

1 Synthesis of data products for ocean carbonate chemistry

2
3 Li-Qing Jiang^{1,2}, Amanda Fay³, Jens Daniel Müller^{4,5}, **Luke Gregor^{4,6}**, **Alizée Roobaert⁷**, Lydia
4 Keppler⁸, Dustin Carroll^{9,10}, Siv K. Lauvset¹¹, Tim DeVries¹², Judith Hauck^{13,14}, Christian
5 Rödenbeck¹⁵, Nicolas Metz¹⁶, Andrea J. Fassbender¹⁷, Jean-Pierre Gattuso^{18,19}, Peter
6 Landschützer⁶, Rik Wanninkhof²⁰, Christopher Sabine²¹, Simone R. Alin¹⁷, Mario Hoppema¹²,
7 Are Olsen²², Matthew P. Humphreys²³, **Kunal Chakraborty²⁴**, **Ana C. Franco^{25,26}**, Kumiko
8 Azetsu-Scott²⁷, Dorothee C. E. Bakker²⁸, Leticia Barbero^{20,29}, Nicholas R. Bates^{30,31}, Nicole
9 Besemer²⁰, Henry C. Bittig³², Albert E. Boyd^{20,29}, Daniel Broullón³³, Wei-Jun Cai³⁴, Brendan R.
10 Carter^{35,17}, Thi-Tuyet-Trang Chau^{36,37}, Chen-Tung Arthur Chen³⁸, Frédéric Cyr^{39,40}, John E.
11 Dore⁴¹, Ian Enochs²⁰, Richard A. Feely¹⁷, Hernan E. Garcia², Marion Gehlen³⁶, **Prasanna Kanti**
12 **Ghoshal²⁴**, Lucas Gloege³, Melchor González-Dávila⁴², Nicolas Gruber⁴, **Debby Ianson⁴³**,
13 Yosuke Iida⁴⁴, Masao Ishii⁴⁵, **A.P. Joshi²⁴**, Esther Kennedy⁴⁶, Alex Kozyr^{1,2}, Nico Lange¹⁰, Claire
14 Lo Monaco¹⁶, Derek P. Manziello⁴⁷, Galen A. McKinley³, Natalie M. Monacci⁴⁸, Xose A.
15 Padin³³, Ana M. Palacio-Castro^{20,29}, Fiz F. Pérez³³, J. Magdalena Santana-Casiano⁴², Jonathan
16 Sharp^{35,17}, Adrienne Sutton¹⁷, Jim Swift⁴⁹, Toste Tanhua⁵⁰, Maciej Telszewski⁵¹, Jens Terhaar⁵².
17 ⁵³, Ruben van Hooidonk⁵⁴, Anton Velo³³, Andrew J. Watson⁵⁵, Angelique E. White²¹, Zelun
18 Wu³⁴, **Liang Xue⁵⁶**, Hyelim Yoo^{1,2}, Jiye Zeng⁵⁷, **Guorong Zhong⁵⁸**.

20 ¹Cooperative Institute for Satellite Earth System Studies, Earth System Science Interdisciplinary Center, University
21 of Maryland, College Park, Maryland 20740, United States.

22 ²NOAA/NESDIS National Centers for Environmental Information, Silver Spring, Maryland 20910, United States.

23 ³Columbia University and Lamont-Doherty Earth Observatory, Palisades, New York 10964, United States.

24 ⁴Environmental Physics, Institute of Biogeochemistry and Pollutant Dynamics, ETH Zürich, Zürich, Switzerland.

25 ⁵Carbon to Sea Initiative, Washington, District of Columbia, United States.

26 ⁶Swiss Data Science Center, ETH Zurich and EPFL, Zurich, Switzerland.

27 ⁷Flanders Marine Institute (VLIZ), Jacobsenstraat 1, 8400 Ostend, Belgium.

28 ⁸Vycarb Inc., Brooklyn, New York, United States.

29 ⁹Moss Landing Marine Laboratories, San José State University, Moss Landing, California, United States.

30 ¹⁰Jet Propulsion Laboratory, California Institute of Technology, Pasadena, California, United States.

31 ¹¹NORCE Research AS, Bjerknes Centre for Climate Research, Bergen, Norway.

32 ¹²Department of Geography and Earth Research Institute, University of California, Santa Barbara, California, United
33 States.

34 ¹³Alfred Wegener Institute Helmholtz Centre for Polar and Marine Research, Bremerhaven, Germany

35 ¹⁴University of Bremen, Department 02 Biology/Chemistry Bremen, Germany.

36 ¹⁵Max Planck Institute for Biogeochemistry, Jena, Germany.

37 ¹⁶Laboratoire LOCEAN/IPSL, Sorbonne Université-CNRS-IRD-MNHN, 75005 Paris, France.

38 ¹⁷NOAA/OAR Pacific Marine Environmental Laboratory, Seattle, Washington 98115, United States.

39 ¹⁸Sorbonne Université, CNRS, Laboratoire d'Océanographie de Villefranche, 06230 Villefranche-sur-Mer, France.

40 ¹⁹Institute for Sustainable Development and International Relations, Paris, France.

41 ²⁰NOAA/OAR Atlantic Oceanographic and Meteorological Laboratory, Miami, Florida 33149, United States.

42 ²¹Department of Oceanography, University of Hawai'i at Mānoa, 1000 Pope Rd., Honolulu, Hawaii 96822, United
43 States.

44 ²²Geophysical Institute, University of Bergen and Bjerknes Centre for Climate Research, Bergen, Norway.

45 ²³Department of Ocean Systems, NIOZ Royal Netherlands Institute for Sea Research, Texel, the Netherlands.

46 ²⁴Indian National Center for Ocean Information Services, Ministry of Earth Sciences, Hyderabad, India.

47 ²⁵Department of Earth, Ocean and Atmospheric Sciences, University of British Columbia, Vancouver, BC, Canada.

48 ²⁶Current affiliation: Earth Sciences Department, Barcelona Supercomputing Center, Barcelona, Spain.

49 ²⁷Fisheries and Oceans, Canada, Bedford Institute of Oceanography, Dartmouth, Nov Scotia, Canada.

50 ²⁸Centre for Ocean and Atmospheric Sciences, School of Environmental Sciences, University of East Anglia,
51 Norwich NR4 7TJ, United Kingdom.

52 ²⁹Cooperative Institute for Marine and Atmospheric Studies, Rosenstiel School of Marine and Atmospheric Science,
53 University of Miami, Miami, Florida 33149, United States.

54 ³⁰Bermuda Institute of Ocean Sciences, ASU-BIOS, 17 Biological Lane, St. Georges, GEO1, Bermuda.

55 ³¹School of Ocean Futures, Arizona State University, Tempe, Arizona 85281, United States.

56 ³²Leibniz Institute for Baltic Sea Research Warnemünde (IOW), Rostock, Germany.

57 ³³Instituto de Investigaciones Mariñas, IIM – CSIC, Vigo, Spain.

58 ³⁴School of Marine Science and Policy, University of Delaware, Newark, Delaware 19716, United States.

59 ³⁵Cooperative Institute for Climate, Ocean, and Ecosystem Studies, University of Washington, Seattle, Washington,
60 United States.

61 ³⁶Laboratoire des Sciences du Climat et de l'Environnement, LSCE-IPSL, CEA-CNRS-UVSQ, Université Paris-
62 Saclay, 91191 Gif-sur-Yvette, France.

63 ³⁷Laboratoire Interdisciplinaire des Sciences du Numérique (LISN), Centre de recherches INRIA, Université Paris-
64 Saclay, René Thom, F-91190, Gif-sur-Yvette, France.

65 ³⁸Department of Oceanography, National Sun Yat-Sen University, Kaohsiung, Taiwan.

66 ³⁹Northwest Atlantic Fisheries Centre, Fisheries and Oceans Canada, St. John's, Newfoundland and Labrador,
67 Canada.

68 ⁴⁰Current affiliation: Centre for Fisheries Ecosystems Research, Fisheries and Marine Institute of Memorial
69 University of Newfoundland, St. John's, Canada.

70 ⁴¹Department of Land Resources and Environmental Sciences, Montana State University, Bozeman, Montana,
71 United States.

72 ⁴²Instituto de Oceanografía Cambio Global, IOCAG, Universidad de Las Palmas de Gran Canaria, 35017 Las
73 Palmas de Gran Canaria, Spain.

74 ⁴³Institute of Ocean Sciences, Fisheries and Oceans Canada, Sidney, British Columbia, Canada.

75 ⁴⁴Atmosphere and Ocean Department, Japan Meteorological Agency, 3-6-9 Toranomon, Minato City, Tokyo, Japan.

76 ⁴⁵Meteorological Research Institute, Japan Meteorological Agency, Tsukuba, Japan.

77 ⁴⁶University of California Davis, Bodea Marine Laboratory, Davis, California, United States.

78 ⁴⁷Coral Reef Watch, U.S. National Oceanic and Atmospheric Administration, College Park, Maryland, United
79 States.
80 ⁴⁸College of Fisheries and Ocean Sciences, University of Alaska Fairbanks, Fairbanks, Alaska, United States.
81 ⁴⁹Scripps Institution of Oceanography, La Jolla, California, United States.
82 ⁵⁰GEOMAR Helmholtz Centre for Ocean Research Kiel, Kiel, Germany.
83 ⁵¹International Ocean Carbon Coordination Project, Institute of Oceanology of Polish Academy of Sciences, Sopot,
84 Poland.
85 ⁵²Climate and Environmental Physics, Physics Institute, University of Bern, Bern, Switzerland.
86 ⁵³Oeschger Centre for Climate Change Research, University of Bern, Bern, Switzerland.
87 ⁵⁴Science for Climate Change Resilience, Boulder, Colorado 80302, United States.
88 ⁵⁵Global Systems Institute, University of Exeter, Exeter, United Kingdom.
89 ⁵⁶First Institute of Oceanography, and Key Laboratory of Marine Science and Numerical Modeling, Ministry of
90 Natural Resources, Qingdao, China.
91 ⁵⁷National Institute for Environmental Studies, Tsukuba, Japan.
92 ⁵⁸Institute of Oceanology, Chinese Academy of Sciences, Qingdao, China.
93 *Correspondence to:* Li-Qing Jiang (liqing.jiang@noaa.gov)

94 **Abstract.** As the largest active carbon reservoir on Earth, the ocean is a cornerstone of the global carbon cycle,
95 playing a pivotal role in modulating ocean health and the Earth's climate system. Understanding these crucial roles
96 requires access to a broad array of data products documenting the changing chemistry of the global ocean as a vast
97 and interconnected system. This review article provides an overview of 68 existing ocean
98 carbonate chemistry data products and data product sets, encompassing compilations of cruise datasets, derived gap-
99 filled data products, model simulations, and compilations thereof. It is intended to help researchers identify and
100 access data products that best align with their research objectives, thereby advancing our understanding of the
101 ocean's evolving carbonate chemistry. [The list will be updated periodically to incorporate new data products. The](#)
102 [most up-to-date list is available at https://oceanco2.github.io/co2-products/](https://oceanco2.github.io/co2-products/). [New data products can be submitted](https://forms.gle/g8hYm37Wg1Uifg8E8)
103 [through https://forms.gle/g8hYm37Wg1Uifg8E8](https://forms.gle/g8hYm37Wg1Uifg8E8).

104 **1 Introduction**

105 Since the onset of the Industrial Revolution in 1750, human activities, such as the burning of fossil fuels, cement
106 production, and land-use change, have emitted ~2600 Gt carbon dioxide (CO₂) ([1 Gt = 10¹⁵g, 1 Gt CO₂ = 3.667 Gt](#)
107 [Carbon, or Gt C](#)) into the atmosphere, causing the atmospheric CO₂ levels to increase by ~50% (DeVries, 2022a;
108 Friedlingstein et al., 2025; Tans and Keeling, 2025). The global carbon cycle, encompassing the exchange of CO₂
109 among the atmosphere, oceans, terrestrial ecosystems, and geosphere, plays a critical role in regulating atmospheric
110 CO₂ levels (Archer, 2010; DeVries, 2022a; Friedlingstein et al., 2025). As the largest dynamic CO₂ reservoir, the
111 ocean holds approximately 45 times the amount of carbon found in the atmosphere currently and actively exchanges

112 it with the air above and sediments below. On timescales from decades to millennia, the ocean imposes a dominant
113 control over atmospheric CO₂ levels (Revelle and Suess, 1957; Broecker, 1982; Archer et al., 2009; DeVries,
114 2022a).

115 The ocean currently absorbs about a quarter of human-caused CO₂ emissions (Sabine et al., 2004a; Gruber et al.,
116 2019a; Carroll et al., 2022; Crisp et al., 2022; Terhaar et al., 2022a; Gruber et al., 2023; DeVries et al., 2023; Müller
117 et al., 2023a; Schimel and Carroll, 2024; [Terhaar, 2025](#)). The chemistry of the ocean has been shifting as a result of
118 anthropogenic CO₂ increase in the ocean (Feely et al., 2023; Ma et al., 2023; Müller et al., 2023a; Fassbender et al.,
119 2023; Keppler et al., 2023a; Jiang et al., 2023; Müller and Gruber, 2024a; [Terhaar et al., 2020, 2021a, and 2024](#)).
120 Since the beginning of the Industrial Revolution, the total amount of dissolved inorganic carbon (DIC) in the
121 [layer from 0 to 200m](#) has risen from 1690 to 1730 Gt of Carbon, and from 35,400 to
122 35,560 Gt C [below 200m](#) (Sabine et al., 2004a; Müller et al., 2023a). The seemingly small increase of 0.5%
123 [results in a substantial drop of](#) the oceans' buffer capacity (DeVries, 2022a). [Buffer capacity](#)
124 [refers to the ocean's ability to resist changes in pH, and thus also the partial pressure of CO₂ \(pCO₂\), when CO₂ or](#)
125 [any other acid or base is added or removed.](#)

126 As anthropogenic CO₂ enters seawater, it reacts with water to form carbonic acid. This is the first in
127 a series of rapid acid-base reactions that release protons (H⁺) and decrease the availability of carbonate ions, which
128 are building materials that many marine organisms, such as mollusks, crustaceans, and corals, use to construct their
129 shells and skeletons (Gattuso and Hansson, 2011). This process, termed as “ocean acidification (OA)”, has already
130 decreased surface ocean pH by roughly 0.11 (~30% increase in acidity) since 1750 (Orr et al., 2005; Jiang et al.,
131 2019a; Kwiatkowski et al., 2020; Jiang et al., 2023; IPCC, 2023). In [some parts of](#) the subsurface ocean, the trends
132 of some acidification [variables](#), e.g., pH, and total hydrogen ion content ([H⁺]_{total}), can be even greater
133 due to the increasing sensitivity of [H⁺] to changes in DIC with depth (Chen et al., 2017; [Perez et al., 2021](#);
134 Fassbender et al., 2023; Müller and Gruber, 2024a). This ongoing acidification threatens critical ocean ecosystem
135 services, including food security, fisheries, aquaculture, and the broader Blue Economy, for billions of people
136 globally (Cooley and Doney, 2009; [Perez et al., 2018](#); Doney et al., 2020).

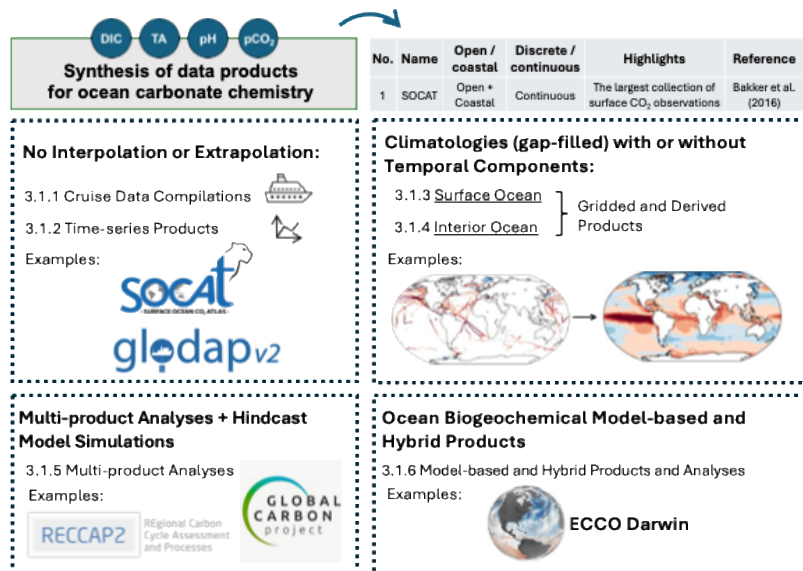
137 In some parts of the ocean, OA is driven not only by the uptake of carbon but also by other processes (Delaigue
138 et al., 2024), for example via alkalinity changes driven by freshening of the Arctic Ocean (Terhaar et al., 2021a) or
139 changes in the carbon and alkalinity export from [the Pacific Ocean and](#) Arctic rivers (Terhaar et al., 2019; Qi et al.,
140 [2017 and 2022](#); Bertin et al., 2023). Local anthropogenic inputs through rivers or from air pollution also lead to OA
141 (e.g. Sarma et al, 2015; Sridvi and Sarma, 2021). [Furthermore, eutrophication and hypoxia in coastal regions may](#)
142 [exacerbate OA in oxygen-deficient bottom waters, as biologically produced CO₂ weakens the natural buffering](#)
143 [capacity of seawater.](#) (Cai et al., 2011). If anthropogenic CO₂ emissions continue without mitigation, as per the
144 shared socioeconomic pathway (SSP5-8.5) scenario, surface ocean pH could decrease by a further 0.3 to 0.4 by
145 2100, equivalent to a 100–150% increase in acidity (Kwiatkowski et al., 2020; Jiang et al., 2023). If society,
146 however, succeeds at reducing emissions, the future acidity level becomes highly uncertain as it sensitively depends
147 on the transient response of the Earth system and the amount of reductions of non-CO₂ radiative agents (Terhaar et

148 al., 2023).

149 In summary, monitoring ocean carbonate chemistry is essential for (a) tracking the evolving ocean carbon sink,
150 and (b) understanding OA and its ecological impacts. Additionally, monitoring ocean carbonate chemistry is crucial
151 when considering marine carbon dioxide removal (mCDR) strategies such as ocean alkalinity enhancement (OAE),
152 artificial upwelling, ocean fertilization and electrochemical ocean CO₂ removal (Kheshgi, 1995; Bach et al., 2019;
153 Schimel and Carroll, 2024; Oschlies et al., 2025). The ocean's vast and interconnected nature necessitates that data
154 from individual oceanographic cruises be meticulously preserved, subject to rigorous quality control, and uniformly
155 formatted to promote their usability (Brett et al., 2020; Schoderer et al., 2024). Following Lange et al. (2023), we
156 curate an exhaustive catalogue of synthesis products pertaining to ocean carbonate chemistry, including cruise data
157 compilations, gridded gap-filled data products, and other derived data products. This compilation spans both global
158 and regional scales, providing a holistic view of the current state of ocean biogeochemistry data aggregation.

159 2 Methods

160 In this paper, data products are defined as outputs that quality-control, aggregate, and transform individual
161 datasets from multiple sources into a unified, structured format to support research, decision-making, or operational
162 needs for specific end users. The data products included in this study were identified through a literature review and
163 discussions with researchers via the Ocean Acidification Information Exchange (OAIE) platform.



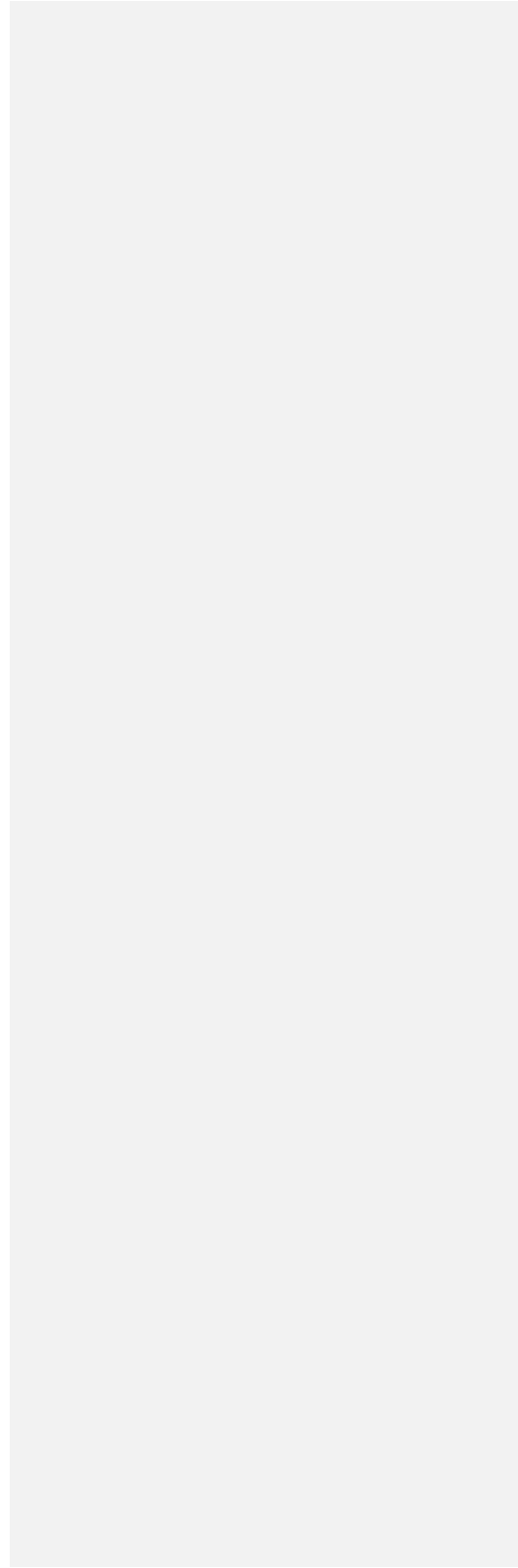
164
165 **Figure 1.** An overview diagram outlining the paper's structure and flow.

166 The products are organized [into six categories](#) based on end-user needs [and listed within each class with no](#)
167 [particular order](#) (Figure 1):

- 168 1. Cruise data compilations (no interpolation or gap filling).
- 169 2. Time-series data products (no interpolation or gap filling).
- 170 3. Derived gap-filled (e.g., interpolated) products for the surface ocean, starting with products offering a cli-
171 matological snapshot of the ocean, followed by those showing temporal changes.
- 172 4. Derived gap-filled (e.g., interpolated) products for the interior ocean, also starting with products offering a
173 climatological snapshot of the ocean, followed by those showing temporal changes.
- 174 5. Multi-product analyses of 3 and 4. These compilations also include hindcast model simulations of the
175 ocean carbon cycle and biogeochemistry.
- 176 6. Model and hybrid data products projecting ocean carbonate system variables into the future [Note: Here the
177 term “model” refers to ocean biogeochemical models (Fennel et al., 2022). If a statistical model or machine
178 learning model is used for gap filling, the product is not categorized as a model output product in this com-
179 pilation.

180 Each category includes numbered descriptions of each data product in that class, as well as a summary table of
181 the data products with corresponding IDs so the user can easily jump to the associated product description. [For each](#)
182 [data product, the description is followed by its access links. Persistent identifiers \(e.g., digital object identifiers, or](#)
183 [DOIs\) and links to all data products are also summarized in the table in Section 4. Data availability.](#)

184 Although some data products, such as Surface Ocean CO₂ Atlas (SOCAT) and Lamont-Doherty Earth
185 Observatory (LDEO) surface [partial pressure of carbon dioxide \(\$p\text{CO}_2\$ \)](#) Database report only one ocean carbonate
186 [system](#) variable, i.e., fugacity of carbon dioxide ($f\text{CO}_2$) [or \$p\text{CO}_2\$](#) , they provide a foundation from which additional
187 variables can be derived using empirical algorithms. For instance, total alkalinity content (TA) can be estimated
188 from salinity and temperature and other factors (Lee et al., 2006) and by neural network approaches such as those
189 developed by Velo et al. (2013) and Broullón et al. (2019). Beyond TA, neural network algorithms have been
190 extended to estimate [dissolved inorganic carbon \(\$\text{DIC}\$ \)](#) [DIC](#) as demonstrated by Broullón et al. (2020a), and even the
191 full marine carbonate system (MCS) through frameworks like CANYON-B/CONTENT (Bittig et al., 2018) and
192 Empirical Seawater Property Estimation Routines (ESPERs) (Carter et al., 2021). While these methods primarily
193 employ neural networks, both Velo et al. (2013) and Carter et al. (2021) provide alternative estimation approaches
194 based on local interpolation, through their 3-dimensional moving window multilinear regression algorithm
195 (3DwMLR) and locally interpolated regression (LIR) methods, respectively. Utilizing such derived data, the
196 complete suite of ocean carbonate [system parameters/variables](#) can then be calculated using computer software, such
197 as CO2SYS (Lewis and Wallace, 1998; van Heuven et al., 2011; Orr et al., 2018; Sharp et al., 2023) or its Python
198 implementation PyCO2SYS (Humphreys et al., 2022). An in-depth explanation of the methods employed for these
199 calculations can be found in the Supplementary material of Jiang et al. (2022a).



201 3 Results and Discussion

202 3.1 Data products for ocean carbonate chemistry

203 3.1.1 Cruise Data Compilations (no interpolation or gap filling):

204 The data compilations described in this section standardize datasets collected from individual research vessels,
205 ships of opportunity, and [uncrewed](#) platforms, presenting them in a uniform format for easy
206 access. These datasets typically undergo both primary QC (identifying outliers and obvious errors within an
207 individual cruise dataset) and secondary QC ([when possible, to objectively compare](#) data from one cruise
208 against another or a previously synthesized dataset to quantify systematic differences in reported values). [It's](#)
209 [important to note that data providers are expected to carry out rigorous QC prior to data submission.](#)

210 1) **SOCAT:** The Surface Ocean CO₂ Atlas features surface *f*CO₂
211 measurements from both the open ocean and the coastal ocean, predominantly sourced from research
212 vessels, [ships of opportunity](#), and autonomous platforms including fixed moorings and
213 [uncrewed](#) surface vehicles (USVs) (Bakker et al., 2016). It represents the most extensive collection of
214 observational ocean CO₂ data for the global surface ocean. Since 2013, SOCAT has been updated annually.
215 [Dataset flags indicate the estimated uncertainty and completeness of metadata in](#)
216 [SOCAT synthesis products. The SOCAT gridded product contains *f*CO₂ values with an estimated](#)
217 [uncertainty of less than 5 μatm.](#) To access the latest version
218 of the SOCAT data product (with 40 million data points), visit <https://socat.info/> (Bakker et al., 2025).

219 2) **LDEO Surface *p*CO₂ Database:** Dr. Taro Takahashi [[LDEO](#),
220 Palisades, New York] started synthesizing global surface ocean CO₂ data in 1997, compiling three decades
221 of observations (~250,000 measurements) to create inaugural monthly global surface *p*CO₂ maps
222 (Takahashi et al., 1997; Takahashi et al., 2002). The most recent version (V2019) expanded this dataset to
223 approximately 14.2 million surface water *p*CO₂ measurements spanning from 1957–2019. Distinct from the
224 SOCAT database, the LDEO database reports *p*CO₂, instead of *f*CO₂, exclusively from equilibrator-CO₂
225 analyzer systems, with an average estimated uncertainty of ± 2.5 μatm. The database is also interpolated
226 onto a global surface ocean 4° × 5° grid for a reference year 2000 (Takahashi et al., 2009) and 2010 (Fay et
227 al., 2024). Access to the LDEO surface *p*CO₂ database (Version 2019) is provided by the Ocean Carbon
228 and Acidification Data System (OCADS)
229 at: <https://www.ncei.noaa.gov/data/oceans/ncei/ocads/metadata/0160492.html> (Takahashi et al., 2017).
230 Additionally, there is a dedicated webpage for the LDEO Database at OCADS:
231 [https://www.ncei.noaa.gov/access/ocean-carbon-acidification-data-](https://www.ncei.noaa.gov/access/ocean-carbon-acidification-data-system/oceans/LDEO_Underway_Database/)
232 [system/oceans/LDEO_Underway_Database/](https://www.ncei.noaa.gov/access/ocean-carbon-acidification-data-system/oceans/LDEO_Underway_Database/).

233 3) **GLODAPv2:** The Global Ocean Data Analysis Project Version 2 (GLODAPv2) aggregates

234 biogeochemical data collected from discrete bottle samples, offering extensive global coverage from the
235 surface to depths (Key et al., 2015; Olsen et al., 2016; Lauvset et al., 2024). While GLODAP is primarily a
236 product for basin-scale ~~repeat~~ hydrography data, it also includes coastal datasets and observations from a
237 few time-series. The GLODAPv2 data product provides rigorously quality-controlled measurements for 14
238 essential oceanographic variables: temperature, salinity, dissolved oxygen (DO), nitrate, silicate, phosphate,
239 ~~dissolved inorganic carbon (DIC)~~ **DIC**, ~~total alkalinity~~ (TA, pH, chlorofluorocarbons (CFC-11, CFC-12,
240 CFC-113), carbon tetrachloride (CCl₄), and sulfur hexafluoride (SF₆). These variables, excluding
241 temperature, undergo both primary and secondary quality control procedures to detect outliers and adjust
242 for significant measurement biases. GLODAPv2 was first published in 2016 and ~~has been~~ **was** updated
243 annually through a living data process in Earth System Science Data ~~since from~~ 2019 **through “v2023,”**
244 **which was published in 2024.** For these updates, new data (including historical data not previously included
245 in the data product) are quality controlled and adjusted to the 2016 version (Olsen et al., 2019; Olsen et al.,
246 2020; Lauvset et al., 2021; Lauvset et al., 2022; Lauvset et al., 2024). Since the global repeat hydrography
247 programs operate with decadal repetitions, the aim is to produce a completely new version of GLODAP,
248 where all cruise datasets will be reevaluated, every decade. Release of the GLODAPv3 data product is
249 planned for 2026, **and is expected to evolve the secondary data quality control practices relative to those**
250 **used in GLODAPv2.** For more information on the secondary quality control process, refer to Tanhua et al.
251 (2010) and Lauvset and Tanhua (2015). GLODAPv2 offers two kind of products: the collection of quality
252 controlled data from discrete bottle samples taken at sampling location (Key et al., 2015; Olsen et al., 2016;
253 Olsen et al., 2019; Olsen et al., 2020; Lauvset et al., 2021; Lauvset et al., 2022; Lauvset et al., 2024), and a
254 gridded product, interpolated to a 1° × 1° grid and the 33 standard depth levels of ~~WOA~~ (World Ocean
255 Atlas (**WOA**) (Lauvset et al., 2016). All versions of the GLODAPv2 data product can be accessed at
256 <https://glodap.info/>.

257 **GLODAPv2 builds upon three foundational data products: the original GLODAP (Sabine et al., 2004a),**
258 **CARbon dioxide IN the Atlantic Ocean (CARINA, Key et al., 2010), and PACIFIC ocean Interior Carbon**
259 **(PACIFICA, Suzuki et al., 2013). These data products remain available at NCEI:**
260 **<https://www.ncei.noaa.gov/data/oceans/ncei/ocads/metadata/0001644.html> (GLODAP, Sabine et al.,**
261 **2004b), <https://www.ncei.noaa.gov/data/oceans/ncei/ocads/metadata/0113899.html> (CARINA, Tanhua et**
262 **al., 2013), and <https://www.ncei.noaa.gov/data/oceans/ncei/ocads/metadata/0110865.html> (PACIFICA,**
263 **Suzuki et al., 2013), respectively.**

264 **3)4) Quality Edited Hydrographic Data **JOA Suite:** The **Quality Edited Hydrographic Data Suite** product
265 offers both a user-friendly application and a library of ocean profile data curated by Jim Swift (Scripps
266 Institution of Oceanography, La Jolla, California, **United States**SA). Similar to GLODAPv2, this data
267 product serves as a comprehensive repository of quality-controlled discrete bottle-based measurements (and
268 limited CTD), spanning from the surface to the depths of the global ocean. Unlike GLODAPv2, no offset**

269 corrections were applied to this data product. It encompasses a range of oceanographic variables including
270 temperature, salinity, DO, DIC, TA, silicate, phosphate, nitrate, nitrite, CFC-11, CFC-12, ~~and SF₆ and~~
271 ~~CTD parameters associated with the water sample data~~. To access the ~~JOA~~-application and data, visit:
272 <https://joa.ucsd.edu/>. Currently, there is not a peer-reviewed paper or public-accessible report for this data
273 product. Cite the data product itself as: “Swift, J. (2022), [Quality Edited Hydrographic DataJava](#)
274 ~~OceanAtlas Data~~, https://joa.ucsd.edu/Data_homepage”, or cite the entire ~~JOA Suite~~data product as: “Swift,
275 J. and Osborne, J. (2022), The [Quality Edited Hydrographic DataJava-OceanAtlas Suite](#),
276 <https://joa.ucsd.edu>”.

277 **4)5) WOD:** In addition to the [GLODAPv2 \(No. 3\)](#) and [Quality Edited Hydrographic Data \(No. 4\)](#),
278 users can also access historical and recent original biogeochemical data collected from discrete bottle
279 samples in a uniform format and units, along with their originator quality control (QC) flags, through the
280 World Ocean Database (WOD) (Mishonov et al., 2024). Like the [Quality Edited Hydrographic Data](#),
281 these measured data remain unaltered. The WOD allows users to filter and subset data with specific
282 variables, platforms, institutions, projects, regions, or time periods (Garcia et al., 2024). Users can visualize
283 sampling locations on a “distribution plot” and access a cruise list for all selected data and variables. Users
284 also have the option of exporting data in NetCDF or Comma-Separated Values (CSV) formats.
285 Additionally, all data in the WOD are reproducible and traceable to their original data sources archived at
286 NOAA’s National Centers for Environmental Information (NCEI). The WOD is accessible at
287 <https://www.ncei.noaa.gov/products/world-ocean-database>.

288 **5)6) SNAPO-CO₂:** Metzl et al. (2024) aggregated over 44,400 measurements of DIC and TA from a series of
289 research cruises and [ships of opportunity](#) across various oceanic regions from 1993-2022, under
290 several French research programs, to create a product called “Service National d’Analyse des
291 Paramètres Océaniques du CO₂ (SNAPO-CO₂)”. The majority of the samples were analyzed by the Service
292 National d’Analyse des Paramètres Océaniques du CO₂ (SNAPO-CO₂) at the LOCEAN laboratory in Paris,
293 France. Sampling was performed either from CTD-rosette casts (Niskin bottles) or collected from the ship’s
294 flow-through system (intake at roughly 5m depth). DIC and TA determinations were conducted
295 simultaneously through potentiometric titration in a closed-cell setup, calibrated with certified reference
296 material to achieve an accuracy of $\pm 4 \mu\text{mol kg}^{-1}$ for both [variables](#), as per Edmond (1970). This
297 methodology was also applied for real-time measurements during OISO cruises, with data from the South
298 Indian Ocean for 1998-2018 included in this compilation. The data is split into two sets: one for the global
299 ocean and coastal zones, and another for the Mediterranean Sea, both accessible in the same format:
300 <https://doi.org/10.17882/95414>. Additionally, this data product is available at OCADS
301 : <https://www.ncei.noaa.gov/data/oceans/ncei/ocads/metadata/0285681.html> (Metzl
302 et al., 2023)

303 **6)7) CODAP-NA:** Jiang et al. (2021) synthesized two decades of discrete measurements of carbonate system

304 variables, DO, and nutrient data from the North American continental shelves to generate the first version
305 of Coastal Ocean Data Analysis Data Product in North America (CODAP-NA). The 2021 release
306 encompasses 3,391 oceanographic profiles from 61 research cruises spanning the North American
307 continental shelves from Alaska to Mexico in the west and from Canada to the Caribbean in the east. It
308 includes 14 key variables, including temperature, salinity, DO, DIC, TA, pH, carbonate ion, $f\text{CO}_2$, silicate,
309 phosphate, nitrate, all of which have undergone rigorous quality control. Note that certain datasets meeting
310 the GLODAPv2 QC standards are also included in the GLODAPv2 since its 2022 release (No. 3 above).
311 CODAP-NA is available at OCADS (~~DOI: "10.25921/531n-e230"~~):
312 <https://www.ncei.noaa.gov/data/oceans/ncei/ocads/metadata/0219960.html> (Jiang et al., 2020).

313 **7)8) AZMP Carbon:** Gibb et al. (2023) compiled [ocean carbonate system variables](#) data from the
314 Canadian Atlantic Zone Monitoring Program (AZMP Carbon) since 2014. More than 100 seagoing
315 missions are represented in this dataset. The sample strategy corresponds generally to full-depth water
316 samples mostly collected along standardized hydrographic sections. The majority of these data were
317 collected as part of the Atlantic Zone Monitoring Program (AZMP) of Fisheries and Oceans Canada
318 (DFO). Implemented in 1998, the AZMP aims to characterize and understand the causes of oceanic
319 variability at the seasonal, inter-annual and decadal scales in support of, among other things, fisheries
320 management in the Atlantic Zone (including the Gulf of St. Lawrence, the Scotian shelf and the
321 Newfoundland and Labrador shelf). Since 2014, a minimum of two of the three following carbonate [system](#)
322 [variables](#), DIC, TA, and pH, are also acquired by the program at standardized hydrographic
323 stations across the zone (sampled up to three times a year). Each measurement is completed with
324 corresponding temperature, salinity and, when available, nutrients and DO concentration data. This dataset
325 also includes samples collected as part of ships of opportunity, fishing and other scientific trips. The entire
326 dataset comprises 19,531 discrete samples [last updated 21 August 2024]. Among this number, 18,085 have
327 at least two of the three carbonate system [variables](#) (e.g., TA, DIC and pH), allowing the
328 derivation of other [variables](#) such as the saturation state relative to aragonite and calcite (Ω_{arag}
329 and Ω_{calc}) and $p\text{CO}_2$ (in μatm) using the CO2SYS program modified for Python
330 (<https://github.com/mvdh7/PyCO2SYS/tree/v1.2.1>, last access: 8 January 2023; Humphreys et al., 2022).
331 The full dataset of measured and derived [variables](#) is available from the Federated Research
332 Data Repository: <https://doi.org/10.20383/102.0673> (Cyr et al., 2022) and is updated annually.

333 **8)9) MOCHA:** Kennedy et al. (2023) curated a comprehensive coastal ocean data product called "Multistressor
334 Observations of Coastal Hypoxia and Acidification (MOCHA)", encompassing temperature, salinity, DO,
335 ocean carbonate [system](#) variables (DIC, TA, pH, $p\text{CO}_2$, $f\text{CO}_2$), nutrients, and chlorophyll measurements
336 from the full water column along the U.S. west coast. The synthesis integrates observations from 71
337 different sources, including high-resolution autonomous sensors, synoptic oceanographic cruises, and
338 shoreline samples. The MOCHA synthesis spans from the shoreline to well-beyond the continental shelf

339 and incorporates observations from CODAP-NA ([see No. 7 above](#)), [California Cooperative Oceanic](#)
340 [Fisheries Investigations](#) (CalCOFI), and other large-scale oceanographic cruises to facilitate linking
341 nearshore, high-resolution observations to broader oceanographic conditions. As of 2025, MOCHA
342 includes 15.9 million temperature readings, 5.0 million salinity measurements, 3.9 million DO records, and
343 2.3 million pH measurements, along with 8,368 [dissolved inorganic carbon](#) [DIC](#), 10,144 [total alkalinity](#) [TA](#),
344 and 505,000 $p\text{CO}_2/f\text{CO}_2$ measurements, with limited additional chlorophyll and nutrient observations. To
345 reduce the computational load from high-resolution sensors, the synthesis is also available as a “daily
346 aggregated” dataset, with all data sources averaged by day, location, and depth. All data in the MOCHA
347 synthesis product has been quality controlled to a “plausible and reasonable” standard, but researchers
348 requiring high-precision coastal data may need to apply additional QC tests. The data product is available at
349 OCADS ([DOI: “10.25921/2vve-fh39”](#)):
350 <https://www.ncei.noaa.gov/data/oceans/ncei/ocads/metadata/0277984.html> ([Kennedy et al., 2023](#)), while
351 the methods and product are described in [Kennedy et al. \(2024\)](#).

352 **9)10) ARIOS:** The Acidification in the Rias and the Iberian Continental Shelf (ARIOS) project involved
353 compiling and analyzing the historical record of [ocean carbonate](#) system measurements and associated
354 [variables](#) conducted by the Instituto de Investigaciones Mariñas (IIM-CSIC) in Vigo, Spain.
355 This dataset comprises 3,343 oceanographic stations and 17,653 discrete samples, combining
356 measurements of pH, [TA](#), and other physical (pressure, temperature and salinity) and
357 biogeochemical [variables](#) (DO, nitrate, phosphate, and silicate) off the northwestern Iberian
358 Peninsula from June 1976 to September 2018 ([Padin et al., 2020](#)). The oceanography cruises funded by 24
359 projects were primarily carried out in the Ría de Vigo coastal inlet, but also in an area ranging from the Bay
360 of Biscay to the Portuguese coast. Robust seasonal cycles and long-term trends were calculated along a
361 longitudinal section, gathering data from the coastal and oceanic zone of the Iberian upwelling system.
362 A synthesis paper is available at <https://doi.org/10.5194/essd-12-2647-2020> ([Padin et al., 2020](#)), and the
363 A synthesis paper is available at <https://doi.org/10.5194/essd-12-2647-2020> ([Padin et al., 2020](#)), and the
364 A synthesis paper
365 is available at <https://doi.org/10.5194/essd-12-2647-2020> ([Padin et al., 2020](#)), and the data product is
366 available at <https://doi.org/10.20350/digitalCSIC/12498> ([Pérez et al., 2020](#)).

367 **10)11) Marine Inorganic Carbon-Carbonate Chemistry in the Northern Gulf of Alaska:** [Monacci et](#)
368 [al. \(2023\)](#) compiled a data product of discrete seawater samples collected each May and September over a
369 10-year period from 2008 to 2017 along the long-term hydrographic line in the Gulf of Alaska (GAK Line).
370 Samples were collected from a sampling rosette on a profiling CTD. Data variables include profiled
371 seawater temperature, salinity, and DO. Discrete sample variables include DO (i.e., Winkler titrations),
372 macronutrients (nitrate, nitrite, phosphate, silicic acid), [dissolved inorganic carbon \(DIC\)](#) [DIC](#), and [total](#)
373 [alkalinity \(TA\)](#) [TA](#). The repeat hydrographic cruises were funded by the Alaska Ocean Observing System

374 (AOOS), the Exxon Valdez Oil Spill Trustee Council (EVOS), Gulf Watch Alaska, and the North Pacific
375 Research Board (NPRB) and were mostly conducted aboard the United States Fish and Wildlife Service
376 (USFWS) R/V Tíglaġ. All carbonate ~~system parameters/variables~~ were analyzed at the Ocean Acidification
377 Research Center (OARC) at the University of Alaska Fairbanks (UAF). This data product is available at
378 ~~OCADS (DOI: 10.25921/x9sg-9b08)-;~~
379 <https://www.ncei.noaa.gov/data/oceans/ncei/ocads/metadata/0277034.html> (Monacci et al., 2023), and the
380 synthesis paper can be accessed at <https://doi.org/10.5194/essd-16-647-2024> (Monacci et al., 2024).

381 **12) Coral Reef Carbonate Chemistry Off the Florida Keys:** Palacio-Castro et al. (2023) compiled discrete
382 seawater samples from 38 permanent stations located along 10 inshore-offshore transects at the Florida
383 Coral Reef. These samples were collected as part of NOAA's National Coral Reef Monitoring Program
384 (NCRMP) and the South Florida Ecosystem Restoration Research (SFER) cruises. Sampling efforts
385 commenced in 2010, with every two months collections initiated in 2015, resulting in a total of 47 sampling
386 cruises and 1,538 discrete seawater samples. For all samples, a minimum of two of the carbonate
387 ~~system variables~~ (TA, DIC) were measured, in addition to salinity and temperature.
388 The Ω_{calc} , $p\text{CO}_2$, and pH were derived from the measured
389 ~~variables~~ using the R package seacarb (Gattuso et al., 2021a). The time-series analysis provides
390 insight into the dynamic carbonate conditions spanning the inshore to offshore gradients, encompassing four
391 distinct regions of the Florida Coral Reef: Biscayne Bay, the Upper Keys, Middle Keys, and Lower Keys.
392 Data is available at NCEI: <https://www.ncei.noaa.gov/access/metadata/landing->
393 Data is available at NCEI:
394 <https://www.ncei.noaa.gov/access/metadata/landing-page/bin/iso?id=gov.noaa.nodc:NCRMP-CO3-Atlantic>
395 (Manzello et al., 2018).

396 **13) Salish Cruise and Cruise Data Package and Multi-stressor Data Product:** Alin et al.
397 (2024/2025a) compiled data from 35-61 individual cruise data sets that sampled marine waters of the
398 southern Salish Sea and northern Washington coast (United States/SA) from 2008 to 2018/2024. ~~These data~~
399 ~~sets were collected in support of research and monitoring efforts of the University of Washington Puget~~
400 ~~Sound Regional Synthesis Model (2008–2013), Washington Ocean Acidification Center (WOAC, 2014–~~
401 ~~present), NOAA Ocean Acidification Observing Network, Northwest Association of Networked Ocean~~
402 ~~Observing Systems, and NOAA Pacific Marine Environmental Laboratory.~~ Ongoing seasonal sampling
403 occurred during April, July, and September for Puget Sound cruises has occurred ~~under WOAC support~~
404 since 2014 and most frequently during May and October for Sound-to-Sea cruises, which sample from
405 Puget Sound through the Strait of Juan de Fuca to the northern Washington coast. The Salish cruise data
406 package contains observations from ~~a total of 715 oceanographic water column~~ profiles, with ~~CTD7490~~
407 sensor measurements of temperature, salinity, and ~~oxygen/DO; as well as ≥ 6070 measurements of discrete~~
408 ~~measurements of DO/oxygen and, nutrients~~ (nitrate, phosphate, silicate, ammonium, nitrite), ~~DIC, and TA~~

409 samples; and ≥ 4462 measurements of inorganic carbon variables (DIC and TA). A follow-on data product is
410 also available, containing based on the Salish cruise data package, which only included the 3971 samples
411 with complete information records for temperature, salinity, and DO from sensors, and oxygen DO,
412 nutrients, DIC, and TA from discrete measurements, along with is also available (Alin et al., 2023). To
413 facilitate applications of this data product to understanding multi-stressor ocean conditions in Pacific
414 Northwest marine waters by various end-users, Alin et al. (2023) also included the most commonly used
415 calculated carbonate system parameters/variables: in this data product pH (total scale), $f\text{CO}_2$, $p\text{CO}_2$, Ω_{arag} , and
416 Ω_{calc} (Alin et al., 2025b). The data package is available at OCADS (DOI: "10.25921/zgk5-ep63"):
417 [https://www.ncei.noaa.gov/access/ocean-carbon-acidification-data-](https://www.ncei.noaa.gov/access/ocean-carbon-acidification-data-system/oceans/SalishCruise_DataPackage.html)
418 [system/oceans/SalishCruise_DataPackage.html](https://www.ncei.noaa.gov/access/ocean-carbon-acidification-data-system/oceans/SalishCruise_DataPackage.html). The multi-stressor data product is available at:
419 [https://www.ncei.noaa.gov/access/ocean-carbon-acidification-data-](https://www.ncei.noaa.gov/access/ocean-carbon-acidification-data-system/oceans/SalishCruises_DataProduct.html)
420 [system/oceans/SalishCruises_DataProduct.html](https://www.ncei.noaa.gov/access/ocean-carbon-acidification-data-system/oceans/SalishCruises_DataProduct.html). Furthermore, two synthesis papers describing the Salish
421 cruises, as well as seasonality and extreme ocean acidification conditions observed during the 2008–2018
422 part of the time-series, data package and interpreting the data product can be found at:
423 <https://essd.copernicus.org/articles/16/837/2024/> (Alin et al., 2024a) and
424 <https://bg.copernicus.org/articles/21/1639/2024/> (Alin et al., 2024b). A preliminary description of the 2019–
425 2024 Salish cruises can be found at <https://www.psp.wa.gov/psmarinewatersoverview.php> (Alin et al.,
426 2025c).

427 **12)14) Line P Marine Carbonate Chemistry Compilation:** This dataset contains marine carbonate
428 system measurements collected during 55 Line P cruises from 1990 to 2019 in the subarctic Northeast
429 Pacific. The dataset contains discrete profiles of DIC, TA, seawater temperature, salinity, DO and nutrients.
430 From a total of 27 hydrographic time-series stations, only the five major stations where DIC and TA are
431 routinely sampled were included in this compilation. Among them is the outermost station P26, also known
432 as Ocean Station Papa (Freeland, 2007). Cruises were conducted approximately three times per year,
433 typically in February, May/June and August/September. Each vertical profile was individually inspected
434 and contrasted with the whole pool of data (including historical data) relative to salinity, density, and
435 oxygen to detect and flag poor quality data following the World Ocean Circulation Experiment
436 (WOCE) quality control convention (Jiang et al., 2022a). Additionally, the recommended cruise-specific
437 adjustments from PACIFICA were applied (Suzuki et al.,
438 2013). The Line P marine carbonate chemistry compilation is described and analyzed in (Franco et al.,
439 2021a) and is publicly available as a single synthesis product at OCADS:
440 <https://www.ncei.noaa.gov/data/oceans/ncei/ocads/metadata/0234342.html> (Franco et al., 2021b). The Line
441 P carbonate chemistry timeseries is maintained by Fisheries and Oceans Canada and continues to the
442 present day. Data are available and continuously updated in the Line P repository, which can be publicly
443 accessed after generating an account at <https://waterproperties.ca>.

444 **13|15** **Anthropogenic Carbon in the Arctic Ocean:** This dataset includes anthropogenic carbon
 445 estimates in the Arctic Ocean based on measurements of transient tracers, such as CFC-12 and SF₆ (Terhaar
 446 et al., 2020; Tanhua et al., 2009). Using the transient time distribution (TTD) method, anthropogenic
 447 carbon estimates were estimated at measurement locations across all basins of the Arctic Ocean between
 448 1983 and 2005. In addition to these estimates, adjusted estimates of anthropogenic carbon at these locations
 449 are provided to account for differences in the saturation of transient tracers and anthropogenic carbon in
 450 Arctic Ocean surface waters that caused anthropogenic carbon estimates to be biased low (Terhaar et al.,
 451 2020). It is recommended to use the adjusted estimates. This dataset can be accessed at
 452 <https://doi.org/10.17882/103920> (Terhaar et al., 2024).

453 **Table 1. Ocean carbonate chemistry data products out of cruise data compilations (no gridding or gap filling).**

No.	Name	Open or coastal ocean	Surface or water column	Discrete bottle or continuous	Highlights	Reference
1	SOCAT	Open + Coastal	Surface	Continuous	The largest collection of surface ocean carbon observations	Bakker et al. (2016)
2	LDEO Surface pCO ₂ Database	Open + Coastal	Surface	Continuous	The LDEO database reports pCO ₂ exclusively from equilibrator-CO ₂ analyzer systems	Takahashi et al. (2017)
3	GLODAPv2	Open ocean	Water column	Discrete bottle	Adjustments are applied by comparing data in the deep ocean (>2000 m) using a crossover and inversion method as described by Johnson et al. (2001).	Lauvset et al. (2024)
4	Quality Edited Hydrographic Data+OA Suite	Open ocean	Water column	Discrete bottle	Similar to GLODAPv2, with no adjustments	Swift (2022)
5	WOD	Open ocean	Water column	Discrete bottle	Similar to GLODAPv2, with no adjustments	Mishonov et al. (2024)
6	SNAPO-CO ₂	Open + Coastal	Water column	Discrete bottle and semi-continuous	A compilation of cruises from multiple French initiatives	Metzl et al. (2024)
7	CODAP-NA	Coastal ocean	Water column	Discrete bottle	Like GLODAPv2, but for the coastal ocean	Jiang et al. (2021)
8	AZMP Carbon	Continental shelf and slope	Water column	Discrete bottle	A compilation of cruises from the Atlantic Zone Monitoring Program (AZMP) since 2014	Gibb et al. (2023)
9	MOCHA	Coastal ocean	Water column	Discrete bottle + Continuous	U.S. West Coast	Kennedy et al. (2024)
10	ARIOS	Coastal ocean	Water column	Discrete bottle	An OA Database for the Galician Upwelling Ecosystem off the NW Iberian Peninsula from 1976 to 2018	Padin et al., (2020)

11	Marine Inorganic Carbonate Chemistry in the Northern Gulf of Alaska	Coastal ocean	Water column	Discrete bottle	A synthesis of twenty cruises from 2008 to 2017 on the Gulf of Alaska (GAK) Line	Monacci et al. (2023)
12	Coral Reef Carbonate Chemistry Off the Florida Keys	Coastal / regional	Water column	Discrete bottle	Temporal trends of DIC, TA, $p\text{CO}_2$, pH, Ω_{arag} , in different areas of the Florida Keys	Palacio-Castro et al. (2023)
13	Salish Cruise and Cruise Data Package and Multi-stressor Data Product	Coastal / estuarine	Water column	Discrete bottle	A data compilation and multi-stressor (OA, hypoxia, temperature) data product based on cruises from 2002 to 2018 in the southern Salish Sea and Washington coast	Alin et al. (2025a, b)
14	Line P Marine Carbonate Chemistry Compilation	Open ocean	Water column	Discrete bottle	A compilation of fifty-five Line P cruises containing discrete DIC and TA profiles at five stations in the Northeast Pacific Ocean. Sampled approximately three times per year from 1990 to 2019	Franco et al. (2021a, b)
15	Anthropogenic carbon in the Arctic Ocean	Open ocean	water column	Discrete bottle (normalized adjusted to year-2005)	Observation-based estimates of anthropogenic carbon in the Arctic Ocean	Tanhua et al. (2009, 2020)

454 **3.1.2 Time-series Products (no interpolation or gap filling):**

455 The time-series products described in this section include observations collected at regular time intervals, over a
456 sustained period, and at fixed locations. The data often represent changes in a particular oceanographic variable over
457 time, such as temperature, salinity, TA and DIC. The list below includes both climate-quality time-series data
458 products compiled at selected stations, and data products compiling time-series measurements at multiple locations.
459 Additionally, some hydrographic sections are measured regularly enough to warrant being called a time-series, e.g.,
460 Line P in the northeast Pacific (Franco et al., 2021b, Freeland, 2007), sections in the northwest Pacific (Ishii et al.,
461 2011a), the [Observatoire de la Variabilité Interannuelle à DÉcennale \(OVIDE\)](#) lines (Mercier et al., 2024).
462 Measurements from these sections are typically included in cruise data compilations (3.1.1) and are not listed
463 separately here.

464 [1416](#) **BATS**: The Bermuda Atlantic Time-series Study (BATS) observations and data products extend
465 to forty years of observations of DIC and TA and OA indicators, and constitute the longest continuous
466 record of warming, salinification, ocean deoxygenation, and OA in the open ocean (Bates and Johnson,
467 2023). The sustained observations at the BATS site began in October 1988, approximately 80 km to the
468 south-east of Bermuda (<https://bios.asu.edu/bats>). The program comprises monthly cruises with CTD,
469 water-column biogeochemical sampling and rate measurements (e.g., primary and export production) plus
470 additional cruises in the spring period and annual transects between the Gulf Stream and Puerto Rico. CO_2 -

471 carbonate chemistry sampling includes full-depth bottle DIC and [TAalkalinity](#) data (including additional
472 surface measurements going back to 1983 collected at the Hydrostation S site). Hydrostation S is located
473 ~25 km south-east of Bermuda (<https://bios.asu.edu/research/projects/hydrostation-s>) and began in 1954
474 with biweekly cruises each year. Underway $f\text{CO}_2/p\text{CO}_2$ data collected from the R/V *Atlantic Explorer* that
475 supports the BATS and Hydrostation S sites constitutes part of the annual data submission to SOCAT. The
476 BATS project page at the Biological and Chemical Oceanography Data Management Office (BCO-DMO)
477 includes metadata and data streams (<https://demo.bco-dmo.org/project/2124>). Hydrostation S data and
478 DOIs are also available at BCO-DMO (<https://www.bco-dmo.org/project/859583>).

479 [15|17](#) **HOT:** The Hawaii Ocean Time-series (HOT) CO₂ measurement program documents 35+ years of
480 inorganic carbon dynamics in the open waters of the central North Pacific. Since October 1988, full ocean
481 depth profiles of DIC and TA have been analyzed, and direct measurements of pH have been made over
482 most of this longest-running Pacific Ocean time-series study.

483 The program is based on shipboard observations and experiments conducted on ~10 expeditions per annum

484 The program is based on

485 shipboard observations and experiments conducted on ~10 expeditions per annum to Station ALOHA
486 (22.75°N, 158°W). HOT program background information and details of sampling strategy may be found
487 in Karl and Lukas (1996) and Karl et al. (2001). Results from the HOT CO₂ measurement program can be
488 found in Winn et al. (1994, 1998), Dore et al. (2003, 2009, 2014), and Knor et al. (2023, [2025](#)). The HOT
489 project page, metadata, data streams and data identifiers are listed at [https://www.bco-](https://www.bco-dmo.org/project/2101)
490 [dmo.org/project/2101](https://www.bco-dmo.org/project/2101). A MAPCO₂ system on the Woods Hole Oceanographic Institution Hawaii Ocean
491 Time-series Site mooring (WHOTS; <https://www.soest.hawaii.edu/whots/>) has provided a near-continuous
492 record of surface $p\text{CO}_2$ since 2004, and is anchored by the longer high-accuracy HOT ship-based program
493 (see Sutton et al., 2019 and Knor et al., 2023). A surface ocean data product that includes CO2SYS-
494 calculated values of $p\text{CO}_2$, carbonate mineral saturation states and other derived quantities may be found at
495 <https://hahana.soest.hawaii.edu/hot/hotco2/hotco2.html> and <https://doi.org/10.5281/zenodo.15060930>.

496
497
498 [16|18](#) **ESTOC:** The European Station for Time-series in the Ocean (ESTOC) began carbon dioxide
499 monitoring in October 1995, providing a 30-year record on DIC, TA, and pH. This dataset represents the
500 longest continuous monthly record of warming, rising carbon dioxide levels, and acidification in the eastern
501 North Atlantic (González-Dávila and Santana-Casiano, 2023). ESTOC is located 100 km north of the
502 Canary Islands archipelago (<https://plocan.eu/en/installations/ocean-observatory>). The program includes a
503 ship-based observation system, measuring physical, chemical, and biological [parametersvariables](#)
504 throughout the 3,670-meter water column. It also features a moored platform for surface meteorological
505

506 and oceanic observations as well as subsurface measurements, maintained by the Canary Island Oceanic
507 Platform (PLOCAN, <https://plocan.eu/en>) and the University of Las Palmas de Gran Canaria
508 (<https://iocag.ulpgc.es/research/research-units/quima>). ~~Carbon dioxide~~Carbonate system measurements
509 include full-depth bottle sampling for photometric pH, ~~total alkalinity~~TA, and DIC, conducted monthly
510 from 1995 to 2008, every two months until 2018, and semiannually in recent years due to limited ship time,
511 timed to coincide with moored structure maintenance. ESTOC is also visited every two weeks by a
512 volunteer observing ship, ES-SOOP-CanOA (https://meta.icos-cp.eu/resources/stations/OS_687B), part of
513 the European Research Infrastructure ICOS (<https://www.icos-cp.eu/observations/ocean/stations>), which
514 provides real-time surface data on carbon dioxide fluxes and OA. The program also includes the CO₂-
515 ESTOC oceanographic buoy (<https://meta.icos-cp.eu/labeling/>). The full dataset with DOIs is accessible on
516 Pangaea (González-Dávila and Santana-Casiano, 2023).

517 **17)19) Point B Time-series:** The Point B Time-series documents the carbonate chemistry at a coastal site
518 of the Bay of Villefranche (43.686200N 7.314800E) in Villefranche-sur-mer, France, northwestern
519 Mediterranean Sea. Since January 2007, seawater is sampled weekly at 1 and 50 m, and analyzed for
520 DIC and TA (Kapsenberg et al., 2017). Salinity and temperature
521 are extracted from CTD profiles. Variables of the carbonate system such as pH (total
522 scale) are calculated using the R package seacarb (Gattuso et al., 2021a). Data are available at Pangaea:
523 <https://doi.org/10.1594/PANGAEA.727120> (Gattuso et al., 2021b).

524 **18)20) Ny-Ålesund Time-series:** The Ny-Ålesund Time-series documents the carbonate chemistry at a
525 coastal site of Kongsfjorden, Spitsbergen (78.930660N 11.920030E) during the period 2015-2021. It is the
526 first high-frequency (1 hour), multi-year (6 years) dataset of salinity, temperature,
527 pCO₂, pH, ~~as well as calculated DIC and TA~~ in the High-Arctic Ocean (Gattuso et
528 al., 2023a). Data are available at Pangaea: <https://doi.org/10.1594/PANGAEA.957028> (Gattuso et al.,
529 2023b).

530 **19)21) SPOTS:** The Synthesis Product for Ocean Time-Series (SPOTS) is a ship-based biogeochemical
531 pilot, aiming at regularly providing high quality data from fixed time-series stations with consistent format
532 and semantics (Lange et al., 2024a). The pilot includes data from 12 fixed ship-based time-series programs
533 with a focus on the Global Ocean Observing System's biogeochemical essential ocean variables. These
534 stations represent unique marine environments across a variety of spatiotemporal resolutions and ranges,
535 with data from 1983 to 2021. While implementing the FAIR principles (Wilkinson et al., 2016) and
536 promoting open data, the metadata of the time-series stations ~~were enhanced~~ to interoperate with the IOC-
537 UNESCO Ocean Data and Information System (ODIS). Additionally, an extensive quality assessment
538 resulted in enhanced intra- and inter-station comparability. ~~Altogether, SPOTS' pilot increased the~~
539 ~~readiness of biogeochemical time-series (Lange et al., 2023) and facilitates a variety of applications that~~
540 ~~benefit from the collective value of biogeochemical time-series observations.~~ Data are available at

541 https://www.bco-dmo.org/dataset/896862_with_the_DOI_10.26008/1912/bco-dmo.896862.2 (Lange et al.,
 542 2024b).

543 **20)22) pCO₂ and pH Time-series from 40 Surface Buoys**: Sutton et al. (2019)
 544 established a living dataset comprising 40 individual autonomous moored surface ocean pCO₂ time-series
 545 established between 2004 and 2013, 17 of them also include autonomous pH measurements. These time-
 546 series characterize a wide range of surface ocean carbonate system conditions, across a variety of
 547 environments, including 17 oceanic and 13 coastal locations, as well as 10 coral reefs.
 548 Data are available at OCADS: <https://www.ncei.noaa.gov/data/oceans/ncei/ocads/metadata/0173932.html>
 549 Data are available at OCADS:
 550 <https://www.ncei.noaa.gov/data/oceans/ncei/ocads/metadata/0173932.html> (Sutton et al., 2018).
 551 Additionally, there is a dedicated webpage for this project at OCADS:
 552 <https://www.ncei.noaa.gov/access/ocean-carbon-acidification-data-system/oceans/Moorings/ndp097.html>.

553 **Table 2. Time-series based ocean carbonate chemistry data synthesis products.**

No.	Name	Open or coastal ocean	Surface or water column	Discrete bottle or continuous	Highlights	Reference
16	BATS	Open ocean	Top 4600 m	CTD profiles, discrete bottle data from hydrocast, rate measurements (primary, export and bacterial production), biomass and other biological measurements, underway measurements	One of the longest continuous records of warming, salinification, ocean deoxygenation, and OA in the open ocean	Bates and Johnson (2020, 2023)
17	HOT	Open ocean	Top 4500 m	Discrete Bottle for shipboard measurements; sensor measurements on WHOTS mooring	35+ years of inorganic carbon dynamics in the open waters of the central North Pacific	Dore et al. (2009)
18	ESTOC	Open ocean	Top 3570m	Discrete Bottle for shipboard measurements; sensor measurements on ESTOC mooring	The longest continuous monthly record of warming, rising carbon dioxide levels, and OA in the eastern North Atlantic	González-Davila and Santana-Casiano (2023)
19	Point B Time-series	Coastal ocean	5 and 50 m	CTD profiles, discrete bottle data	Carbonate chemistry at a coastal site of the Bay of Villefranche, France	Kapsenberg et al. (2017)
20	Ny-Ålesund Time-series	Coastal ocean	12 m	CTD, discrete bottle data, sensor measurements at the COSYNA/MOSES-AWIPEV underwater observatory	Carbonate chemistry at a coastal site of Kongsfjorden, Spitsbergen	Gattuso et al. (2023a, b)

21	SPOTS	Open + Coastal	Water column	Discrete	The pilot includes biogeochemical data from 12 fixed ship-based time-series programs	Lange et al. (2024a_b); Lange et al. (2024b)
22	Autonomous pCO ₂ and pH Time-series from 40 Surface Buoys	Open + Coastal	Surface	Continuous	Based on 40 moored surface pCO ₂ time-series, with 17 of them containing pH	Sutton et al. (2019)

554

555 **3.1.3 Gridded and Derived Products – Surface Ocean:**

556 Although cruise data compilations are valuable for making data available in a uniform format, they often are
557 constrained by their sampling strategies and can have significant gaps in space and time. Gridded and derived data
558 products address this limitation by making some variables available at all grid points on a standardized spatial grid
559 and at standardized depth levels through processes such as interpolation and gap filling. This section describes
560 gridded data products that have been derived from observations through interpolation and other gap filling
561 procedures, depicting the surface ocean. Note that this compilation focuses primarily on data products with global
562 coverage, acknowledging that many regional gap-filled products became available in recent years and shall be
563 include in future updates:

564 **21)23) Takahashi Delta $f\text{CO}_2$ and Flux Climatology:** Following on previous climatologies published
565 by the late Taro Takahashi in 1997 and 2009, Fay et al. (2024) created a legacy climatology using his
566 methodology and the updated SOCAT database of observations. This product provides 12 months of delta
567 $f\text{CO}_2$ values and corresponding fluxes for a base year of 2010 at $4^\circ \times 5^\circ$ resolution subsequently subgridded
568 to $1^\circ \times 1^\circ$ resolution and near-global coverage. This climatology represents the mean of ocean conditions
569 over the last four decades and is distinctive relative to many other mechanistic machine learning
570 approaches in that it interpolates in time and space using only the available $f\text{CO}_2$ data and a surface water
571 advection scheme rather than using proxy variables for gap filling. It uses the median of observations to
572 determine a reference year of 2010 and fluxes are provided using air-sea partial pressure differences and
573 inputs from the SeaFlux product (Fay et al., 2021). The climatology product is available at OCADS
574 : <https://www.ncei.noaa.gov/data/oceans/ncei/ocads/metadata/0282251.html>. The
575 related manuscript is available at ESSD: <https://doi.org/10.5194/essd-16-2123-2024> (Fay et al., 2024).

576 **22)24) MPI-ULB-SOM-FFN:** Landschützer et al. (2020a) created a uniform $p\text{CO}_2$ climatology
577 combining open and coastal oceans. It is a monthly gridded global surface ocean $p\text{CO}_2$ data product
578 without adjusting for a specific reference year. Developed on a higher-resolution $0.25^\circ \times 0.25^\circ$ global
579 surface-ocean grid, this product is the result of combining two neural network-based $p\text{CO}_2$ products: the
580 open ocean product described below (i.e., Landschützer et al., 2016) and the coastal product created by
581 Laruelle et al. (2017). Consequently, it represents coastal zones better. Data collected between 1998 and
582 2015 from the SOCAT database (Version 5) were used to create this data product. The merged climatology
583 is available at OCADS:
584 <https://www.ncei.noaa.gov/data/oceans/ncei/ocads/metadata/0209633.html>. Additionally, there is a
585 dedicated web page at OCADS for this project: [https://www.ncei.noaa.gov/access/ocean-carbon-](https://www.ncei.noaa.gov/access/ocean-carbon-acidification-data-system/oceans/MPI-ULB-SOM_FFN_clim.html)
586 [acidification-data-system/oceans/MPI-ULB-SOM_FFN_clim.html](https://www.ncei.noaa.gov/access/ocean-carbon-acidification-data-system/oceans/MPI-ULB-SOM_FFN_clim.html).

587 **23)25) VLIZ-SOM-FFN:** Landschützer et al. (2016) employed the Self-Organizing-Map Feed-Forward
588 Network (SOM-FFN) neural network method (Landschützer et al., 2013) to map sea surface $p\text{CO}_2$ from

589 SOCAT (see No. 1 above) (Bakker et al., 2014) to generate monthly $p\text{CO}_2$ fields on a $1^\circ \times 1^\circ$ global
590 surface ocean grid, covering the period from 1982 to near present. It is based on the gridded $p\text{CO}_2$
591 measurements from SOCAT and is updated regularly. The creation of the $p\text{CO}_2$ fields involve a two-step
592 neural network approach, which has been extensively detailed and validated in previous works by
593 Landschützer et al. (2013, 2014, 2016). In the initial step, the global ocean is clustered into biogeochemical
594 provinces, and subsequently, the non-linear relationship between CO_2 driver variables and gridded data
595 from SOCAT (Bakker et al., 2016) is reconstructed. Air-sea CO_2 fluxes are also computed based on the air-
596 sea $p\text{CO}_2$ difference, utilizing a bulk gas transfer formulation as described by Landschützer et al. (2013,
597 2014, 2016). The product is available at OCADS ([DOI: "10.7289/v5z899n6"](https://doi.org/10.7289/v5z899n6)):
598 <https://www.ncei.noaa.gov/data/oceans/ncei/ocads/metadata/0160558.html>. Additionally, there is a
599 dedicated page at OCADS for this project: [https://www.ncei.noaa.gov/access/ocean-carbon-acidification-
600 data-system/oceans/SPCO2_1982_present_ETH_SOM_FFN.html](https://www.ncei.noaa.gov/access/ocean-carbon-acidification-data-system/oceans/SPCO2_1982_present_ETH_SOM_FFN.html).

601 **24)26) JMA-MLR:** Iida et al. (2021) developed a monthly data product for inorganic carbonate
602 variables on a $1^\circ \times 1^\circ$ global surface ocean grid for the period 1993–2018. Variables include
603 [DIC](#), [TA](#), $p\text{CO}_2$, sea-air CO_2 flux, pH, and
604 Ω_{arag} . They leveraged data products such as SOCAT.v2019 (Bakker et al., 2016)
605 and GLODAPv2.2019 (Olsen et al., 2019), as well as satellite-based variables, including sea-surface
606 dynamic height (SSDH), mixed layer depth (MLD), and chlorophyll-a. The product is updated annually
607 using the latest SOCAT and GLODAPv2 data. The data product can be accessed at:
608 https://www.data.jma.go.jp/kaiyou/english/co2_flux/co2_flux_data_en.html.

609 **25)27) OceanSODA-ETHZ:**
610 (a) **OceanSODA-ETHZv1** is a monthly gridded global surface ocean data product for multiple ocean
611 carbonate system variables, including [DIC](#), [TA](#),
612 $p\text{CO}_2$, pH (total scale),
613 Ω_{arag} , and Ω_{calc} (Gregor and Gruber, 2020; Gregor and Gruber, 2021; Gregor and Gruber, 2023; Ma et al.,
614 2023). This dataset is structured on a $1^\circ \times 1^\circ$ global surface ocean grid with monthly resolution from 1982–
615 2022, facilitating research on OA over seasonal to decadal scales. The OceanSODA-ETHZ data product
616 was created by extrapolating in time and space the surface ocean observations of $f\text{CO}_2$ from SOCATv2022
617 (Bakker et al., 2016) and TA from GLODAPv2.2022 using the newly developed Geospatial Random
618 Cluster Ensemble Regression (GRaCER) method (Gregor, 2021). TA and $p\text{CO}_2$ were then used to calculate
619 the remaining [variables](#) of the marine carbonate system with the PyCO2SYS software
620 (Humphreys et al., 2022). Phosphate and silicate from [WOA_2018](#) product were used
621 (Boyer et al., 2018; Garcia et al., 2018a). The OceanSODA-ETHZ data product is available at OCADS
622 : [https://www.ncei.noaa.gov/data/oceans/ncei/ocads/
623 metadata/0220059.html](https://www.ncei.noaa.gov/data/oceans/ncei/ocads/metadata/0220059.html).

624 (b) **OceanSODA-ETHZv2** is a surface $f\text{CO}_2$ product with a $0.25^\circ \times 0.25^\circ$ spatial resolution and an 8-day
625 temporal resolution, providing estimates starting from 1982 (Gregor et al., 2024a; Gregor et al., 2024b).
626 The high-resolution outputs are suitable for investigating the shorter- and finer-scale dynamics of surface
627 $f\text{CO}_2$. Despite sharing a name with its predecessor, OceanSODA-ETHZv2 does not provide TA estimates
628 and employs a different methodology, as described in the following steps: 1) The atmospheric trend of CO_2
629 is removed by subtracting marine boundary layer CO_2 concentrations from SOCAT $f\text{CO}_2$ producing a new
630 target $\Delta^*\text{CO}_2$ to reduce the biases at the start and end of the time-series. 2) An 8-day seasonal climatology
631 of $\Delta^*\text{CO}_2$ is estimated using Gradient Boosted Decision Trees (GBDT), which is later used as a predictor.
632 3) The non-seasonal thermal component is removed from $\Delta^*\text{CO}_2$, resulting in a new target, $\Delta^*\text{CO}_2^{\text{nonT}}$. 4)
633 The new target is estimated using a feed-forward neural network, with the GBDT as one of the forcing
634 variables. 5) Steps 4 through to 1 are inverted to arrive at $f\text{CO}_2$. 6) Air-sea CO_2 fluxes are computed using
635 ERA5 winds. Data are available at <https://doi.org/10.5281/zenodo.11206365> and are updated annually.

636 **26)28) LDEO-HPD $f\text{CO}_2$:** The LDEO Hybrid Physics Data (LDEO-HPD) estimates the
637 temporal evolution of surface ocean $f\text{CO}_2$ and air-sea CO_2 exchange, utilizing the strengths of observations
638 and global ocean biogeochemical models (GOBMs) (Gloege et al., 2022). GOBMs are internally
639 consistent, mechanistic representations of the ocean circulation and carbon cycle, and have long been the
640 standard for making spatiotemporally resolved estimates of air-sea CO_2 fluxes. However, there is often a
641 bias between the modelled $f\text{CO}_2$ and available surface ocean measurements (Fay and McKinley 2021). The
642 LDEO-HPD approach trains an eXtreme Gradient Boosting (XGB) algorithm to learn a non-linear
643 relationship between model-data $f\text{CO}_2$ mismatch and observed predictor variables: [sea surface temperature](#)
644 ([SST](#)), [sea surface salinity](#) (SSS), chlorophyll concentration, mixed layer depth). The GOBM $f\text{CO}_2$ is then
645 corrected with the predicted model-data misfit to estimate real-world $f\text{CO}_2$ for the observation period
646 (Gloege et al., 2022). This results in reconstructed monthly surface ocean $f\text{CO}_2$ and air-sea CO_2 fluxes on a
647 $1^\circ \times 1^\circ$ grid in the open ocean beginning in 1982. Additional information can be found at
648 oceanarbon.ldeo.columbia.edu. The data product is available at: <https://zenodo.org/records/4760205>.

649 **27)29) LDEO-HPD product with Extended Temporal Coverage:** Building on the work of Gloege et
650 al. (2022), the LDEO-HPD product as mentioned above (No. 28) can be extended back in time to predict
651 $f\text{CO}_2$ for all available model years. Bennington et al. (2022a) find that the largest component of the GOBM
652 corrections is climatological. The smaller corrections at other timescales suggest either that these are well
653 captured by the GOBMs or the data are insufficient. The dominance of climatological corrections supports
654 the extension of the LDEO-HPD $f\text{CO}_2$ product backwards in time. A climatology of model-observation
655 misfits for the best-observed period (2000–present) is applied to the GOBMs for 1959–1981, while an
656 inter-annually varying correction is used for 1982 onward. (Bennington et al., 2022a). This results in
657 reconstructed monthly surface ocean $f\text{CO}_2$ and air–sea CO_2 fluxes on a $1^\circ \times 1^\circ$ grid covering the open
658 ocean, beginning in 1959. Since 2022, the LDEO-HPD Back in Time product has been included in the

659 annual release of the Global Carbon Budget (GCB). Additional information can be found at
660 ocean.carbon.ldeo.columbia.edu. The data product can be accessed via Zenodo at
661 <https://zenodo.org/records/13891722>.

662 **28)30) LDEO $f\text{CO}_2$ - Residual Method:** A frequently used approach for estimating full-coverage $f\text{CO}_2$ is
663 to train a machine learning algorithm on sparse in situ $f\text{CO}_2$ data and associated physical and
664 biogeochemical observations. While these associated variables have well-known relationships to $f\text{CO}_2$, it is
665 often unclear how they mechanistically drive $f\text{CO}_2$ around the world. The LDEO $f\text{CO}_2$ -Residual method
666 takes the basic approach and enhances connections between physical understanding and reconstructed
667 $f\text{CO}_2$. The novel approach used here includes applying pre-processing to the $f\text{CO}_2$ data to remove the direct
668 effect of temperature – a relationship well-documented in literature and lab experiments (Takahashi et al.,
669 2002). This enhances the biogeochemical/physical component of $f\text{CO}_2$ in the target variable (now $f\text{CO}_2$ -
670 Residual) and reduces the complexity that the machine learning must disentangle. The resulting algorithm
671 has physically understandable connections between input data and the output biogeochemical/physical
672 component of $f\text{CO}_2$ (Bennington et al., 2022b). This results in reconstructed monthly surface ocean $f\text{CO}_2$
673 and air–sea CO_2 fluxes on a $1^\circ \times 1^\circ$ grid covering the open ocean, beginning in 1982 and extended to the
674 most recent year of available data. Additional information can be found at ocean.carbon.ldeo.columbia.edu.
675 The data product can be accessed via Zenodo at <https://zenodo.org/records/13941548>.

676 **29)31) CMEMS-LSCE Surface Ocean Carbonate Data Products:**

677 (a) **CMEMS-LSCEv1:** Monthly surface ocean $p\text{CO}_2$ and air–sea CO_2 fluxes on a $1^\circ \times 1^\circ$ grid in both the
678 open ocean and coastal seas from 1985–2019 were reconstructed by Chau et al., (2022). CMEMS-LSCE is
679 short for Copernicus Marine Environment Monitoring Service - Laboratoire des Sciences du Climat et de
680 l'Environnement. This product is generated from an ensemble-based reconstruction of $p\text{CO}_2$ maps trained
681 with gridded data from SOCATv2020 (Bakker et al., 2016). Sea-surface $p\text{CO}_2$ values (converted from the
682 original $f\text{CO}_2$ values in SOCATv2020) were regressed against a set of predictors with non-linear functions,
683 i.e., feed-forward neural network (FFNN) models. The predictors include: sea-surface height (SSH), SST,
684 SSS, MLD, chlorophyll a (Chl-a), atmospheric CO_2 mole fraction ($x\text{CO}_2$), and geographical coordinates
685 (longitudes and latitudes). This data product is accessible at:
686 <https://data.ipsl.fr/catalog/srv/eng/catalog.search#/metadata/a2f0891b-763a-49e9-af1b-78ed78b16982>.

687 (b) **CMEMS-LSCEv2:** CMEMS-LSCEv2 corresponds to the latest version of the CMEMS-LSCE FFNN.
688 It uses the same ensemble-based reconstruction method for $p\text{CO}_2$ maps as CMEMS-LSCEv1.
689 Improvements include downscaling the spatial resolution to $0.25^\circ \times 0.25^\circ$ and reproducing additional
690 surface ocean carbonate system variables on a global grid from 1985 onwards (Chau et al., 2024a). The
691 additional surface ocean carbonate system variables are: $p\text{CO}_2$, DIC, TA, pH, and saturation states with
692 respect to aragonite (Ω_{arag}) and calcite (Ω_{calc}). Surface ocean $p\text{CO}_2$ is reconstructed based on an ensemble of
693 neural network models mapping gridded observation-based data provided by SOCATv2022 (Bakker et al.,

694 2016). Surface ocean TA is estimated with a multiple linear regression approach (Carter et al., 2016, 2017).
695 The remaining carbonate variables are calculated from $p\text{CO}_2$ and TA using a MATLAB version of
696 CO2SYS (Lewis and Wallace, 1998; Van Heuven et al., 2011). The CMEMS-LSCE product is updated
697 yearly for surface ocean $p\text{CO}_2$, air-sea fluxes, and the carbonate system variables. Updates are phased with
698 release of the SOCAT database. For surface ocean $p\text{CO}_2$ and air-sea fluxes the temporal coverage is
699 extended to the present date with a latency of 1 month (Chau et al., 2024b). Both the multi-year
700 reconstruction and the near-real time prediction can be accessed through the CMEMS portal:
701 <https://doi.org/10.48670/moi-00047>.

702 **30)32) CarboScope (Jena-MLS):** The Jena Mixed-Layer Scheme (within the CarboScope family of
703 data-based estimates of carbon-cycle variability) is based on observed sea surface $p\text{CO}_2$ from
704 SOCAT (see above No. 1) (Bakker et al., 2014). It provides daily global fields of $p\text{CO}_2$
705 and sea-air CO_2 fluxes from 1957 to the year before present, on a resolution of $2.5^\circ \times 2^\circ$ degrees. In the
706 original method (Rödenbeck et al, 2013), a diagnostic model of the carbon balance in the ocean mixed layer
707 is being fitted to the $p\text{CO}_2$ data, by adjusting the ocean-interior sources and sinks of carbon of the mixed
708 layer. The multi-decadal trend is derived from the data-based Ocean Circulation Inverse Model (OCIM)
709 estimate provided by DeVries (2022b). Since a later extension described in Rödenbeck et al. (2022),
710 the variability in the ocean-interior sources and sinks is first regressed against variability in SST and wind
711 speed. The regression step is followed by a correction step with explicit temporal variability, to also
712 represent data variability not yet represented by the predictors of the regression. The CarboScope product is
713 updated yearly. The results from current and previous releases can be downloaded from [https://www.bgc-](https://www.bgc-jena.mpg.de/CarboScope/)
714 [jena.mpg.de/CarboScope/](https://www.bgc-jena.mpg.de/CarboScope/).

715 **31)33) UOEx-Watson:** This product is an estimate of the atmosphere-ocean flux of CO_2 that takes into
716 account near-surface temperature deviations (Watson et al., 2020). Most estimates use data on surface
717 ocean $p\text{CO}_2$ without considering corrections due to temperature gradients within the uppermost few
718 millimeters of the sea surface (“Skin temperature effects”) or small effects due to changes in temperature
719 that occur during sampling and measurement, especially when the measurement is from a commercial
720 vessel rather than a research ship. This product takes these effects into account by recalculating $p\text{CO}_2$ from
721 the SOCAT data base (v2019) using co-located satellite observations of skin temperature. The result is a
722 substantial increase in the calculated net global uptake of CO_2 . In other respects, the methodology for this
723 data product follows the two-step neural network approach described by Landschützer et al. (2013, 2014).
724 The gridded data set of sea surface $f\text{CO}_2$ adjusted to satellite-derived subskin surface temperature, is
725 available at <https://doi.org/10.1594/PANGAEA.905316>. Ocean-atmosphere fluxes interpolated to monthly
726 and $1^\circ \times 1^\circ$ spatial resolution is available at OCADS:
727 <https://www.ncei.noaa.gov/data/oceans/ncei/ocads/metadata/0301544.html>.

728 **32)34) NIES-ML3:** The National Institute for Environmental Studies (NIES-ML3) product includes

729 monthly global surface ocean $f\text{CO}_2$ in 1982-2023 on a $1^\circ \times 1^\circ$ grid. Using a leave-one-year-out (LOYO)
730 validation method and three machine learning models, Zeng et al. (2022) found that the time variant trends
731 of ocean CO_2 could be estimated approximately by a harmonic function fitting of the annual atmospheric
732 CO_2 . They removed the estimated trends from the ocean CO_2 and applied the LOYO to the trend-removed
733 data to obtain the trend that could not be approximated by the fitting for trend correction. The trend-
734 removed data by the corrected trends were used to train the models. The gap-filled CO_2 maps were
735 constructed by adding the trends to model predictions. The product is available at NIES:
736 <https://doi.org/10.17595/20220311.001> (Zeng 2022).

737 **33)35) CSIR-ML6:** Provides monthly $1^\circ \times 1^\circ$ estimates of surface $p\text{CO}_2$ (Gregor et al., 2019a). The
738 approach uses the conceptual two-step approach of clustering and performing regressions for each cluster
739 as Landschützer et al. (2016). CSIR-ML6 investigates the efficacy of various machine learning (ML)
740 methods in estimating surface $p\text{CO}_2$, namely, feed-forward neural networks (FFNN), extremely
741 randomized trees (ERT), gradient boosting machines (GBM), and support vector regression (SVR). It is
742 found that the ensemble of all but the ERT method resulted in the best estimate, highlighting the fact that
743 various ML methods do not produce the same outcome, particularly when data is sparse. Further, the
744 variance between ensemble members can inform us about regions where uncertainty may be large due to
745 methodological differences. Despite this, all methods achieve roughly the same uncertainty – a barrier, or
746 wall beyond which the community has yet to overcome. The data are available at OCADS
747 : <https://www.ncei.noaa.gov/data/oceans/ncei/ocads/metadata/0206205.html>
748 (Gregor et al., 2019b). The product is one of the six ensemble members of the SeaFlux dataset.

749 **34)36) Stepwise-FFNN:** Zhong et al. (2022) constructed a monthly global $1^\circ \times 1^\circ$ surface ocean $p\text{CO}_2$
750 product from January 1992 to December 2024, by combining the stepwise regression algorithm and a feed-
751 forward neural network (FFNN) to select predictors of $p\text{CO}_2$ based on the mean absolute error in each of
752 the 11 biogeochemical provinces defined by the self-organizing map (SOM) method. The methodology for
753 this data product used regionally optimal predictors to account for differences in $p\text{CO}_2$ drivers, lowering
754 local biases relative to a single global predictor set. The developed data product is available at:
755 <http://dx.doi.org/10.12157/IOCAS.20250814.001>.

756 **35)37) AOML-ET:** Wanninkhof et al. (2024, 2025) developed a monthly global ocean data product of
757 seawater $p\text{CO}_2$ and sea-air CO_2 fluxes, referred to as AOML-ET, using an extremely randomized trees (ET)
758 machine learning technique. These maps are created on $1^\circ \times 1^\circ$ spatial grids, providing global surface
759 ocean coverages from 1998 to 2023. AOML-ET incorporates several predictor variables, including time,
760 location, SST, SSS, MLD, and chlorophyll-a. The model was trained using the v2020 and v2023 releases of
761 the SOCAT data product (No. 1). Sea-air CO_2 fluxes were calculated using the air-sea CO_2 [partial pressure](#)
762 [difference \(\$\Delta p\text{CO}_2\$ \)](#) and a bulk gas transfer formulation incorporating windspeed. The dataset contains
763 monthly $1^\circ \times 1^\circ$ NetCDF files of the AOML-ET outputs, along with the predictor variables. The data are

764

available at OCADS (DOI: "10.25921/0s8y-q287");

765

<https://www.ncei.noaa.gov/data/oceans/ncei/ocads/metadata/0298989.html> (Wanninkhof et al., 2024).

766 **38) ULB-SOM-FFN-Coastalv2.1:** Roobaert et al. (2024) present high-resolution ($0.25^\circ \times 0.25^\circ$ grid) monthly
767 maps showing the distribution of sea surface $p\text{CO}_2$ across the global coastal oceans, spanning from 1982 to
768 2020. This product (ULB-SOM-FFN-coastalv2.1) builds upon the work by Laruelle et al. (2017),
769 incorporating a two-step methodology that utilizes Self Organizing Maps (SOM) and Feed Forward
770 Networks (FFN). This updated product now captures temporal variability, enabling the assessment of
771 interannual variability and long-term trends in coastal air-sea CO_2 exchange, unlike the product by Laruelle
772 et al. (2017), which only offers a climatology for a short period (1998-2015). The enhancements include
773 additional environmental predictors and an expanded dataset for training and validation, featuring
774 approximately 18 million direct coastal observations from the SOCAT database,
775 specifically the SOCATv2022 release (Bakker et al., 2016). The product is available at OCADS
776 : <https://www.ncei.noaa.gov/data/oceans/ncei/ocads/metadata/0279118.html>
777 (Roobaert et al., 2023).

778 **36)39) RFR-LME:** Sharp et al. (2024a) developed a data product delineating the temporal trends of OA
779 indicators mapped on a $0.25^\circ \times 0.25^\circ$ spatial grid, across eleven U.S. Large Marine Ecosystems (LMEs),
780 with monthly coverage from 1998–2023. These indicators, which include the $p\text{CO}_2$, pH, Ω_{arag} , DIC, TA,
781 Revelle Factors, among others, were derived from SOCATv2023, along with other oceanographic
782 properties, e.g., SST, SSS, SSH, and MLD. The methodology combined Gaussian Mixture Models to
783 categorize the data into environmentally similar subregions, Random Forest Regressions for the spatial and
784 temporal extrapolation of observational $f\text{CO}_2$ data, and regressions to estimate TA (Carter et al., 2021) to
785 provide a second carbonate system constraint. The resulting maps are available at OCADS
786 : <https://www.ncei.noaa.gov/data/oceans/ncei/ocads/metadata/0287551.html> (Sharp
787 et al., 2024b), while an online portal at <https://ecowatch.noaa.gov/thematic/ocean-acidification> presents
788 regionally averaged time-series for three key indicators: $p\text{CO}_2$,
789 Ω_{arag} , and pH.

790 **37)40) ReCAD-NAACOM- $p\text{CO}_2$:** Wu et al. (2025) developed a reconstructed $p\text{CO}_2$ product for the
791 North American Atlantic Coastal Ocean Margins (NAACOM), spanning from the Gulf of Mexico/Gulf of
792 America to the Grand Banks, called the Reconstructed Coastal Acidification Database- $p\text{CO}_2$ (ReCAD-
793 NAACOM- $p\text{CO}_2$). This product employed a two-step approach combining random forest regression and
794 linear regression to generate monthly $p\text{CO}_2$ data at 0.25° spatial resolution from 1993–2021. The model
795 was trained using SOCAT v2023 observations as ground-truth values, incorporating various satellite-
796 derived and reanalysis environmental variables known to influence sea surface $p\text{CO}_2$. ~~The ReCAD-
797 NAACOM- $p\text{CO}_2$ product demonstrates robust performance, with a coefficient of determination of 0.83, a
798 root-mean-square error of $18.64 \mu\text{atm}$, and an accumulative uncertainty of $23.83 \mu\text{atm}$ when compared
799 against all SOCAT observation samples. This high accuracy was maintained across model training and
800 validation phases. The model exhibits robust performance when validated against independent test data~~

801 from a period excluded from both training and validation, underscoring the product's capability to reliably
802 reconstruct $p\text{CO}_2$ in periods lacking direct observational data within the NAACOM. Significantly, the
803 product enables detailed investigation of regional spatial differences, seasonal cycles, and decadal changes
804 in $p\text{CO}_2$ across the NAACOM. The ReCAD-NAACOM- $p\text{CO}_2$ dataset is publicly accessible
805 (<https://doi.org/10.5281/zenodo.11500974>) and will be updated regularly.

806 **38)41) Gridded Surface OA Indicators in the Northern Caribbean Sea:**

807 This dataset contains a high-quality dataset of derived products from over a million observations of surface
808 water partial pressure/fugacity of carbon dioxide ($p\text{CO}_2\text{w}/f\text{CO}_2\text{w}$), for the Caribbean Sea, Gulf of
809 Mexico/Gulf of America and North-West Atlantic Ocean covering the timespan from 2002-01-01 to 2019-
810 12-30. The derived quantities include TA, acidity (pH), Ω_{arag}
811 and air-sea CO_2 flux (Wanninkhof et al., 2020). This data product is available at OCADS:
812 <https://www.ncei.noaa.gov/data/oceans/ncei/ocads/metadata/0207749.html> (Wanninkhof et al., 2019)

813 **39)42) OA Data in the Gulf of Mexico/Gulf of America and Wider Caribbean:** The Acidification,

814 Climate, and Coral Reef Ecosystems Team (ACCRETE) Lab within AOML's Ocean Chemistry and
815 Ecosystems Division (OCED) developed a data product for tracking OA in the Caribbean and Gulf of
816 Mexico/Gulf of America from 2014 to 2020 (van Hooijdonk, 2022). Utilizing satellite imagery and a data-
817 assimilative hybrid model, the tool maps key indicators of the water's carbonate system, including $p\text{CO}_2$,
818 TA, pH, Ω_{arag} , and Ω_{calc} . This innovation builds upon an update to the experimental OA Product Suite
819 (OAPS) developed by NOAA's Coral Reef Watch. The data product is available at OCADS:
820 <https://www.ncei.noaa.gov/data/oceans/ncei/ocads/metadata/0245950.html> (van Hooijdonk, 2022).

821 **40)43) $p\text{CO}_2$ Climatology of the Baltic Sea:** Bittig et al. (2024) used biogeochemical model
822 output to inform the mapping of sea surface $p\text{CO}_2$ observations in the Baltic Sea and to build a mean
823 monthly climatology for the period 2003 to 2021, with spatial resolutions of $0.10^\circ \times 0.05^\circ$ (approximately 3
824 nautical miles in both directions). In a first step, spatial patterns of
825 variability were extracted from 20 years of model surface $p\text{CO}_2$ data by an EOF analysis. These spatial
826 patterns were then used to map surface $p\text{CO}_2$ observations from SOCAT (see
827 above No. 1) (Bakker et al., 2014) onto the Baltic Sea domain. By using an ensemble approach with
828 varying number of EOF patterns, the spatial scales of the mapping were locally adjusted based on the
829 observation's data density. Mapped monthly fields of $p\text{CO}_2$ from 2003-2021 were combined for the product
830 into a mean monthly climatology and a spatially-resolved linear trend. The climatology product is available
831 at PANGAEA: <https://doi.org/10.1594/PANGAEA.961119> (Bittig et al., 2023).

832 **41)44) INCOIS-ReML:** The Indian National Centre for Ocean Information Services-Regional Machine
833 Learning model (INCOIS-ReML) $p\text{CO}_2$ data product offers machine learning based monthly climatological
834 sea surface $p\text{CO}_2$ and the corresponding air-sea CO_2 flux for the Bay of Bengal (Joshi et al., 2024). This

835 data product integrates publicly available open-ocean observations with data from the Indian Exclusive
 836 Economic Zone. This high-resolution ($0.083^\circ \times 0.083^\circ$) monthly climatological $p\text{CO}_2$ data product is
 837 available from the INCOIS Portal: <https://las.incois.gov.in>, and from OCADS (~~DOI: "10.25921/2sjr-~~
 838 ~~pg16"~~, ~~link: <https://www.ncei.noaa.gov/data/oceans/ncei/ocads/metadata/0307627.html>~~) (Joshi et al.,
 839 2025a).

840 [42/45](#) **INCOIS_TA**: The Indian National Centre for Ocean Information Services-Total Alkalinity
 841 (INCOIS_TA) data product offers a machine learning based monthly interannual surface ~~Total~~
 842 ~~Alkalinity~~TA from 1993-2020 for the North Indian Ocean (Joshi et al., 2025b). This data product integrates
 843 publicly available open-ocean observations with data collected during Indian scientific expeditions and
 844 from the Indian Exclusive Economic Zone. This high-resolution ($0.083^\circ \times 0.083^\circ$) long-term monthly TA
 845 data product is available from the INCOIS Portal: <https://las.incois.gov.in>, and from OCADS (~~DOI:~~
 846 ~~"10.25921/7as7-et15"~~, ~~link: <https://www.ncei.noaa.gov/data/oceans/ncei/ocads/metadata/0307789.html>~~
 847 (Joshi et al., 2025c).

Field Code Changed

848 **Table 3. Gridded and derived ocean carbonate chemistry data synthesis products in the surface ocean.**

No.	Name	Open or coastal ocean	Spatial resolution	Temporal resolution	Methodology	Highlights	Reference
23	Takahashi Delta $f\text{CO}_2$ and Flux Climatology	Open ocean	$1^\circ \times 1^\circ$	12-month climatology for a base year referenced to 2010	Advection Scheme	Does not use proxy variables for extrapolation. Only produced as monthly climatology.	Fay et al. (2024)
24	MPI-ULB-SOM-FFN	Open + Coastal	$0.25^\circ \times 0.25^\circ$	12-Month climatology (January through December) without a reference year	2-step machine learning: Merged product of the SOM-FFN approach applied to the open ocean (Landschützer et al., 2016) and the coastal ocean (Laruelle et al., 2017)	Monthly gridded $p\text{CO}_2$ without adjusting for a specific reference year, high-resolution coastal ocean coverage	Landschützer et al. (2020a)
25	VLIZ SOM-FFN	Open ocean	$1^\circ \times 1^\circ$	Monthly from January 1982 onwards	2-step machine learning: Self organizing map clustering followed by a feed forward network (SOM-FFN)	Monthly gridded $p\text{CO}_2$ from 1982 through near present	Landschützer et al. (2016)
26	JMA-MLR	Open ocean	$1^\circ \times 1^\circ$	Monthly from January 1990 onwards	Multiple linear regressions	Temporal trends of DIC, TA, $p\text{CO}_2$, air-sea CO_2 flux, pH, and Ω_{arag}	Iida et al. (2021)

27(a)	OceanSODA-ETHZv1	Open ocean	1° × 1°	Monthly from 1982 to 2023	Ensemble of 2-step members: K-means clustering with gradient boosting and SVR regression	Temporal trends of DIC, TA, pCO ₂ , pH, Ω _{arag} , and Ω _{calc}	Gregor and Gruber (2021)
27(b)	OceanSODA-ETHZv2	Open + Coastal ocean	0.25° × 0.25°	8-day from 1982 to 2022	FFNN	Highlighting fine-scale and short-term variability of the ocean carbon sink	Gregor Shutler, and Gruber et al. (2024a, b)
28	LDEO-HPD fCO ₂ -product	Open ocean	1° × 1°	Monthly from 1982	XGBoost algorithm	Temporal evolution of surface ocean fCO ₂ and air-sea CO ₂ exchange	Gloege et al. (2022)
29	LDEO-HPD with Extended Temporal Coverage	Open ocean	1° × 1°	Monthly from 1959	XGBoost algorithm	Uses model-data misfit climatology to extend estimate back in time to 1959	Bennington et al. (2022a)
30	LDEO fCO ₂ - Residual Method	Open ocean	1° × 1°	Monthly from 1982	XGBoost algorithm	Removes the temperature component before ML	Bennington et al. (2022b)
31(a)	CMEMS-LSCEv1	Open + Coastal	1° × 1°	Monthly from 1985 to 2019	FFNN	Seamless reconstruction from coastal to open ocean	Chau et al. (2022)
31(b)	CMEMS-LSCEv2	Open + Coastal	0.25° × 0.25°	Monthly from 1985 to 2025 ⁴	FFNN	Yearly extension of time-series & monthly reconstruction at low latency	Chau et al. (2024a, b)
32	CarboScope (Jena-MLS)	Open ocean	2.5° × 2°	Daily from 1957	Multi-linear regression against long-term predictors, plus auto-regressive correction	Variability of pCO ₂ and sea-air CO ₂ fluxes since 1957, sensitivities to SST and wind speed variations	Rödenbeck et al. (2022)
33	UOEx-Watson	Open ocean	1° × 1°	Monthly from January 1992	Two-step neural network approach described by Landschützer et al. (2013, 2014, 2016)	Air-sea fluxes of CO ₂ with adjusted skin temperature effect	Watson et al., 2020
34	NIES-ML3	Open ocean	1° × 1°	Monthly from 1982 to 2023	FNN, GBM, RF	The prediction of a ML method was obtained from ten trainings with different seeds. The mean of the three methods was taken as the final prediction.	Zeng (2022), Zeng et al. (2022)

35	CSIR-ML6	Open ocean	$1^\circ \times 1^\circ$	Monthly from 1982 to 2016	Ensemble: FFNN, SVR, ERT, Gradient Boosted Trees	Various ML methods produce different results when data is sparse, but all still achieving roughly the same uncertainty.	Gregor et al. (2019a)
36	Stepwise-FFNN	Open ocean	$1^\circ \times 1^\circ$	Monthly from 1992 to 2024	SOM, FFNN, Stepwise regression	ML-based selection of predictors considering regional differences of $p\text{CO}_2$ drivers	Zhong et al. (2022)
37	AOML-ET	Open ocean	$1^\circ \times 1^\circ$	Monthly from 1998 to 2023	Extremely randomized trees (ET) machine learning technique	Monthly global sea-air CO_2 flux maps in modern era	Wanninkhof et al. (2015)
38	ULB-SOM-FFN-Coastalv2.1	Coastal ocean	$0.25^\circ \times 0.25^\circ$	Monthly from 1982 to 2020	2-step machine learning: Self organizing map clustering followed by a feed forward network (SOM-FFN)	Global temporal trends of coastal $p\text{CO}_2$ and air-sea CO_2 fluxes based on SOCATv2022 with data collected from 1982–2020	Roobaert et al. (2024)
39	RFR-LME	Coastal ocean	$0.25^\circ \times 0.25^\circ$	Monthly from 1998 to 2023	Gaussian mixture models and random forest regressions	Temporal trends of OA indicators and estimated uncertainties across 11 U.S. Large Marine Ecosystems (LMEs), with monthly coverage from 1998–2023.	Sharp et al. (2024a)
40	ReCAD-NAACOM- $p\text{CO}_2$	Coastal ocean	$0.25^\circ \times 0.25^\circ$	Monthly from 1993 to 2021	2-step machine learning: random forest regression followed by linear regression	Sea surface $p\text{CO}_2$ in the North American Atlantic Coastal Ocean Margins (NAACOM)	Wu et al. (2025)
41	Gridded Surface OA Indicators and Air-sea CO_2 Fluxes in the Northern Caribbean Sea	Coastal ocean	$1^\circ \times 1^\circ$	Monthly from 2002 to 2019	Gridding of the observations of $f\text{CO}_2$, SST and SSS was performed by binning and averaging the data in ($1^\circ \times 1^\circ$ by month) cells	A 17-year record of $f\text{CO}_2$, TA, pH, Ω_{arag} , and air-sea CO_2 flux in the Caribbean Sea	Wanninkhof et al. (2020)

42	OA data in the Gulf of Mexico/Gulf of America and Wider Caribbean	Regional	$0.088^\circ \times 0.88^\circ$	Monthly from 2014 to 2020	Utilizing satellite imagery and a data-assimilative hybrid model, the tool maps key indicators of the water's carbonate system, including $p\text{CO}_2$, TA, pH, Ω_{arag} , and Ω_{calc} .	A new tool to monitor OA over the wider Caribbean and Gulf of Mexico/Gulf of America.	van Hooidonk (2022)
43	Regional $p\text{CO}_2$ Climatology of the Baltic Sea	Regional	$0.10^\circ \times 0.05^\circ$	12-month climatology for a base year of referenced to 2013; linear trend 2003-2021	Extrapolation using model-based patterns of variability	Does not use proxy variables for extrapolation. Spatial scales adjust locally to data density	Bittig et al. (2024)
44	INCOIS-ReML	Regional	$0.083^\circ \times 0.083^\circ$	Monthly climatology referenced to 2013; linear trend 2003-2021 for this dataset is 2015.	Xtreme Gradient Boosting (XGB) based Machine Learning Model	This data product integrates publicly available open-ocean observations with data from the Indian EEZ region in the Bay of Bengal to provide surface $p\text{CO}_2$ and air-sea CO_2 flux estimates.	Joshi et al. (2024)
45	INCOIS_TA	Regional	$0.083^\circ \times 0.083^\circ$	Monthly from 1993 to 2020	Xtreme Gradient Boosting (XGB) based Machine Learning Model	Integrates publicly available open-ocean observations with data collected during Indian scientific expeditions and from the Indian Exclusive Economic Zone to provide surface TA estimates for the North Indian Ocean.	Joshi et al. (2025b)

849 **3.1.4 Gridded and Derived Products – Interior Ocean:**

850 This section describes gridded data products that have been derived from observations through interpolation and other
851 gap filling procedures, depicting the interior ocean.

852 ~~43~~⁴⁶ ~~Global interior ocean mapped climatology from GLODAPv2~~ **Climatology** (referenced to
853 **2002**): Lauvset et al. (2016) generated a comprehensive set of global interior ocean climatologies, mapping
854 key biogeochemical variables on a $1^\circ \times 1^\circ$ grid for 33 depth levels from surface to 5500 m. These
855 climatologies cover temperature, salinity, ~~DO~~^{oxygen}, nitrate, phosphate, silicate, DIC, TA, pH, ~~and the~~

856 ~~saturation states of aragonite and calcite~~ (Ω_{arag} and Ω_{calc}). This data product was created based on the
857 quality-controlled and internally consistent GLODAPv2.2016 (Olsen et al., 2016) using the data-
858 interpolating variational analysis (DIVA) method (Barth et al., 2014). The conceivably confounding
859 temporal trends in DIC, pH, Ω_{arag} and Ω_{calc} due to anthropogenic influence were removed prior to mapping
860 by normalizing their values to a reference year of 2002 using first-order calculations of anthropogenic
861 carbon accumulation rates. For all variables, all data from the full 1972–2013 period were used, including
862 data that did not receive full secondary quality control. This data product is not updated each year along
863 with the main GLODAPv2 data product. The mapped data product is available at OCADS (~~DOI:~~
864 ~~“10.3334/ediac/otg.ndp093_glodapv2”~~):
865 <https://www.ncei.noaa.gov/data/oceans/ncei/ocads/metadata/0286118.html> (Lauvset et al., 2023a). It can
866 also be accessed from the GLODAP website: <https://glodap.info/>. For reference, the original GLODAP
867 Climatology (Version 1.1) is accessible at:
868 <https://www.ncei.noaa.gov/data/oceans/ncei/ocads/metadata/0001644.html> (Sabine et al., 2004b).

869 **44)47) Aragonite Saturation State Climatology:** Jiang et al. (2015a) developed an
870 interior ocean Ω_{arag} climatology (referenced to 2000), on a $1^\circ \times 1^\circ$ grid at 9 standardized depth levels from
871 the surface down to 4000m. This was accomplished by integrating data from the first version of GLODAP
872 (Key et al., 2004), CARINA (Key et al., 2010), and PACIFICA (Suzuki et al., 2013), along with additional
873 recent cruise datasets up to 2012. Calculations of Ω_{arag} utilized a MATLAB version of the CO2SYS
874 program (Orr et al., 2015), with the dissociation constants for carbonic acid of Lueker et al. [2000],
875 potassium bisulfate (KHSO_4^-) of Dickson [1990], hydrofluoric acid (HF) of Perez and Fraga (1987), and
876 the total borate concentration equations of Lee et al. [2010]. Temporal adjustments were made to a
877 reference year of 2000, accounting for an annual increase of $f\text{CO}_2$ of $1.6 \mu\text{atm}$ in the surface mixed layer
878 (SML), with a rate that decreases linearly to zero $\mu\text{atm yr}^{-1}$ from the bottom of the SML to a depth of 1000
879 m (Sabine et al., 2008). The data product is available at OCADS:
880 <https://www.ncei.noaa.gov/data/oceans/ncei/ocads/metadata/0139360.html> (Jiang et al., 2015b).

881 **48) Mapped Observation-Based Oceanic Dissolved Inorganic Carbon (MOBO-DIC):**

882 **(a) MOBO-DIC (Version 2020):** Kepler et al. (2020) produced a global interior ocean DIC monthly
883 climatology (average climatological values for January through December) on a $1^\circ \times 1^\circ$ grid at 33
884 standardized depth levels from the surface to 2000 m. The MOBO-DIC mapping method adapts and
885 extends the SOM-FFN technique originally introduced by Landschützer et al. (2013). It starts by
886 categorizing the ocean into clusters with comparable physical and biogeochemical characteristics using
887 self-organizing maps (SOM). Subsequently, within each SOM-defined cluster, a feed-forward network
888 (FFN) is employed to estimate and enforce the statistical correlation between the targeted ~~dissolved~~
889 ~~inorganic carbon (DIC)~~ **DIC** data and the predictor data available in globally mapped fields. The product
890 uses data from January 2004 to December 2017, and is thus centered around the years 2010/2011. The data

891 product is available at OCADS (DOI: "10.25921/yvzj-zx46"): [https://www.ncei.noaa.gov/access/ocean-](https://www.ncei.noaa.gov/access/ocean-carbon-acidification-data-system/oceans/ndp_104/ndp104.html)
892 [carbon-acidification-data-system/oceans/ndp_104/ndp104.html](https://www.ncei.noaa.gov/access/ocean-carbon-acidification-data-system/oceans/ndp_104/ndp104.html).

893 **(b) MOBO-DIC (Version 2023):** Keppler et al. (2023a) extended the temporal resolution of MOBO-DIC
894 to resolve monthly fields from January 2004 to December 2019, as opposed to the average climatological
895 values in Keppler et al. (2020). This data product is on a $1^\circ \times 1^\circ$ grid at 28 depth levels from the surface to
896 1500 m. The data product is available at OCADS:

897 <https://www.ncei.noaa.gov/data/oceans/ncei/ocads/metadata/0277099.html> (Keppler et al., 2023b).

898 **45)49) Monthly Interior Ocean TA Climatology:** Broullón et al. (2019) developed a monthly
899 global interior ocean TA climatology using a feed-forward neural network approach. This dataset offers a
900 spatial resolution of $1^\circ \times 1^\circ$ in the horizontal, spans 102 depth levels (ranging from 0–5500 m) in the
901 vertical dimension, and features a temporal resolution that varies from monthly (0–1500 m) to annual
902 (1550–5500 m). The development of this climatology was based on the analysis of TA in relation to several
903 key predictor variables, including temperature, salinity, nutrients (phosphate, nitrate, and silicate), DO, and
904 sampling position (coordinates and depth), as outlined in Velo et al. (2013). Both TA and these predictor
905 variables were sourced from GLODAPv2 (version 2016) (Olsen et al., 2016). The global interior ocean TA
906 climatology was constructed by leveraging the established relationships between TA and the predictor
907 variables, as well as the monthly climatologies of temperature, salinity, and DO from the
908 [WOA](#) 2013 (Locarnini et al., 2013; Zweng et al., 2013; Garcia et al., 2014), and nutrients
909 data that were obtained through the CANYON-B neural network process, applied to the previously
910 mentioned fields. The data product is available at OCADS:

911 <https://www.ncei.noaa.gov/data/oceans/ncei/ocads/metadata/0222470.html> (Broullón et al., 2020b).

912 **46)50) Monthly Global Interior Ocean DIC Climatology:** Broullón et al. (2020a) employed a feed-
913 forward neural network approach to create a monthly global interior ocean DIC climatology, centered
914 around the year 1995. This dataset offers a $1^\circ \times 1^\circ$ spatial resolution in the horizontal domain,
915 encompassing 102 depth levels ranging from 0–5500 m vertically. The temporal resolution varies, ranging
916 from monthly (0–1500 m) to annual (1550–5500 m). In contrast to their previous work on TA (Broullón et
917 al., 2019), this analysis includes the variable "year" to account for anthropogenic DIC pool changes. It also
918 incorporates data from the ~~Lamont-Doherty Earth Observatory~~ (LDEO $p\text{CO}_2$ database (Takahashi et al.,
919 2017) alongside GLODAPv2.2019 (Olsen et al., 2019) to establish relationships between DIC and its input
920 variables: temperature, salinity, DO, as well as location, pressure, and time. The DIC climatology was
921 derived using these relationships, along with monthly climatological data for temperature, salinity, and DO
922 from ~~the World Ocean Atlas~~ [WOA](#) 2013 (Locarnini et al., 2013; Zweng et al., 2013; Garcia et al., 2014), as
923 well as phosphate, nitrate, and silicate values computed from the CANYON-B neural network fed with the
924 aforementioned fields. The data product is available at OCADS (DOI: "10.25921/ndgj-jp24"):

925 <https://www.ncei.noaa.gov/data/oceans/ncei/ocads/metadata/0222469.html> (Broullón et al., 2020c).

926 **51) Acidification Metrics in the Ocean Interior:** Fassbender et al. (2023) generated estimates of global
927 interior ocean changes to pH, $[H^+]$, Ω_{org} , pCO_2 , and the Revelle sensitivity factor driven by the
928 accumulation of anthropogenic carbon (C_{ant}) from the preindustrial period to the year 2002, and quantified
929 the component of those changes caused by nonlinearities in the carbonate system. For each OA metric, the
930 dataset includes year 2002 values and quasi-preindustrial values, which were estimated by subtracting C_{ant}
931 from the year 2002 carbonate chemistry information and recomputing each OA metric without considering
932 any warming, circulation, or biological changes that may have occurred since the preindustrial era. Data
933 from the upper 2000 m of the GLODAPv2.2016b mapped data product
934 , described in Lauvset et al., 2016, and from the preformed
935 properties product of Carter et al., 2021 were used to make these estimates on the GLODAPv2.2016b $1^\circ \times$
936 1° grid for 26 depth levels from surface to 2000 m. The provided uncertainties were estimated using a
937 1000-iteration Monte Carlo simulation. Calculation details are described in Fassbender et al. (2023). Year
938 2002 (Ω_{org}) and pH values, and their uncertainties, are reproduced from the
939 GLODAPv2.2016b mapped data product and are provided in this dataset for user convenience with the
940 permission of the original data producer. This data product is available at OCADS
941 : <https://www.ncei.noaa.gov/data/oceans/ncei/ocads/metadata/0290073.html> (Fassbender et al.,
942 [2024](#)).

943 **52) Ocean Interior Acidification Over the Industrial Era:** Building on the total anthropogenic carbon
944 estimates for 1994 from Sabine et al. (2004) and the decadal changes between 1994 and 2014 reconstructed
945 by Müller et al. (2023a), Müller and Gruber (2024a) quantified ocean interior acidification over the
946 industrial era. To convert the increasing anthropogenic carbon concentrations into acidification estimates,
947 their approach relied on time-invariant climatologies of ocean interior DIC, TA, temperature, salinity, and
948 other relevant variables to determine the background state of the marine carbonate system. Hence, their
949 estimates resolve exclusively the acidification driven by the anthropogenic carbon accumulation. In
950 contrast to direct observations of acidification variables, such as those collected at time-series stations, this
951 approach does not account for changes in the natural carbon cycle or the displacement of water masses. The
952 approach by Müller and Gruber (2024a) is conceptually similar to that of Fassbender et al. (2023), but
953 provides temporally resolved estimates, enabling the tracking of both the spatial distribution and temporal
954 evolution of ocean interior acidification. The data product is available at OCADS
955 : <https://www.ncei.noaa.gov/data/oceans/ncei/ocads/metadata/0298993.html> (Müller and Gruber,
956 [2024b](#)).

957 **53) Decadal changes of anthropogenic CO_2 :**

958 **(a) Anthropogenic CO_2 from 1994 to 2007:** Gruber et al. (2019a) estimated the decadal time-scale
959 changes in the oceanic content of anthropogenic CO_2 (ΔC_{ant}) between for the years 1994, 2004, and 2014
960 to 2007. The results have been derived from the GLODAPv2.2016 product (Olsen et al., 2016),

961 utilizing the eMLR(C*) methodology pioneered by Clement and Gruber (2018). [The product is combined](#)
962 [with the estimated amount of C_{ant} for 1994 derived by Sabine et al. \(2004\) from GLODAPv1 to infer C_{ant}](#)
963 [for 2007](#). All estimates are geospatially distributed on a horizontal grid with a resolution of 1° × 1°. Two
964 primary files are available: one providing the complete three-dimensional distribution of ΔC_{ant}, and the
965 other containing vertically integrated values, i.e., the column inventories. This data product is available at
966 OCADS ([DOI: "10.25921/wdn2-pt10"](#)):
967 <https://www.ncei.noaa.gov/data/oceans/ncei/ocads/metadata/0186034.html> (Gruber et al., 2019b).

968 **(b) Decadal Trends in Anthropogenic CO₂ from 1994 to 2014:** Müller et al. (2023_a) extended the
969 analysis by Gruber et al. (2019a) to reconstruct decadal trends in the oceanic storage of
970 ΔC_{ant} in the global ocean interior from [mid-year 1994 to mid-year 2004, and further to mid-year](#)
971 [2014](#). They applied the extended multiple linear regression (eMLR) method (Clement and Gruber, 2018) to
972 ship-borne observations of DIC and other biogeochemical variables from GLODAPv2.2021 (Lauvset et al.,
973 2021). All estimates are provided on a 1° × 1° horizontal grid. Two principal data files are provided: one
974 featuring the comprehensive three-dimensional distribution of ΔC_{ant} [for the two time periods](#), and the other
975 presenting the vertically integrated quantities, i.e., the column inventories. The data product is available at
976 OCADS:
977 <https://www.ncei.noaa.gov/data/oceans/ncei/ocads/metadata/0279447.html> (Müller et al., 2023_b).

978 **47)54) Tracer-based rapid anthropogenic carbon estimation from 1750 to 2500:** Carter et al. (2025)
979 developed a method for estimating C_{ant} based on a machine learning translation of ocean circulation
980 information inferred from transient tracer distributions. They applied it to the gridded GLODAPv2
981 climatology to obtain estimates of the past and projected C_{ant} distribution between 1750 and 2500.
982 Projections are made using a range of simple assumptions and shared socioeconomic pathway projections.
983 Estimates are provided on [1° × 1° spatial grids at 33 standard depth](#)
984 [levels](#) in micromoles C_{ant} per kg of seawater. [This data product is available at:](#)
985 <https://doi.org/10.5281/zenodo.15692788>.

986 **55) Preformed TA and other biogeochemical properties:** Carter et al. (2020) estimated preformed seawater
987 TA, nitrate, silicate, phosphate, and oxygen using empirical seawater property estimation routines (Carter et
988 al., 2017) with ocean circulation pathway information from ocean circulation transport matrices (John et
989 al., 2020). Preformed properties are estimated property contents that seawater had when it last left contact
990 with the atmosphere, and are used as an aid in interpretation of measured ocean property distributions. [This](#)
991 [data product is available at: https://doi.org/10.5281/zenodo.3745002](#).

992 **48)56) Monthly Interior Ocean pH Climatology from 1992 to 2020:** Zhong et al. (2025) developed a
993 monthly 1° × 1° gridded global seawater pH (total scale) [product climatology from 1992 to 2020](#) at in situ
994 temperature, derived using a machine learning algorithm trained on pH observations from [the Global Ocean](#)

995 [Data Analysis Project \(GLODAPv2 \(Lauvset et al., 2024\)\)](#). The product spans from 1992 to 2020 and
 996 covers depths from the surface to 2000 m across 41 vertical levels. Its development involved a three-step
 997 machine-learning approach: (1) regional division using a self-organizing map neural network, (2) predictor
 998 selection via stepwise regression, which iteratively adds or removes variables based on their impact on
 999 reconstruction error, and (3) nonlinear regression using feedforward neural networks (FFNNs). The
 1000 developed data product is available at: <http://dx.doi.org/10.12157/IOCAS.20230720.001>.

1001 **57. CODAP-NA Climatology:** Jiang et al. (2024) developed a coastal OA indicators climatology on a $1^\circ \times 1^\circ$
 1002 grid, covering North American ocean margins from surface to 500 m at 14 standardized depth levels
 1003 . This product includes 10 key oceanographic
 1004 [variables](#): $f\text{CO}_2$, pH, $[\text{H}^+]_{\text{total}}$, free
 1005 hydrogen ion content ($[\text{H}^+]_{\text{free}}$), carbonate ion content ($[\text{CO}_3^{2-}]$), Ω_{arag} , Ω_{calc} , DIC, TA, and Revelle Factor
 1006 (RF), as well as temperature and salinity. The climatology was produced with the
 1007 WOA gridding technologies of the NOAA National Centers for Environmental Information (NCEI), based
 1008 on the recently released Coastal Ocean Data Analysis Product in North America (CODAP-NA) (Jiang et
 1009 al., 2021), along with GLODAPv2.2022 (Lauvset et al., 2022). The relevant variables were adjusted to the
 1010 year of 2010 before the gridding. The first-guess fields for this analysis were calculated using ESPERs
 1011 (Carter et al., 2021), based on the WOA (Version 2018) climatologies for salinity (Zweng et al., 2019),
 1012 temperature (Locarnini et al., 2019) and DO (Garcia et al., 2018b). The data product is available in NetCDF
 1013 at OCADS:
 1014 <https://www.ncei.noaa.gov/data/oceans/ncei/ocads/metadata/0270962.html> (Jiang et al., 2022b).
 1015 Additionally, maps of these indicators are available in jpeg at: [https://www.ncei.noaa.gov/access/ocean-](https://www.ncei.noaa.gov/access/ocean-carbon-acidification-data-system/synthesis/nacoastal.html)
 1016 [carbon-acidification-data-system/synthesis/nacoastal.html](https://www.ncei.noaa.gov/access/ocean-carbon-acidification-data-system/synthesis/nacoastal.html) (Jiang et al., 2022b).

1017 **Table 4. Gridded and derived ocean carbonate chemistry data synthesis products in the subsurface ocean.**

No.	Name	Open or coastal ocean	Resolution	Temporal resolution	Methodology	Highlights	Reference
46	Global interior ocean-mapped climatology from GLODAPv2 Climatology	Open ocean	$1^\circ \times 1^\circ$	Referenced to 2002	Data Interpolating Variational Analysis (DIVA)	Ocean interior climatology for multiple variables from surface to the bottom of the ocean (referenced to year 2002)	Lauvset et al. (2016)
47	Aragonite Saturation State Climatology	Open ocean	$1^\circ \times 1^\circ$	Referenced to 2000	Data Interpolating Variational Analysis (DIVA)	Ocean interior climatology for (Ω_{arag}) aragonite saturation state from surface to 4000 m (referenced to year 2000)	Jiang et al. (2015a)

48(a)	MOBO-DIC (Version 2020)	Open ocean	1° × 1°	Monthly climatology centered around 20 referenced to January 2011	Machine learning	Seasonal variability of DIC in the interior ocean from surface to 2000 m	Keppler et al. (2020)
48(b)	MOBO-DIC (Version 2023)	Open ocean	1° × 1°	Monthly from Jan 2004 to Dec 2019	Machine learning	Temporal trends and interannual variability of DIC in the interior ocean from surface to 1500 m	Keppler et al. (2023 _{a,b})
49	Monthly I glo b al interior Ocean TA Climatology	Open ocean	1° × 1°	Monthly climatology	Machine learning	Ocean interior climatology for TA from surface to bottom	Broullón et al. (2019, 2020 _b)
50	Monthly I glo b al interior Ocean DIC Climatology	Open ocean	1° × 1°	Monthly from 1957 to 2018	Machine learning	Ocean interior climatology for DIC from surface to bottom (referenced to year 1995)	Broullón et al. (2020 _{a,c})
51	Acidification Metrics in the Ocean Interior	Open ocean	1° × 1°	2002 and preindustrial	Reproduced from GLODAPv2.2016 b (Lauvset et al., 2016) and the preformed properties of Carter et al., (2021)	Metrics of acidification in the ocean interior (to 2000 m) and the component of those changes caused by carbonate system nonlinearities	Fassbender et al. (2023)
52	P rogression of Ocean Interior Acidification over the Industrial Era	Open ocean	1° × 1°	1800-1994 to 2004-2014	Conversion of anthropogenic carbon accumulation into acidification rates	Temporal trends in the progression of acidification in the interior ocean are resolved	Müller et al. and Gruber (2024 _a)
53(a)	Anthropogenic CO ₂ from 1994 to 2007	Open ocean	1° × 1°	1994 and 2007	e MLR(C*) extended Multiple Linear Regression applied to the tracer C*Extended multiple linear regression (eMLR)	The oceanic sink for anthropogenic CO ₂ over the period 1994 to 2007	Gruber et al. (2019a)
53(b)	Decadal Trends in Anthropogenic CO ₂ from 1994 to 2014	Open ocean	1° × 1°	Decadal from 1994 to 2014	eMLR(C*) extended Multiple Linear Regression applied to the tracer C*	Temporal trends in the accumulation of anthropogenic CO ₂ in the interior ocean are resolved	Müller et al. (2023 _a)
54	A nthropogenic carbon from 1750 to 2500 (TRACE)	O pen ocean	1° × 1°	R eferenced to 20 years ranging from ~1750 to 2500	E stimated from atmospheric transients and ocean tracer distributions	E stimates over time based on assumptions of steady state ocean circulation and CO ₂ exchange	C arter et al. (2025)

55	Preformed TA and other biogeochemical properties	Open ocean	$1^\circ \times 1^\circ$	Not referenced in time	Empirical algorithms with inversions to find source outcrops	Estimates of the properties of seawater at the time of last contact with the atmosphere	Carter et al. (2021)
56	Monthly Interior Ocean pH from 1992 to 2020 Climatology	Open ocean	$1^\circ \times 1^\circ$	Monthly from Jan 1992 to Dec 2020	Machine learning	Temporal variability of pH in the interior ocean from surface to 2000 m over 3 decades	Zhong et al. (2025)
57	CODAP-NA Climatology	Coastal	$1^\circ \times 1^\circ$	Referenced to 2010	Objective analysis approach of the World Ocean Atlas WOA	The first discrete bottle based climatology in the North American ocean margins	Jiang et al. (2024)

1018

1019 3.1.5 Multi-product Analyses:

1020 This section includes data products that have been generated by community synthesis efforts designed to inform
1021 [global carbon budget](#) [the GCB](#).

1022 [49\)58\)](#) [SeaFlux](#): Harmonization of air–sea CO₂ fluxes from surface pCO₂ data products using a
1023 standardized approach (Gregor and Fay, 2021). This resource provides an ensemble of six pCO₂ products
1024 with air-sea CO₂ fluxes computed consistently. The six included products are: CMEMS-[LSCEv1](#) [FFNN](#),
1025 CSIR-ML6, JENA-MLS, JMA-MLR, MPI-SOMFFN, and NIES-FNN. First, missing areas of pCO₂
1026 estimates (mostly high-latitude and marginal seas) are filled using a linear-regression approach, thus
1027 addressing differences in spatial coverage between the mapping products. Further, also accounts for
1028 methodological inconsistencies in flux calculations. Fluxes are calculated using three wind products
1029 (CCMPv2, ERA5, and JRA55) along with the application of a scaled gas exchange coefficient for each of
1030 the wind products. Through these steps, SeaFlux presents a product ensemble of interpolated global surface
1031 ocean pCO₂ and air–sea carbon flux estimates for the years 1990–2019. For more details, refer to Fay et al.
1032 (2021).

1033 [50\)59\)](#) [RECCAP2](#): In the context of the second iteration of the project REgional Carbon Cycle
1034 Assessment and Processes (RECCAP2), the ocean carbon community compiled, quality controlled and
1035 harmonized (in the sense of providing output on the same regular grid at the same spatial and temporal
1036 resolution) 12 [global ocean biogeochemical model](#) [GOBMs](#) simulations, 11 pCO₂ products, one ocean
1037 interior DIC product, and three data assimilation models to constrain the ocean carbon sink between 1985
1038 and 2018. The RECCAP2 synthesis effort stands as a distinct but complementary resource to the [Global
1039 Carbon Budget](#) (GCB project (Friedlingstein et al., 2025), which primarily focuses on anthropogenically
1040 perturbed surface CO₂ fluxes from a global budgeting perspective. The individual chapters of RECCAP2
1041 were published in this special issue of Global Biogeochemical Cycles:
1042 [https://agupubs.onlinelibrary.wiley.com/doi/toc/10.1002/\(ISSN\)2169-8961.RECCAP2](https://agupubs.onlinelibrary.wiley.com/doi/toc/10.1002/(ISSN)2169-8961.RECCAP2). The data products
1043 of this assessment are available on a $1^\circ \times 1^\circ$ horizontal grid, with monthly resolution for surface ocean

1044 variables such as air-sea CO₂ fluxes, and annual resolution for interior ocean variables, such as DIC
1045 content. The data compilation, which is described in detail in DeVries et al. (2023), is available at:
1046 <https://zenodo.org/records/7990823> (Müller, 2023).

1047 ~~51~~60 **Global Carbon Budget:** The GCB collects annually updated estimates of the ocean carbon sink
1048 from currently nine *f*CO₂-products and ten ~~Global Ocean Biogeochemical Models~~GOBMs for the period
1049 1959 to the past calendar year (Friedlingstein et al., 2025, <https://globalcarbonbudget.org/gcb-2024>). In
1050 contrast to Earth System Models, the GOBMs are here forced with atmospheric reanalysis that ingested
1051 atmosphere and ocean observations and are thus thought to be closer to the observed climate. Gridded
1052 fields are provided on a 1° × 1° horizontal grid and monthly resolution. In addition, globally and regionally
1053 integrated air-sea CO₂ fluxes from the native model grids are provided. Globally integrated time-series are
1054 adjusted for full ocean coverage and model bias and drift and are available for each individual *f*CO₂-
1055 product and GOBM (<https://globalcarbonbudget.org/download/1442/?tmstv=1731323337>). The model data
1056 goes well beyond surface fluxes and includes data to analyze drivers of carbon fluxes, including several 3D
1057 variables. The model data request has been updated since RECCAP2 and also provides, for example,
1058 monthly interior ocean data of DIC, ~~alkalinity~~TA, nutrients and ~~DO~~oxygen. The GOBM data request was
1059 also updated to have all variables available that are needed to serve as a testbed for *f*CO₂-products (e.g., sea
1060 surface height). Gridded surface data of sea surface fugacity and air-sea CO₂ flux of all *f*CO₂-products and
1061 GOBMs as used in the latest release of GCB (2024) are published on Zenodo
1062 (<https://zenodo.org/records/14639761>, Hauck et al., 2025). All other GOBM output is available via
1063 <https://globalcarbonbudgetdata.org/closed-access-requests.html>.

1064 **Table 5. Ocean carbonate chemistry data product synthesis and harmonizations.**

No.	Name	Open or coastal ocean	Surface or water column	Spatial resolution	Temporal resolution	Methodology	Highlights	Reference
58	SeaFlux	Open + Coastal	Surface only	1° × 1°	Monthly from 1990 to 2022	Consistent flux calculations for 6 pCO ₂ products to produce an ensemble estimate	Careful consideration of flux calculation provides a resource and code to the community for independent flux calculations	Gregor and Fay (2021)
59	RECCAP2	Open + Coastal	Surface + Water column	1° × 1° (open) 0.25° × 0.25° (coastal)	Monthly from 1985 to 2018	Harmonized compilation of surface fCO ₂ products, model simulations and ocean interior products	Quality controlled data compilation with a harmonized horizontal grid and temporal resolution	Müller (2023), DeVries et al. (2023), Resplandy et al. (2024)
60	Global Carbon Budget	Open + Coastal	Surface + Water column	1° × 1°	Monthly from 1959 to 2023	Harmonized compilation of surface fCO ₂ products, and GOBM global ocean biogeochemical model simulations	Annually updated and quality controlled data sets. Availability of monthly 4D ocean model output.	Friedlingstein et al. (2025)

1065

1066 **3.1.6 Model-based and Hybrid Products and Analyses:**

1067 Model-based projections of biogeochemical variables are often available from global and regional models, such
 1068 as those in the ~~Sixth-Seven~~ Coupled Model Intercomparison Project (CMIP7) (Dunne et al., 2024; Durack et al.,
 1069 2025). This section further includes hybrid data products, which adjust model estimates towards observation-based
 1070 constraints.

1071 [5261](#) **Decadal Trends in the Ocean Carbon Sink:** The DeVries et al. (2019) analysis examines
 1072 decadal trends in global and regional air-sea CO₂ fluxes from a variety of ocean biogeochemical models
 1073 that contributed to the ~~GC~~ Global Carbon Budget (see No. 605). Three sets of model simulations were
 1074 performed. Simulation A uses variable climate forcing (e.g., variable wind stress, heat and freshwater
 1075 fluxes) and observed atmospheric CO₂ forcing, Simulation B uses constant (repeated) climate forcing and
 1076 observed atmospheric CO₂, and simulation C uses both constant climate forcing and constant atmospheric
 1077 CO₂ concentrations. With these simulations, the authors partitioned decadal trends in ocean CO₂ uptake
 1078 into those driven by climate variability and those driven by atmospheric CO₂. They found that climate
 1079 variability drove a weakening trend of the ocean carbon sink during the 1990s, and a strengthening trend
 1080 during the first decade of the 2000s. The magnitude of these trends agreed with those of an OCIM that was
 1081 trained to replicate tracer data from the 1990s and 2000s (DeVries et al., 2017), indicating that the decadal

1082 trends may be driven by variability in ocean circulation. This data from this analysis is accessible through
1083 figshare at <https://doi.org/10.6084/m9.figshare.8091161.v1>.

1084 **53)62) ECCO-Darwin:** Carroll et al. (2022) used the Estimating the Circulation and Climate of the
1085 Ocean-Darwin (ECCO-Darwin) global-ocean biogeochemistry state estimate to generate a data-constrained
1086 DIC budget and investigate how spatiotemporal variability in advection and mixing, air-sea CO₂ flux, and
1087 the biological pump have modulated the ocean sink for 1995–2018. ECCO-Darwin assimilates ocean
1088 circulation and physical tracers, including temperature, salinity, and sea ice, derived from the Estimating
1089 the Circulation and Climate of the Ocean (ECCO) LLC270 global-ocean and sea-ice data synthesis (Zhang
1090 et al., 2018). Additionally, it assimilates biogeochemical observations encompassing the cycling of carbon,
1091 nitrogen, phosphorus (PO₄), iron (Fe), silica (SiO₂), **DO**, and **TA**. This inclusive approach
1092 enhances the model's fidelity by aligning it with a diverse array of observations. All ECCO-Darwin model
1093 output is available on the ECCO Data Portal: <https://data.nas.nasa.gov/ecco/>. The model code and platform-
1094 independent instructions for running ECCO-Darwin simulations can be found at:
1095 https://github.com/MITgcm-contrib/ecco_darwin.

1096 **54)63) Global Surface Ocean Acidification Indicators:**

1097 **(a) Surface pH and Revelle Factor:** Jiang et al. (2019a) produced a high-resolution (1°×1°) data product
1098 delineating regionally varying view of global surface ocean pH, acidity, and Revelle Factor (RF) from 1770
1099 to 2100 by amalgamating recent observational seawater CO₂ data from the SOCAT database (Version 6,
1100 1991–2018, ~23 million observations) (Bakker et al., 2016), and temporal trends at individual locations of
1101 the global surface ocean from an Earth System Model, i.e., GFDL-ESM2M (Dunne et al., 2013). The
1102 calculations were conducted under historical atmospheric CO₂ levels (pre-2005) and four Representative
1103 Concentrations Pathways (post-2005) corresponding to the Intergovernmental Panel on Climate Change
1104 (IPCC)'s 5th Assessment Report, specifically RCP2.6, RCP4.5, RCP6.0, and RCP8.5. Surface ocean TA
1105 was calculated from SSS, SST using the updated locally interpolated alkalinity regression (LIARv2)
1106 method (Carter et al., 2017). Surface ocean pH, acidity, and RF were then calculated using a MATLAB
1107 version of the CO2SYS program (Orr et al., 2015). The data product is available at OCADS
1108 : <https://www.ncei.noaa.gov/data/oceans/ncei/ocads/metadata/0206289.html> (Jiang
1109 et al., 2019b).

1110 **(b) Surface OA Indicators:** Jiang et al. (2023) developed a comprehensive model-data fusion product that
1111 delineates the trajectory of 10 OA indicators: fCO₂, pH, ~~[H⁺]_{total}, total hydrogen ion content, free hydrogen~~
1112 ~~ion content, [H⁺]_{free}~~ [CO₃²⁻], Ω_{arag}, Ω_{calc}, DIC, TA, and RF, as well as temperature and salinity at all
1113 locations of the global surface ocean from 1750 to 2100. This product marks a significant breakthrough in
1114 OA forecasting by refining temporal trends with data from 14 Earth System Models (ESMs) within ~~the~~
1115 ~~Coupled Model Interecomparison Project Phase 6~~ (CMIP6, and by applying bias and drift corrections from

1116 three updated observational ocean carbonate system data products: SOCAT (Version 2022) (Bakker et al.,
1117 2016), GLODAPv2.2022 (Lauvset et al., 2022), and CODAP-NA (Jiang et al., 2021). This dataset offers
1118 10-year averages on a $1^\circ \times 1^\circ$ global surface ocean grid, capturing trends from preindustrial times (1750),
1119 through historical conditions (1850–2010), and projects future conditions to 2100 across five Shared
1120 Socioeconomic Pathways: SSP1-1.9, SSP1-2.6, SSP2-4.5, SSP3-7.0, and SSP5-8.5. The gridded data
1121 product is available in NetCDF at OCADS (DOI: ~~“10.25921/9ker-
1122 be48”~~): <https://www.ncei.noaa.gov/data/oceans/nci/ocads/metadata/0259391.html> (Jiang et al., 2022c),
1123 and global maps of these indicators are available in jpeg at: [https://www.ncei.noaa.gov/access/ocean-
1124 carbon-acidification-data-system/synthesis/surface-oa-indicators.html](https://www.ncei.noaa.gov/access/ocean-carbon-acidification-data-system/synthesis/surface-oa-indicators.html) (Jiang et al., 2022c).

1125 **64) Simulated and Constrained Global and Southern Ocean Carbon Sink**

1126 : These two datasets include spatially-integrated and annually averaged values for the
1127 ocean carbon sink from 1850 to 2100 for different scenarios over the 21st century for the global ocean
1128 (Terhaar et al., 2022a, 2022b) and the Southern Ocean (Terhaar et al., 2021b, 2021c). All results are based
1129 on CMIP5 and CMIP6 models. For the global ocean carbon sink, values are available for SSP1-2.6, SSP2-
1130 4.5, and SSP5-8.5. For the Southern Ocean, values are also available for SSP1-2.6, SSP2-4.5, and SSP5-8.5
1131 and additionally also for RCP2.6, RCP4.5, and RCP8.5. In addition, to the raw simulated values,
1132 constrained estimates of the annually averaged ocean carbon sink estimates are available. These
1133 constrained estimates adjusted the simulated carbon sink estimates for biases on the ocean’s circulation and
1134 surface carbonate chemistry (see Terhaar et al., 2021b, 2022a for details). It is recommended to use the
1135 constrained estimates. The datasets are available at <https://doi.org/10.17882/103934> and
1136 <https://doi.org/10.17882/103938>.

1137 **55)65) Composite model-based estimate of the ocean carbon sink from 1959 to 2022:** This data
1138 product, developed by Terhaar (2025), presents an estimate of the global ocean carbon sink by combining
1139 forced hindcast simulations and simulations made by coupled earth system models. Hindcast models
1140 manage to adequately simulate the short-term variability of the ocean, but struggle to simulate the long-
1141 term climate change trend (Huguenin et al., 2022; Takano et al., 2023; Hollitzer et al., 2024). Earth system
1142 models cannot simulate the observed short-term variability by definition, but accurately simulate long-term
1143 trends (Takano et al., 2023; Hollitzer et al., 2024). The composite model-based estimate combines the
1144 simulated short-term variability from hindcast simulations and the long-term trend from earth system
1145 models. The output is supplied with the associated study (<https://bg.copernicus.org/articles/22/1631/2025/>)
1146 (Terhaar, 2025).

1147 **56)66) pCIBR_Clim and pCIBR_Int:** A machine learning (ML) model is employed to correct biases in
1148 surface $p\text{CO}_2$ simulations generated by the INCOIS-BIO-ROMS model ($p\text{CO}_2$ model) over the period
1149 1980–2019. The ML model is trained using the differences between observed ($p\text{CO}_2$ obs) and modeled
1150 $p\text{CO}_2$ to estimate the spatio-temporal deviations ($p\text{CO}_2$ obs – $p\text{CO}_2$ model). These interannually and

1151 climatologically varying deviations are then added back to the original model output, resulting in two
 1152 improved data products: pCIBR_Int and pCIBR_Clim (Ghoshal et al., 2025a). Evaluation against
 1153 independent datasets, including moored observations (BOBOA), the gridded SOCAT product, and other
 1154 ML-based $p\text{CO}_2$ products (such as CMEMS-LSCEv2-FFNN and OceanSODA), demonstrates a significant
 1155 improvement of approximately $40\% \pm 3.31\%$ in RMSE compared to the original model. This high-
 1156 resolution ($0.083^\circ \times 0.083^\circ$), long-term monthly $p\text{CO}_2$ data product is available from the INCOIS Portal
 1157 (<https://las.incois.gov.in>) and from OCADS: (DOI: “10.25921/r2q9-d197”, link:
 1158 <https://www.ncei.noaa.gov/data/oceans/ncei/ocads/metadata/0307788.html> (Ghoshal et al., 2025b)).

1159 **57)67) INCOIS-BIO-ROMS Simulated Surface $p\text{CO}_2$ and pH for the Indian Ocean:**

1160 This data product presents a comprehensive assessment of OA trends across the Indian Ocean and its sub-
 1161 regions from 1980 to 2019, leveraging outputs from a regional, high-resolution coupled ocean-ecosystem
 1162 model (INCOIS-BIO-ROMS), an offline biogeochemical (BGC) model, and two machine learning-based
 1163 products (Chakraborty et al., 2024). INCOIS-BIO-ROMS, configured at $1/12^\circ$ resolution for the Indian
 1164 Ocean, was developed in accordance with the “RECCAP-2: Ocean Modeling Protocol” for regional oceans.
 1165 The INCOIS-BIO-ROMS simulated surface $p\text{CO}_2$ and pH data product is available from the INCOIS Portal
 1166 (<https://las.incois.gov.in>) and from OCADS:
 1167 <https://www.ncei.noaa.gov/data/oceans/ncei/ocads/metadata/0307663.html> (Chakraborty et al., 2025).

1168 **68) Annual gridded anthropogenic carbon estimates from 1780-2020:** DeVries (2022b) utilized a two-step
 1169 procedure to estimate anthropogenic carbon in the ocean interior using an ocean inverse model. First, a
 1170 steady-state ocean circulation inverse model (OCIM) was fit to observations of physical circulation tracers
 1171 such as temperature, salinity, radiocarbon, and CFCs (Holzer et al., 2021). Then, the circulation model was
 1172 coupled to an abiotic carbon cycle model, spun up to equilibrium in 1780 and then forced by observed at-
 1173 mospheric CO_2 time history from 1781-2020. Simulations were run with and without historical changes in
 1174 sea surface temperatures. The difference between preindustrial and transient simulations represents the an-
 1175 thropogenic carbon accumulation in the ocean. Results are provided on a regular grid with a nominal reso-
 1176 lution of 2° in the horizontal with 48 depth levels. The output is available at
 1177 <https://doi.org/10.6084/m9.figshare.19341974.v2>.

1178 **Table 6. Model based data synthesis products and analyses for ocean carbonate chemistry.**

No.	Name	Open or coastal ocean	Surface or water column	Spatial resolution	Temporal resolution	Highlights	Reference
61	Decadal Trends in the Ocean Carbon Sink	Open ocean	Surface	Variable	Decadal	Climate variability drove weakened ocean CO_2 uptake in the 1990s, and strengthened CO_2 uptake in the 2000s	DeVries et al. (2019)

62	ECCO-Darwin	Open + Coastal	Water column	$\frac{1}{5}^{\circ} \times \frac{1}{5}^{\circ}$	3-hourly, daily, and month fields available	Model-data synthesis product based on the Estimating the Circulation and Climate of the Ocean (ECCO) ocean state estimate. Fully-closed, physically-consistent 3-D biogeochemical budgets.	Carroll et al. (2020, 2022, 2024)
63(a)	Surface pH and Revelle Factor	Open ocean	Surface	$1^{\circ} \times 1^{\circ}$	Decadal from 1770 to 2100	A model-observation fusion product for pH, acidity and Revelle Factor, leveraging GFDL-ESM2M and SOCATv6	Jiang et al. (2019a)
63(b)	Surface OA Indicators	Open ocean	Surface	$1^{\circ} \times 1^{\circ}$	Decadal from 1750 to 2100	A model-observation fusion product for all major OA indicators, leveraging a consortium of 14 Earth System Models and 3 observational data products	Jiang et al. (2023)
64	Simulated and Constrained <u>Global and Southern Ocean Carbon Sink from 1850 to 2100 for the global ocean and the Southern Ocean</u>	Open ocean	Surface	Spatially integrated	Annual from 1850 to 2100	A constrained estimate of the ocean carbon sink based on the simulated carbon sink from CMIP5 and CMIP6 models and constrained with observations of the ocean physics and carbonate chemistry	Terhaar et al. (2021b, 2022a)
65	<u>Composite model-based estimate of the ocean carbon sink from 1959 to 2022</u>	<u>Open ocean</u>	<u>Surface</u>	<u>Spatially integrated</u>	<u>Annual from 1959 to 2022</u>	<u>A model-based estimate of the ocean carbon sink combining the respective strengths of hindcast simulations and simulations by coupled earth system models</u>	<u>Terhaar (2025)</u>
66	pCIBR_Clim and pCIBR_Int	Open + Coastal	Surface	$0.083^{\circ} \times 0.083^{\circ}$	Monthly	This data product has been developed by employing an innovative hybrid approach, where a machine learning algorithm was used to correct high-resolution ($1/12^{\circ}$) coupled ocean-ecosystem model outputs using observational data from SOCAT (1984-2019) and SAS (1991-2019) for the Indian Ocean	Ghoshal et al. (2025a)

67	INCOIS-BIO-ROMS Simulated Surface $p\text{CO}_2$ and pH for the Indian Ocean (1980-2019)	Open + Coastal	Surface	$0.083^\circ \times 0.083^\circ$	Monthly from 1980 to 2019	INCOIS-BIO-ROMS was developed in accordance with the “RECCAP-2: Ocean Modeling Protocol” for regional oceans. By integrating model simulations with available field observations and reconstructed data products, this study advances the current understanding of OA in the Indian Ocean	Chakraborty et al. (2024)
68	<u>Ocean Circulation Inverse Model (OCIM)</u>	Open	<u>Surface and water column</u>	<u>$2^\circ \times 2^\circ$ horizontal, 48 vertical layers</u>	<u>Annual from 1780 to 2020</u>	<u>Data-constrained estimate of anthropogenic CO₂ accumulation in the ocean from inverting physical ocean circulation tracers</u>	<u>DeVries (2022b)</u>

1179 3.2 Overlaps and history

1180 Many of the data products described above exhibit significant overlap in various forms. In some cases, one or more
1181 products are used to generate new ones, while in others, the same collection-level cruise datasets underpin multiple
1182 products. There are a few foundational data products, such as GLODAPv2 and SOCAT, which are widely utilized to
1183 develop other data products, including their respective gridded products (e.g., Lauvset et al., 2016). For instance,
1184 SOCAT forms the backbone of nearly all derived products listed in Table 3, serving as a key resource for product
1185 development or validation. Some derived products, such as the JMA-MLR (No. 265) and OceanSODA-ETHZv1
1186 (No. 27a6), incorporate both SOCAT and GLODAPv2 during development. Having overlaps in data and derived
1187 products has provided opportunities for data quality control and intercomparison of different approaches to gap
1188 filling that would not have been available otherwise. Additional overlaps between these data products are provided
1189 below:

1190 3.2.1 SOCAT and LDEO:

1191 The quality control and synthesis of global surface ocean CO₂ data began in 1997 with Dr. Taro Takahashi and his
1192 colleagues at ~~the Lamont-Doherty Earth Observatory~~ (LDEO in Palisades, New York). His pioneering work led to
1193 the creation of the LDEO Surface $p\text{CO}_2$ Database (No. 2), which focused on high-quality data collected by his team
1194 and from various U.S. and international expeditions. Over time, this data set expanded to include contributions from
1195 other laboratories, resulting in a highly influential collection of $p\text{CO}_2$ data and several seminal papers on global
1196 surface ocean CO₂ variations and air-sea CO₂ fluxes (Takahashi et al., 1997; 2002; 2009). The last update to the
1197 LDEO database was in 2019, following Dr. Takahashi’s passing, and no further updates are anticipated (Takahashi
1198 et al., 2017).

1199 The ~~Surface CO₂ Atlas~~ (SOCAT project was developed to address questions around the current and future drivers of

1200 CO₂ fluxes raised at the 2007 Surface Ocean CO₂ Variability and Vulnerability (SOCOVV) workshop in Paris,
1201 France (Metzl et al., 2007). SOCAT was developed to synthesize all of the publicly available, discoverable, and
1202 citable surface CO₂ data. Following the GLODAP model, there was a strong emphasis on an open and transparent
1203 secondary quality control process to ensure the highest data quality. The first data release came in 2011 (Pfeil et al.,
1204 2013; Sabine et al., 2013) and included contributions from numerous laboratories, as well as the freely available CO₂
1205 data from the LDEO database. As of 2024, SOCAT contains ~40 million data points, with new observations added
1206 annually. All data are rigorously standardized, and recalculated as $f\text{CO}_2$. SOCAT represents an ongoing global
1207 community effort, with participants from all continents contributing data and to the quality control process. Initially
1208 new versions were released every other year, but automation allowed annual public releases since version 4.

1209 **3.2.2 GLODAPv2 and Quality Edited Hydrographic Data:**

1210 Starting in the late 1980s, the WOCE, Joint Global Ocean Flux Study
1211 (JGOFS), and the NOAA Ocean-Atmosphere Exchange Study (OACES) collaborated in a multinational effort to
1212 conduct a decadal global hydrographic survey of unparalleled quality and quantity. At the conclusion of the survey
1213 at the end of the 1990s, GLODAP combined and publicly released all of
1214 the available hydrographic data with high-quality [ocean carbonate system](#) measurements as a single database
1215 (Key et al., 2004; Sabine et al., 2005). The data were subjected to extensive secondary quality control checks where
1216 cruise tracks intersected one another, making it the most comprehensive and highest-quality ocean inorganic carbon
1217 dataset ever generated. A gridded, full-depth global ocean carbon climatology was also created and released as part
1218 of the project. These data and associated climatology have been extensively used to evaluate carbon distributions as
1219 well as the accumulation of anthropogenic CO₂ in the ocean. Other regional datasets, like [the CARINA](#)
1220 data synthesis project, an international collaborative effort of the European Union
1221 CARBOOCEAN program (Key et al., 2010; Tanhua et al., 2010) and PACIFICA,
1222 an international synthesis of Pacific Ocean data organized through the North Pacific Marine Science Organization
1223 (PICES) (Ishii et al., 2011b; Suzuki et al., 2013), were combined with GLODAP after its initial release. The
1224 GLODAP database is continuing to grow with new data collected as part of the Global Ocean Ship-Based
1225 Hydrographic Investigations Program (GO-SHIP).

1226 For discrete bottle measurements spanning the entire oceanic water column, GLODAPv2 (No. 3) and the [Quality](#)
1227 [Edited Hydrographic Data](#) ~~Java Ocean Atlas~~ (JOA, No. 4) are the primary data products. Most cruise datasets
1228 contributing to these two data products overlap, but the key difference lies in their approach to data adjustment. The
1229 former applies crossover and inversion analysis for bias correction, while the latter presents the data without such
1230 adjustments. GLODAPv2 achieves consistency by applying adjustments based on deep-ocean offsets, whereas
1231 [Quality Edited Hydrographic Data](#) ~~JOA~~ provides the data in its original form. While there is substantial overlap
1232 between the two, data from a specific expedition might differ slightly due to GLODAPv2's secondary quality control
1233 adjustments. Both GLODAPv2 and [Quality Edited Hydrographic Data](#) ~~JOA~~ offer global coverage, but several
1234 independent regional data products are also available, such as SNAPO-CO₂ (No. 6), CODAP-NA (No. 7), AZMP

1235 Carbon (No. 8), MOCHA (No. 9), and ARIOS (No. 10). Data from these regional products often partially or fully
1236 overlap with GLODAPv2 and [Quality Edited Hydrographic Data](#) [IOA](#).

1237 a) GLODAPv2 and CODAP-NA:

1238 All cruise datasets contributing to CODAP-NA were forwarded to the GLODAPv2 quality control team in 2022.
1239 Data from select cruises with deep-water sampling (>1500 m), enabling crossover analysis, were subsequently
1240 incorporated into the GLODAPv2.2022 data product update (Lauvset et al., 2022).

1241 b) GLODAPv2 and SPOTS:

1242 Some time-series data are included in both GLODAPv2 and the Synthesis Product for Ocean Time-Series (SPOTS).
1243 Usually, data present in both products have not been measured on dedicated time-series cruises but rather collected
1244 as part of a larger cruise passing by a time-series location. As the quality control of SPOTS is restricted to assigning
1245 method flags, adjustments that are applied as a result of the QC of GLODAP are not present in SPOTS. Additional
1246 crossover analyses between SPOTS and GLODAP have revealed a good consistency (Lange et al., 2024a).

1247 3.2.3 RECCAP2 and GCB:

1248 RECCAP2 and GCB are not data products themselves, but analyses and syntheses of data-based and model-based
1249 products. Users should be aware that there is a large degree of overlap between the $f\text{CO}_2$ products and GOBMs that
1250 contributed to both RECCAP2 and GCB [and of the resulting datasets](#). However, [the](#) RECCAP2 and GCB [analyses](#)
1251 serve different purposes. GCB is updated annually to the latest complete calendar year and its main purpose is to
1252 present and estimate the magnitude (and uncertainty) [of the ocean CO₂ sink and the role of CO₂ and climate](#)
1253 [drivers since 1959 with a focus on the last](#) year, while RECCAP2 presents a deeper analysis of the
1254 magnitude, trends, and variability of the [global and regional](#) ocean CO₂ sink over the period 1985-2018.

1255 3.2.4 Jiang et al. (2019a) and Jiang et al. (2023):

1256 Both products contain the projection of surface ocean pH, $[\text{H}^+]_{\text{total}}$, and buffer capacity
1257 from 1750 to 2100. However, the former is based on one GFDL model ESM2M, while the latter is based on a
1258 consortium of 14 Earth system models, and additional observational data. The latter also contains the projection of
1259 seven other OA variables, including carbonate ions, Ω_{arag} , Ω_{calc} , $f\text{CO}_2$,
1260 DIC, and TA.

1261 4 Data availability

1262 Access links for all data products mentioned in this paper are provided in their respective paragraphs. Additionally, their
1263 access links are available in Table 7 below.

1264 Table 7. Access links for the compiled ocean carbonate chemistry data products. N/A is short for not applicable.

No.	Name	Data access link	DOI	Reference
1	SOCAT	https://socat.info/	https://doi.org/10.25921/648f-fv35https://doi.org/10.25921/9wpa-th28	Bakker et al. (2016, 2025)
2	LDEO Surface pCO ₂ Database	https://www.ncei.noaa.gov/data/oceans/ncei/ocads/metadata/0160492.html	https://doi.org/10.3334/cdiac/otg.ndp088(v2015)	Takahashi et al. (2017)
3	GLODAPv2	https://glodap.info/	https://doi.org/10.25921/zyrq-ht66	Lauvset et al. (2023 ^{ba} , 2024)
4	Quality Edited Hydrographic Data/JOA Suite	https://joa.ucsd.edu/	N/A	Swift and Osborne (2022)
5	WOD	https://www.ncei.noaa.gov/products/world-ocean-database	https://doi.org/10.25923/z885-h264	Mishonov et al. (2024)
6	SNAPO-CO ₂	https://www.ncei.noaa.gov/data/oceans/ncei/ocads/metadata/0285681.html	https://doi.org/10.17882/95414	Metzl et al. (2023, 2024)
7	CODAP-NA	https://www.ncei.noaa.gov/data/oceans/ncei/ocads/metadata/0219960.html	https://doi.org/10.25921/531n-c230	Jiang et al. (2020, 2021)
8	AZMP Carbon	N/A	https://doi.org/10.20383/102.0673	Cyr et al. (2022)
9	MOCHA	https://www.ncei.noaa.gov/data/oceans/ncei/ocads/metadata/0277984.html	https://doi.org/10.25921/2vve-fh39	Kennedy et al., (2024)
10	ARIOS	https://digital.csic.es/handle/10261/205135	https://doi.org/10.20350/digitalCSIC/12498	Pérez et al. (2020)
11	Marine Inorganic Carbon Chemistry in the Northern Gulf of Alaska	https://www.ncei.noaa.gov/data/oceans/ncei/ocads/metadata/0277034.html	https://doi.org/10.25921/x9sg-9b08	Monacci et al. (2023, 2024)
12	Coral Reef Carbonate Chemistry Off the Florida Keys	https://www.ncei.noaa.gov/access/metadata/landing-page/bin/iso?id=gov.noaa.nodc:NCRMP-CO3-Atlantic	https://doi.org/10.25921/vfz0-dg77	Manzello et al. (2018)
13	Salish Cruise and Cruise Data Package and Multi-stressor Data Product	https://www.ncei.noaa.gov/access/ocean-carbon-acidification-data-system/oceans/SalishCruise_DataPackage.html , https://www.ncei.noaa.gov/access/ocean-carbon-acidification-data-system/oceans/SalishCruises_DataProduct.html	https://doi.org/10.25921/jgrz-v584https://doi.org/10.25921/zgk5-ep63 , https://doi.org/10.25921/4y18-rw26https://doi.org/10.25921/5g29-q844	Alin et al. (2024a, b, 2025a, b, c)
14	Line P Marine Carbonate Chemistry Compilation	https://www.ncei.noaa.gov/data/oceans/ncei/ocads/metadata/0234342.html	https://doi.org/10.25921/zrw8-kn24	Franco et al. (2021a, b)

15	Anthropogenic Carbon in the Arctic Ocean	https://www.seanoe.org/data/00927/103920/	https://doi.org/10.17882/103920	Terhaar et al. (2024)
16	BATS	https://demo.bco-dmo.org/project/2124	https://doi.org/10.26008/1912/bco-dmo.894099.4 , https://doi.org/10.26008/1912/bco-dmo.893182.4 , https://doi.org/10.26008/1912/bco-dmo.926534.4 , https://doi.org/10.26008/1912/bco-dmo.893521.6 , https://doi.org/10.26008/1912/bco-dmo.917255.5 , https://doi.org/10.26008/1912/bco-dmo.939210.7 , https://doi.org/10.26008/1912/bco-dmo.3782.6 , https://doi.org/10.26008/1912/bco-dmo.3918.8 , https://doi.org/10.26008/1912/bco-dmo.881861.5	Bates et al. (2024a, b, c, d, e), Johnson et al. (2024a, b, c), Steinberg and Cope (2024)
17	HOT	https://www.bco-dmo.org/project/2101 , https://dhoi.org/10.5281/zenodo.15060930	https://doi.org/10.1575/1912/bco-dmo.3773.1 , https://doi.org/10.5281/zenodo.15060931	Winn et al. (1994, 1998), Dore et al. (2003, 2009, 2014, 2025), Knor et al. (2023, 2025)
18	ESTOC	N/A	https://doi.org/10.1594/PANGAEA.959856 , https://doi.pangaea.de/10.1594/PANGAEA.856590 , https://doi.pangaea.de/10.1594/PANGAEA.856615 , https://doi.pangaea.de/10.1594/PANGAEA.856608 , https://doi.pangaea.de/10.1594/PANGAEA.856616 , https://doi.pangaea.de/10.1594/PANGAEA.856593 , https://doi.pangaea.de/10.1594/PANGAEA.856612 , https://doi.pangaea.de/10.1594/PANGAEA.856614 , https://doi.pangaea.de/10.1594/PANGAEA.856607 , https://doi.pangaea.de/10.1594/PANGAEA.956272	González-Dávila and Santana-Casiano (2023)
19	Point B Time-series	N/A	https://doi.org/10.1594/PANGAEA.727120	Gattuso et al. (2021b)
20	Ny-Ålesund Time-series	N/A	https://doi.org/10.1594/PANGAEA.957028	Gattuso et al. (2023)

21	SPOTS	https://www.bco-dmo.org/dataset/896862	https://doi.org/10.26008/1912/bco-dmo.896862.2	Lange et al. (2024a, 2024b)
22	Autonomous pCO ₂ and pH Time-series from 40 Surface Buoys	https://www.ncei.noaa.gov/data/oceans/ncei/ocads/metadata/0173932.html	https://doi.org/10.7289/v5db8043	Sutton et al. (2018)
23	Takahashi delta fCO ₂ and flux climatology	https://www.ncei.noaa.gov/data/oceans/ncei/ocads/metadata/0282251.html	https://doi.org/10.25921/295g-sn13	Fay et al. (2023)
24	MPI-ULB-SOM-FFN	https://www.ncei.noaa.gov/data/oceans/ncei/ocads/metadata/0209633.html	https://doi.org/10.25921/qb25-f418	Landschützer et al. (2020a, b)
25	VLIZ SOM-FFN	https://www.ncei.noaa.gov/data/oceans/ncei/ocads/metadata/0160558.html	https://doi.org/10.7289/V5Z899N6	Landschützer et al. (2016), Jersild et al. (2017)
26	JMA-MLR	https://www.data.jma.go.jp/kaiyou/english/co2_flux/co2_flux_data_en.html	N/A	Iida et al. (2021)
27(a)	OceanSODA-ETHZv1	https://www.ncei.noaa.gov/data/oceans/ncei/ocads/metadata/0220059.html	https://doi.org/10.25921/m5wx-ja34	Gregor et al. (2020)
27(b)	OceanSODA-ETHZv2	https://zenodo.org/records/11206366	https://doi.org/10.5281/zenodo.11206365	Gregor et al. (2024b)
28	LDEO-HPD fCO ₂ product	https://zenodo.org/records/4760205	https://doi.org/10.5281/zenodo.4760205	Gloege et al. (2022)
29	LDEO HPD with Extended Temporal Coverage	https://zenodo.org/records/13891722	https://doi.org/10.5281/zenodo.13891722	Bennington et al. (2022a)
30	LDEO fCO ₂ - Residual Method	https://zenodo.org/records/13941548	https://doi.org/10.5281/zenodo.13941548	Bennington et al. (2022b)
31(a)	CMEMS-LSCEv1	https://data.ipsl.fr/catalog/srv/eng/catalog.search#/metadata/a2f0891b-763a-49e9-af1b-78ed78b16982	https://doi.org/10.14768/a2f0891b-763a-49e9-af1b-78ed78b16982	Chau et al. (2022)
30(b)	CMEMS-LSCEv2	https://data.marine.copernicus.eu/product/MULTIOBS_GLO_BIO_CARBON_SURFACE_MYNRT_015_008/services	https://doi.org/10.48670/moi-00047	Chau et al. (2024a, b)
32	CarboScope (Jena-MLS)	https://www.bgc-jena.mpg.de/CarboScope/?ID=oc	10.17871/CarboScope-oc_v2024E (or analogously for previous and upcoming releases)	Rödenbeck et al. (2022)
33	UOEx-Watson	https://www.ncei.noaa.gov/data/oceans/ncei/ocads/metadata/0301544.html	https://doi.org/10.25921/2dp5-xm29	Watson et al. (2025)
34	NIES-ML3	https://db.cger.nies.go.jp/DL/10.17595/20220311.001.html.en	https://doi.org/10.17595/20220311.001	Zeng (2022), Zeng et al. (2022)
35	CSIR-ML6	https://www.ncei.noaa.gov/data/oceans/ncei/ocads/metadata/0206205.html	https://doi.org/10.25921/z682-mn47	Gregor et al. (2019b)

36	Stepwise-FFNN	https://msdc.qdio.ac.cn/data/metadata-special-detail?id=1955061943609876482	http://dx.doi.org/10.12157/IOCAS.20250814.001	Zhong et al. (2022)
37	AOML-ET	https://www.ncei.noaa.gov/data/oceans/ncei/ocads/metadata/0298989.html	https://doi.org/10.25921/0s8y-q287	Wanninkhof et al. (2024, 2025)
38	ULB-SOM-FFN-coastalv2.1	https://www.ncei.noaa.gov/data/oceans/ncei/ocads/metadata/0279118.html	https://doi.org/10.25921/4sdep068	Roobaert et al. (2023, 2024)
39	RFR-LME	https://www.ncei.noaa.gov/data/oceans/ncei/ocads/metadata/0287551.html	https://doi.org/10.25921/h8vve872	Sharp et al. (2024a, b)
40	ReCAD-NAACOM-pCO ₂	https://zenodo.org/records/14038561	https://doi.org/10.5281/zenodo.1150097	Wu et al. (2025)
41	Gridded Surface OA Indicators and Air-sea CO ₂ Fluxes in the Northern Caribbean Sea	https://www.ncei.noaa.gov/data/oceans/ncei/ocads/metadata/0207749.html	https://doi.org/10.25921/2swk-9w56	Wanninkhof et al. (2019)
42	OA data in the Gulf of Mexico/Gulf of America and Wider Caribbean	https://www.ncei.noaa.gov/data/oceans/ncei/ocads/metadata/0245950.html	https://doi.org/10.25921/tt1cdx53	van Hooidonk (2022)
43	Regional pCO ₂ Climatology of the Baltic Sea	N/A	https://doi.org/10.1594/PAN/GAEA.961119	Bittig et al. (2023)
44	INCOIS-ReML	https://www.ncei.noaa.gov/data/oceans/ncei/ocads/metadata/0307627.html	https://doi.org/10.25921/2sjrpg16	Joshi et al. (2024, 2025a)
45	INCOIS_TA	https://www.ncei.noaa.gov/data/oceans/ncei/ocads/metadata/0307789.html	https://doi.org/10.25921/7as7-et15	Joshi et al. (2025b, c)
46	Global interior ocean-mapped climatology from GLODAPv2 Climatology	https://www.ncei.noaa.gov/data/oceans/ncei/ocads/metadata/0286118.html	https://doi.org/10.3334/cdiac/otg.ndp093_glodapv2	Lauvset et al. (2016, 2023a)
47	Aragonite Saturation State Climatology	https://www.ncei.noaa.gov/data/oceans/ncei/ocads/metadata/0139360.html	https://doi.org/10.7289/v5q81b4p	Jiang et al. (2015a, b)
48(a)	MOBO-DIC (Version 2020)	https://www.ncei.noaa.gov/access/ocean-carbon-acidification-data-system/oceans/ndp_104/ndp104.html	https://doi.org/10.25921/yvzj-zx46	Keppler et al. (2020)
48(b)	MOBO-DIC (Version 2023)	https://www.ncei.noaa.gov/data/oceans/ncei/ocads/metadata/0277099.html	https://doi.org/10.25921/z31n-3m26	Keppler et al. (2023a, b)
49	Monthly global interior Ocean TA Climatology	https://www.ncei.noaa.gov/data/oceans/ncei/ocads/metadata/0222470.html	http://doi.org/10.20350/DIGITALCSIC/8564	Broullon et al., (2019, 2020b)

50	Monthly Interior Ocean DIC Climatology	https://www.ncei.noaa.gov/data/oceans/ncei/ocads/metadata/0222469.html	http://doi.org/10.20350/digitalCSIC/10551	Broullon et al., (2020a, c)
51	Acidification Metrics in the Ocean Interior	https://www.ncei.noaa.gov/data/oceans/ncei/ocads/metadata/0290073.html	https://doi.org/10.25921/rdtr-9t74	Fassbender et al. (2023), Fassbender (2024)
52	Progression of Ocean Interior Acidification over the Industrial Era	https://www.ncei.noaa.gov/data/oceans/ncei/ocads/metadata/0298993.html	https://doi.org/10.25921/tefm-x802	Müller et al. and Gruber (2024a, b)
53(a)	Anthropogenic CO ₂ from 1994 to 2007	https://www.ncei.noaa.gov/data/oceans/ncei/ocads/metadata/0186034.html	https://doi.org/10.25921/wdn2-pt10	Gruber et al. (2019a, b)
53(b)	Decadal Trends in A Decadal trends in anthropogenic CO ₂ From 1994 to 2014	https://www.ncei.noaa.gov/data/oceans/ncei/ocads/metadata/0279447.html	https://doi.org/10.25921/ppcf-w020	Müller et al. (2023a, b)
54	Anthropogenic carbon from 1750 to 2500 (TRACE)	https://github.com/BRCScienceProducts/TRACEv1	https://doi.org/10.5281/zenodo.15692788	Carter et al. (2025)
55	Preformed TA and other biogeochemical properties	https://github.com/BRCScienceProducts/PreformedPropertyEstimates	https://doi.org/10.5281/zenodo.3745002	Carter et al. (2020)
56	Monthly Interior Ocean pH from 1992 to 2020 Climatology	https://doi.org/10.12157/IOCAS.20230720.001	https://doi.org/10.12157/IOCAS.20230720.001	Zhong et al. (2025)
57	CODAP-NA Climatology	https://www.ncei.noaa.gov/data/oceans/ncei/ocads/metadata/0270962.html	https://doi.org/10.25921/g8pb-z76	Jiang et al. (2022b), Jiang et al. (2024)
58	SeaFlux	https://zenodo.org/records/8280457	https://doi.org/10.5281/zenodo.5482547	Gregor & Fay. (2021)
59	RECCAP2	https://zenodo.org/records/7990823	https://doi.org/10.5281/zenodo.7990823	Müller (2023)
60	Global Carbon Budget	https://zenodo.org/records/14639761 , https://globalcarbonbudget.org/download/1442/?tmstv=1731323337 , https://globalcarbonbudgetdata.org/closed-access-requests.html	https://doi.org/10.5281/zenodo.14639761	Hauck et al. (2025)
61	Decadal Trends in the Ocean Carbon Sink	N/A	https://doi.org/10.6084/m9.figshare.8091161.v1	DeVries et al. (2019)
62	ECCO-Darwin	https://data.nas.nasa.gov/ecco/	N/A	Carroll et al. (2020)

63(a)	Surface pH and Revelle Factor	https://www.ncei.noaa.gov/data/oceans/ncei/ocads/metadata/0206289.html	https://doi.org/10.25921/kgqr-9h49	Jiang et al. (2019a, b), Jiang et al. (2019b)
63(b)	Surface OA indicators	https://www.ncei.noaa.gov/data/oceans/ncei/ocads/metadata/0259391.html	https://doi.org/10.25921/9ker-bc48	Jiang et al. (2022c), Jiang et al. (2023)
64	Simulated and Constrained Global and Southern Ocean Carbon Sink from 1850 to 2100 for the global ocean and the Southern Ocean	https://www.seanoe.org/data/00927/103934/ , https://www.seanoe.org/data/00927/103938/	https://doi.org/10.17882/103934 , https://doi.org/10.17882/103938	Terhaar et al. (2021c), Terhaar et al. (2022b)
65	Composite model-based estimate of the ocean carbon sink from 1959 to 2022	https://bg.copernicus.org/articles/22/1631/2025/ (the data is in the annex)	https://doi.org/10.5194/bg-22-1631-2025	Terhaar (2025)
66	pCIBR_Clim and pCIBR_Int	https://www.ncei.noaa.gov/data/oceans/ncei/ocads/metadata/0307788.html	https://doi.org/10.25921/r2q9-d197	Ghoshal et al. (2025a, b)
67	INCOIS-BIO-ROMS Simulated Surface pCO ₂ and pH for the Indian Ocean (1980-2019)	https://www.ncei.noaa.gov/data/oceans/ncei/ocads/metadata/0307663.html	https://doi.org/10.25921/z2x4-vt48	Chakraborty et al. (2024, 2025)
68	Ocean Circulation Inverse Model (OCIM)	https://figshare.com/articles/dataset/OCIM-48L_abiotic_ocean_carbon_cycle_model_output/19341974	https://doi.org/10.6084/m9.figshare.19341974.v2	DeVries (2022b)

1265 5 Summary

1266 The synthesis and gridded data products presented here reflect significant community-based efforts that have
1267 been made to advance understanding of the ocean's role in global carbon cycling. This synthesis provides an
1268 ~~comprehensive~~ overview of key data compilations and gridded data products essential for coastal and global ocean
1269 carbonate chemistry research. It highlights the key features of each product, serving as a resource for researchers
1270 seeking the necessary data for their work. ~~The list will be updated periodically to incorporate new data products. The~~
1271 ~~most up-to-date list is available at <https://oceanco2.github.io/co2-products/>. New data products should be submitted~~
1272 ~~through <https://forms.gle/g8hYm37Wg1Uifg8E8>.~~

1273 **Author contributions**

1274 L-QJ prepared the initial draft. [LG designed and implemented the GitHub webpage and supporting scripts to](#)
1275 [present the most current list of products. AR prepared Figure 1.](#) All authors contributed to the writing of the
1276 manuscript. The first 23 authors are listed based on their contributions, while the remaining authors are listed
1277 alphabetically by their last names.

1278 **Competing interests**

1279 One of the (co-)authors, Anton Velo (Instituto de Investigacions Mariñas, IIM - CSIC, Vigo, Spain), is a
1280 member of the editorial board of the Earth System Science Data.

1281 **Acknowledgements**

1282 We extend our gratitude to all scientists who collected and measured the original data and those who compiled
1283 and quality controlled these data products. We thank Pierre Friedlingstein (University of Exeter, Exeter, UK),
1284 Bronte Tilbrook (CSIRO Oceans and Atmosphere and Australian Antarctic Program Partnership, University of
1285 Tasmania, Australia), and Dwight Gledhill (NOAA/OAR Ocean Acidification Program, United States) for their
1286 valuable insights and discussions, which helped shape the vision of this paper. Additionally, we thank Xiping Hu
1287 (University of Texas at Austin, United States), Tessa Hill (University of California, Davis, United States), and
1288 Patrick Duke (University of Victoria, Canada) for recommending numerous data products incorporated into this
1289 compilation. This is PMEL contribution 5728. This is INCOIS contribution no. *** (to be added after the paper is
1290 accepted).

1291 **Financial support**

1292 Funding for L-QJ was from NOAA Ocean Acidification Program (<https://ror.org/02bf4816>) and NOAA grant
1293 NA24NESX432C0001 (Cooperative Institute for Satellite Earth System Studies - CISESS) at the Earth System
1294 Science Interdisciplinary Center, University of Maryland. The authors acknowledge funding from the United States
1295 National Science Foundation (grant no. OCE-2140395) to the Scientific Committee on Oceanic Research (SCOR,
1296 United States) for the International Ocean Carbon Coordination Project (IOCCP). [SKL and NL acknowledge](#)
1297 [funding from OceanICU. OceanICU was funded by the European Union under grant agreement no. 101083922.](#)
1298 [Views and opinions expressed are however those of the author\(s\) only and do not necessarily reflect those of the](#)
1299 [European Union or European Research Executive Agency. Neither the European Union nor the granting authority](#)
1300 [can be held responsible for them.](#) Funding for GLODAPv2 was provided by the EU FP7 project CarboChange (grant
1301 agreement 264879) and the Research Council of Norway project DECApH (grant agreement 214513), and the 2019-
1302 2023 updates were funded by the EU Horizon 2020 innovation action EuroSea (grant agreement 862626). AJF,
1303 SRA, and RAF were supported by the NOAA Pacific Marine Environmental Laboratory. GAM was funded by
1304 NOAA NA24OARX431G0151-T1-01. JPG was supported by the Service d'Observation Rade de Villefranche (SO-

1305 Rade), the Service d'Observation en Milieu Littoral (SOMLIT/CNRS- INSU), the Coastal Observing System for
1306 Northern and Arctic Seas (COSYNA), the two Helmholtz large-scale infrastructure projects ACROSS and MOSES,
1307 the French Polar Institute (IPEV), and the European Commission, Horizon 2020 Framework Programme (grant nos.
1308 871153, 951799, 727890 and 869154). Discrete samples reported by JPG were analyzed for CT and AT by the
1309 Service National d'Analyse des Paramètres Océaniques du CO₂. AV and FFP was supported by BOCATS2
1310 (PID2019-104279GB-C21) project funded by MICIU/AEI/10.13039/501100011033, by FICARAM+ (PID2023-
1311 148924OB-100) and by EuroGO-SHIP project (Horizon Europe #101094690). NM and CLM acknowledge Institut
1312 National des Sciences de l'Univers du Centre National de la Recherche Scientifique (INSU/CNRS) and
1313 Observatoire des Science de l'Univers (OSU ECCE-Terra) for supporting the SNAPO-CO₂ facility housed by the
1314 LOCEAN laboratory in Paris/France. The AZMP Carbon dataset is a contribution to Fisheries and Oceans Canada
1315 Atlantic Zone Monitoring Program. Funding for the HOT program and WHOTS mooring maintenance were
1316 provided by the National Science Foundation (grant no. OCE-9617409). CMEMS-LSCE is supported by the
1317 European Copernicus Marine Environment Monitoring Service (CMEMS, grant no. 83-CMEMSTAC-MOB). The
1318 work of LGr was supported by the ESA OceanHealth-OA project (contract number 4000137603/22/I-DT), the
1319 European Space Agency (OceanSODA project, grant no. 4000112091/14/I-LG), the European Commission
1320 (COMFORT project, grant no. 820989), and the Horizon 2020 (4C project, grant no. 821003). [PL received funding](#)
1321 [through the Horizon Europe research and innovation program under grant agreement No. 101137682 \(A4PEX\), the](#)
1322 [Horizon2020 program \(4C project, grant no. 821003\) and through Schmidt Sciences \(OBVI InMOS\)](#). JH received
1323 funding from the Initiative and Networking Fund of the Helmholtz Association (Helmholtz Young Investigator
1324 Group Marine Carbon and Ecosystem Feedbacks in the Earth System [MarESys], Grant VH-NG-1301), and from
1325 the ERC-2022-STG OceanPeak (Grant 101077209). AK was funded by the NOAA Global Ocean Monitoring and
1326 Observing program (<https://ror.org/037bamf06>). J.T. was funded by the Swiss National Science Foundation under
1327 grant # PZ00P2_209044 (ArcticECO). HCB acknowledges funding by the German Federal Ministry of Education
1328 and Research under grants no. 03F0877D (C-SCOPE project) and 03F0773A (BONUS INTEGRAL project). TD
1329 acknowledges support from the US National Science Foundation through Grant # 1948955. RW, LB, AJS, SRA, and
1330 RAF acknowledge support from the Office of Oceanic and Atmospheric Research of NOAA, U.S. Department of
1331 Commerce, including resources from the Global Ocean Monitoring and Observing Program and the Ocean
1332 Acidification Program (Open Funder Registry numbers 100018302 and 100018228, respectively). SRA and RAF
1333 acknowledge support from the Washington Ocean Acidification Center. KC acknowledges the support of the
1334 Development of Climate Change Advisory Services project, undertaken by the Indian National Centre for Ocean
1335 Information Services (INCOIS) under the Deep Ocean Mission programme of the Ministry of Earth Sciences
1336 (MoES), Government of India. LX was supported by the National Key R&D Program of China (2023YFE0113101
1337 and 2023YFC3108102), the National Natural Science Foundation of China (42176051 and 42376048), and the
1338 Taishan Scholar Project of Shandong Province (tsqn202306294).

1339 **References**

1340 Alin, S. R., Newton, J. A., Feely, R. A., Greeley, D., Curry, B., Herndon, J., and Warner, M.: A decade-long cruise

1341 time series (2008–2018) of physical and biogeochemical conditions in the southern Salish Sea, North America,
1342 Earth Syst. Sci. Data, 16, 837–865, <https://doi.org/10.5194/essd-16-837-2024>, 2024a.

1343 Alin, S. R., Newton, J. A., Feely, R. A., Siedlecki, S., and Greeley, D.: Seasonality and response of ocean
1344 acidification and hypoxia to major environmental anomalies in the southern Salish Sea, North America (2014–
1345 2018), Biogeosciences, 21, 1639–1673, <https://doi.org/10.5194/bg-21-1639-2024>, 2024b.

1346 [Alin, S. R.; Newton, J.; Ikeda, C.; Boyar, A.; Greeley, D.; Herndon, J.; Curry, B.; Kozyr, A.; Feely, R.A.:](#)
1347 [SalishCruiseDataPackage_v2025: An updated compiled data package of sensor profile and discrete physical and](#)
1348 [biogeochemical measurements from 61 individual cruise data sets collected from a variety of ships in the southern](#)
1349 [Salish Sea and northern California Current System \(Washington state marine waters\) from 2008-02-04 to 2024-10-](#)
1350 [22 \(NCEI Accession 0307188\). NOAA National Centers for Environmental Information. Dataset.](#)
1351 <https://doi.org/10.25921/jgrz-v584.2025a>.

1352 [Alin, S.R.; Newton, J.; Feely, R.A.; Ikeda, C.; Boyar, A.; Greeley, D.; Herndon, J.; Kozyr, A.:](#)
1353 [SalishCruiseMultistressor_v2025: An updated multi-stressor data product for marine heatwave, hypoxia, and ocean](#)
1354 [acidification research, including calculated inorganic carbon parameters from the southern Salish Sea and northern](#)
1355 [California Current System from 2008-02-04 to 2024-10-22 \(NCEI Accession 0307626\). NOAA National Centers for](#)
1356 [Environmental Information. Dataset. https://doi.org/10.25921/4y18-rw26.2025b](#).

1357 [Alin, S. R., Newton, J., Feely, R. A., Boyar, A., and Ikeda, C.: The second half decade of Washington Ocean](#)
1358 [Acidification Center cruises, in PSEMP Marine Waters Workgroup. 2025. Puget Sound marine waters: 2024](#)
1359 [overview. J. Apple, R. Wold, K. Stark, and J. Newton \(Eds\). Pgs. 24–25. 2025c.](#)

1360 Archer, D., Eby, M., Brovkin, V., Ridgwell, A., Cao, L., Mikolajewicz, U., Caldeira, K., Matsumoto, K., Munhoven,
1361 G., Montenegro, A., and Tokos, K.: Atmospheric lifetime of fossil fuel carbon dioxide, Annu. Rev. Earth Planet.
1362 Sci., 37(1), 117–134, <https://doi.org/10.1146/annurev.earth.031208.100206>, 2009.

1363 Archer, D.: The Global Carbon Cycle, Princeton University Press, JSTOR, <https://doi.org/10.2307/j.ctvc4m4hx8>,
1364 2010.

1365 Bach, L. T., Gill, S. J., Rickaby, R. E., Gore, S., and Renforth, P.: CO₂ removal with enhanced weathering and ocean
1366 alkalinity enhancement: Potential risks and co-benefits for marine pelagic ecosystems, Front. clim., 1,
1367 <https://doi.org/10.3389/fclim.2019.00007>, 2019.

1368 Bakker, D. C. E., Pfeil, B., Smith, K., Hankin, S., Olsen, A., Alin, S. R., Cosca, C., Harasawa, S., Kozyr, A., Nojiri,
1369 Y., O'Brien, K. M., Schuster, U., Telszewski, M., Tilbrook, B., Wada, C., Akl, J., Barbero, L., Bates, N. R., Boutin,
1370 J., Bozec, Y., Cai, W.-J., Castle, R. D., Chavez, F. P., Chen, L., Chierici, M., Currie, K., de Baar, H. J. W., Evans,
1371 W., Feely, R. A., Fransson, A., Gao, Z., Hales, B., Hardman-Mountford, N. J., Hoppema, M., Huang, W.-J., Hunt,
1372 C. W., Huss, B., Ichikawa, T., Johannessen, T., Jones, E. M., Jones, S. D., Jutterström, S., Kitidis, V., Körtzinger,

1373 A., Landschützer, P., Lauvset, S. K., Lefèvre, N., Manke, A. B., Mathis, J. T., Merlivat, L., Metzl, N., Murata, A.,
1374 Newberger, T., Omar, A. M., Ono, T., Park, G.-H., Paterson, K., Pierrot, D., Ríos, A. F., Sabine, C. L., Saito, S.,
1375 Salisbury, J., Sarma, V. V. S. S., Schlitzer, R., Sieger, R., Skjelvan, I., Steinhoff, T., Sullivan, K. F., Sun, H., Sutton,
1376 A. J., Suzuki, T., Sweeney, C., Takahashi, T., Tjiputra, J., Tsurushima, N., van Heuven, S. M. A. C., Vandemark,
1377 D., Vlahos, P., Wallace, D. W. R., Wanninkhof, R., and Watson, A. J.: An update to the Surface Ocean CO₂ Atlas
1378 (SOCAT version 2), *Earth Syst. Sci. Data*, 6, 69–90, <https://doi.org/10.5194/essd-6-69-2014>, 2014.

1379 Bakker, D. C. E., Pfeil, B., Landa, C. S., Metzl, N., O'Brien, K. M., Olsen, A., Smith, K., Cosca, C., Harasawa, S.,
1380 Jones, S. D., Nakaoka, S., Nojiri, Y., Schuster, U., Steinhoff, T., Sweeney, C., Takahashi, T., Tilbrook, B., Wada,
1381 C., Wanninkhof, R., Alin, S. R., Balestrini, C. F., Barbero, L., Bates, N. R., Bianchi, A. A., Bonou, F., Boutin, J.,
1382 Bozec, Y., Burger, E. F., Cai, W.-J., Castle, R. D., Chen, L., Chierici, M., Currie, K., Evans, W., Featherstone, C.,
1383 Feely, R. A., Fransson, A., Goyet, C., Greenwood, N., Gregor, L., Hankin, S., Hardman-Mountford, N. J., Harlay, J.,
1384 Hauck, J., Hoppema, M., Humphreys, M. P., Hunt, C. W., Huss, B., Ibáñez, J. S. P., Johannessen, T., Keeling, R.,
1385 Kitidis, V., Körtzinger, A., Kozyr, A., Krasakopoulou, E., Kuwata, A., Landschützer, P., Lauvset, S. K., Lefèvre, N.,
1386 Lo Monaco, C., Manke, A., Mathis, J. T., Merlivat, L., Millero, F. J., Monteiro, P. M. S., Munro, D. R., Murata, A.,
1387 Newberger, T., Omar, A. M., Ono, T., Paterson, K., Pearce, D., Pierrot, D., Robbins, L. L., Saito, S., Salisbury, J.,
1388 Schlitzer, R., Schneider, B., Schweitzer, R., Sieger, R., Skjelvan, I., Sullivan, K. F., Sutherland, S. C., Sutton, A. J.,
1389 Tadokoro, K., Telszewski, M., Tuma, M., van Heuven, S. M. A. C., Vandemark, D., Ward, B., Watson, A. J., and
1390 Xu, S. (2016). A multi-decade record of high-quality fCO₂ data in version 3 of the Surface Ocean CO₂ Atlas
1391 (SOCAT), *Earth Syst. Sci. Data*, 8, 383–413, <https://doi.org/10.5194/essd-8-383-2016>.

1392 Bakker, D. C. E.; Alin, S. R.; Aramaki, T.; Barbero, L.; Bates, N. R.; Gkritzalis, T.; Jones, S. D.; Kozyr, A.;
1393 Lauvset, S. K.; Macovei, V.; Metzl, N.; Munro, D. R.; Nakaoka, S.-i.; O'Brien, K. M.; Olsen, A.; Pierrot, D.;
1394 Steinhoff, T.; Sullivan, K. F.; Sutton, A. J.; Sweeney, C.; Wada, C.; Wanninkhof, R.; Akl, J.; Arbilla, L. A.; Azetsu-
1395 Scott, K.; Battisti, R.; Beatty, C. M.; Becker, M.; Benoit-Cattin, A.; Berghoff, C. F.; Bittig, H. C.; Bonin, J. A.; Bott,
1396 R.; Bozzano, R.; Burger, E. F.; Brunetti, F.; Cantoni, C.; Castelli, G.; Chambers, D. P.; Chierici, M.; Corbo, A.;
1397 Cronin, M.; Cross, J. N.; Currie, K. I.; Dentico, C.; Emerson, S. R.; Enochs, I.; Enright, M. P.; Enyo, K.; Ericson,
1398 Y.; Evans, W.; Fay, A. R.; Feely, R. A.; Fragiaco, E.; Fransson, A.; Gehrung, M.; Giani, M.; Glockzin, M.;
1399 Hamna, S.; Holodkov, N.; Hoppema, M.; Ibáñez, J. S. P.; Kadono, K.; Kamb, L.; Kralj, M.; Kristensin, T. O.;
1400 Laudicella, V. A.; Lefèvre, N.; Leseurre, C.; Lo Monaco, C.; Maenner Jones, S. M.; Maenza, R. A.; McAuliffe, A.
1401 M.; Mdokwana, B. W.; Monacci, N. M.; Musielewicz, S.; Neill, C.; Newberger, T.; Nojiri, Y.; Ohman, M. D.;
1402 Ólafsdóttir, S. R.; Olivier, L.; Omar, A.; Osborne, J.; Pensieri, S.; Petersen, W.; Plueddemann, A. J.; Rehder, G.;
1403 Roden, N. P.; Rutgersson, A.; Sallée, J.-B.; Sanders, R.; Sarpe, D.; Schirnik, C.; Schlitzer, R.; Send, U.; Skjelvan, I.;
1404 Sutherland, S. C.; T'Jampens, M.; Tamsitt, V.; Telszewski, M.; Theetaert, H.; Tilbrook, B.; Trull, T.; Tsanwani, M.;
1405 Van de Velde, S.; Van Heuven, S. M. A. C.; Vecchia, M. H.; Voynova, Y. G.; Weller, R. A.; Williams, N. L.: Surface
1406 Ocean CO₂ Atlas Database Version 2025 (SOCATv2025) (NCEI Accession 0304549). NOAA National Centers for
1407 Environmental Information. Dataset. <https://doi.org/10.25921/648f-fv35>, 2025.

1408 Barth, A., Beckers, J.-M., Troupin, C., Alvera-Azcárate, A., and Vandembulcke, L.: DIVAnd-1.0: n-dimensional
1409 variational data analysis for ocean observations, *Geosci. Model Dev.*, 7, 225-241, [https://doi.org/10.5194/gmd-7-](https://doi.org/10.5194/gmd-7-225-2014)
1410 225-2014, 2014.

1411 Bates N. R., Johnson R. J.: Acceleration of ocean warming, salinification, deoxygenation, and acidification in the
1412 surface subtropical North Atlantic Ocean. *Nat. Commun. Earth Environ.* 1, 1–12, 2020.

1413 Bates, N.R., and Johnson, R.J.: Forty years of ocean acidification observations (1983-2023) in the Sargasso Sea at
1414 the Bermuda Atlantic Time-series Study (BATS) site, *Frontiers in Marine Science*, 10,
1415 <https://doi.org/10.3389/fmars.2023.1289931>, 2023.

1416 Bates, N., Johnson, R. J., Lomas, M.W., Steinberg, D.K., Lopez, P., Hayden, M., May, R., Derbyshire, L., Lethaby,
1417 P. J., Smith, D., and Lomas, D.: Determination of carbon, nitrogen, and phosphorus content in sinking particles at
1418 the Bermuda Atlantic Time-series Study (BATS) site from December 1988 to December 2023 using a Particle
1419 Interceptor Trap System (PITS). Biological and Chemical Oceanography Data Management Office (BCO-DMO).
1420 (Version 4) Version Date 2024-11-14 [if applicable, indicate subset used]. doi:10.26008/1912/bco-dmo.894099.4
1421 [access date], 2024a.

1422 Bates, N., Johnson, R. J., Lethaby, P. J., Smith, D., and Medley, C.: Primary productivity estimates from the
1423 incubation of seawater collected at the Bermuda Atlantic Time-series Study (BATS) site from December 1988
1424 through December 2023. Biological and Chemical Oceanography Data Management Office (BCO-DMO). (Version
1425 4) Version Date 2024-11-14 [if applicable, indicate subset used]. doi:10.26008/1912/bco-dmo.893182.4 [access
1426 date], 2024b.

1427 Bates, N., Johnson, R. J., Lethaby, P. J., Smith, D., and Medley, C.: HPLC and fluorometric derived phytoplankton
1428 pigment concentrations from seawater collected on BATS Validation cruises from June 1996 to June 2023.
1429 Biological and Chemical Oceanography Data Management Office (BCO-DMO). (Version 4) Version Date 2024-09-
1430 18 [if applicable, indicate subset used]. doi:10.26008/1912/bco-dmo.926534.4 [access date], 2024c.

1431 Bates, N., Johnson, R. J., Lethaby, P. J., Medley, C., and Smith, D.: HPLC and fluorometric derived phytoplankton
1432 pigment concentrations from seawater collected at the Bermuda Atlantic Time-series Study (BATS) site from
1433 October 1988 through December 2023. Biological and Chemical Oceanography Data Management Office (BCO-
1434 DMO). (Version 6) Version Date 2023-09-13 [if applicable, indicate subset used]. doi:10.26008/1912/bco-
1435 dmo.893521.6 [access date], 2024d.

1436 Bates, N., Johnson, R. J., Smith, D., Lethaby, P. J., Lomas, M.W., and Lomas, D.: Discrete bottle samples collected
1437 during BATS Validation (BVAL) cruises from April 1991 through June 2023. Biological and Chemical
1438 Oceanography Data Management Office (BCO-DMO). (Version 5) Version Date 2024-10-01 [if applicable, indicate
1439 subset used]. doi:10.26008/1912/bco-dmo.917255.5 [access date], 2024e.

1440 Bennington, V., Gloege, L., and McKinley, G. A.: Variability in the global ocean carbon sink from 1959 to 2020 by

1441 correcting models with observations, *Geophys. Res. Lett.*, 49(14), <https://doi.org/10.1029/2022gl098632>, 2022a.

1442 Bennington, V., Galjanic, T., and McKinley, G. A.: Explicit physical knowledge in machine learning for Ocean
1443 Carbon Flux Reconstruction: The $p\text{CO}_2$ -residual method. *J. Adv. Model. Earth Syst.*, 14(10),
1444 <https://doi.org/10.1029/2021ms002960>, 2022b.

1445 Bertin, C., Carroll, D., Menemenlis, D., Dutkiewicz, S., Zhang, H., Matsuoka, A., Tank, S., Manizza, M., Miller, C.
1446 E., Babin, M., Mangin, A., and Le Fouest, V.: Biogeochemical River runoff drives intense coastal Arctic Ocean CO_2
1447 outgassing, *Geophys. Res. Lett.*, 50(8), <https://doi.org/10.1029/2022g1102377>, 2023.

1448 Bittig, H. C., Steinhoff, T., Claustre, H., Fiedler, B., Williams, N. L., Sauzède, R., Körtzinger, A., and Gattuso, J.-P.:
1449 An alternative to static climatologies: Robust estimation of open ocean CO_2 variables and nutrient concentrations
1450 from T, S, and O_2 data using Bayesian Neural Networks, *Frontiers in Marine Science*, 5,
1451 <https://doi.org/10.3389/fmars.2018.00328>, 2018.

1452 Bittig, H. C., Jacobs, E., Neumann, T., and Rehder, G.: A regional $p\text{CO}_2$ climatology of the Baltic Sea, PANGAEA
1453 [data set], <https://doi.org/10.1594/PANGAEA.961119>, 2023.

1454 Bittig, H.C., Jacobs, E., Neumann, T., and Rehder, G.: A regional $p\text{CO}_2$ climatology of the Baltic Sea from in situ
1455 $p\text{CO}_2$ observations and a model-based extrapolation approach, *Earth Syst. Sci. Data*, 16(2), 753–773,
1456 <https://doi.org/10.5194/essd-16-753-2024>, 2024.

1457 Boyer, T. P., Garcia, H. E., Locarnini, R. A., Zweng, M. M., Mishonov, A. V., Reagan, J. R., Weathers, K. A.,
1458 Baranova, O. K., Seidov, D., Smolyar, I. V.: World Ocean Atlas 2018, NOAA National Centers for Environmental
1459 Information, <https://www.ncei.noaa.gov/archive/accession/NCEI-WOA18>, 2018.

1460 Brett, A., Leape, J., Abbott, M., Sakaguchi, H., Cao, L., Chand, K., Golbuu, Y., Martin, T. J., Mayorga, J., and
1461 Myksovoll, M. S.: Ocean Data Need a sea change to help navigate the Warming World. *Nature*, 582(7811), 181–183,
1462 <https://doi.org/10.1038/d41586-020-01668-z>, 2020.

1463 Broecker W. S.: Glacial to interglacial changes in ocean chemistry, *Prog. Oceanogr.*, 11(2), 151–97,
1464 [https://doi.org/10.1016/0079-6611\(82\)90007-6](https://doi.org/10.1016/0079-6611(82)90007-6), 1982.

1465 Broullón, D., Pérez, F. F., Velo, A., Hoppema, M., Olsen, A., Takahashi, T., Key, R. M., Tanhua, T., González-
1466 Dávila, M., Jeansson, E., Kozyr, A., and van Heuven, S. M. A. C.: A global monthly climatology of total alkalinity:
1467 a neural network approach, *Earth Syst. Sci. Data*, 11, 1109–1127, <https://doi.org/10.5194/essd-11-1109-2019>, 2019.

1468 Broullón, D., Pérez, F. F., Velo, A., Hoppema, M., Olsen, A., Takahashi, T., Key, R. M., Tanhua, T., Santana-
1469 Casiano, J. M., and Kozyr, A.: A global monthly climatology of oceanic total dissolved inorganic carbon: A Neural
1470 Network approach, *Earth Syst. Sci. Data*, 12(3), 1725–1743, <https://doi.org/10.5194/essd-12-1725-2020>, 2020a.

1471 Broullón, D.; Pérez, F. F.; Velo, A.; Hoppema, M.; Olsen, A.; Takahashi, T.; Key, R. M.; Tanhua, T.; González-
1472 Dávila, M.; Jeansson, E.; Kozyr, A.; van Heuven, S. M. A. C.: A global monthly climatology of total alkalinity
1473 (AT): a neural network approach (NCEI Accession 0222470). NOAA National Centers for Environmental
1474 Information. Dataset. <https://doi.org/10.25921/5p69-y471>, 2020b.

1475 Broullón, D.; Pérez, F. F.; Velo, A.; Hoppema, M.; Olsen, A.; Takahashi, T.; Key, R. M.; Tanhua, T.; Santana-
1476 Casiano, J. M.; Kozyr, A.: A global monthly climatology of oceanic total dissolved inorganic carbon (DIC): a neural
1477 network approach (NCEI Accession 0222469). NOAA National Centers for Environmental Information. Dataset.
1478 <https://doi.org/10.25921/ndgj-jp24>, 2020c.

1479 Cai, W.-J., Hu, X., Huang, W.-J., Murrell, M. C., Lehrter, J. C., Lohrenz, S. E., Chou, W.-C., Zhai, W., Hollibaugh,
1480 J. T., Wang, Y., Zhao, P., Guo, X., Gundersen, K., Dai, M., and Gong, G.-C.: Acidification of subsurface coastal
1481 waters enhanced by eutrophication, *Nature Geoscience*, 4(11), 766–770, <https://doi.org/10.1038/ngeo1297>, 2011.

1482 Carroll, D., Menemenlis, D., Adkins, J. F., Bowman, K. W., Brix, H., Dutkiewicz, S., Fenty, I., Gierach, M. M.,
1483 Hill, C., Jahn, O., Landschützer, P., Lauderdale, J. M., Liu, J., Manizza, M., Naviaux, J. D., Rödenbeck, C., Schimel,
1484 D. S., Van der Stocken, T., and Zhang, H.: The ECCO-Darwin data-assimilative global ocean biogeochemistry
1485 model: Estimates of seasonal to multidecadal surface ocean pCO₂ and air-sea CO₂ flux, *J. Adv. Model. Earth Syst.*,
1486 12(10), <https://doi.org/10.1029/2019ms001888>, 2020.

1487 Carroll, D., Menemenlis, D., Dutkiewicz, S., Lauderdale, J. M., Adkins, J. F., Bowman, K. W., Brix, H., Fenty, I.,
1488 Gierach, M. M., Hill, C., Jahn, O., Landschützer, P., Manizza, M., Mazloff, M. R., Miller, C. E., Schimel, D. S.,
1489 Verdy, A., Whitt, D. B., and Zhang, H.: Attribution of space-time variability in global-ocean dissolved Inorganic
1490 Carbon, *Global Biogeochemical Cycles*, 36(3), <https://doi.org/10.1029/2021gb007162>, 2022.

1491 Carroll, D., Menemenlis, D., Zhang, H., Mazloff, M., McKinley, G., Fay, A., Dutkiewicz, S., Lauderdale, J., and
1492 Fenty, I.: Evaluation of the ECCO-Darwin Ocean Biogeochemistry State Estimate vs. In-situ Observations (ver 1.0),
1493 Zenodo, <https://doi.org/10.5281/zenodo.10627664>, 2024.

1494 Carter, B. R., Williams, N. L., Gray, A. R., and Feely, R. A.: Locally interpolated alkalinity regression for global
1495 alkalinity estimation, *Limnology and Oceanography: Methods*, 14(4), 268–277, <https://doi.org/10.1002/lom3.10087>,
1496 2016.

1497 Carter, B. R., Feely, R. A., Williams, N. L., Dickson, A. G., Fong, M. B., and Takeshita, Y.: Updated methods for
1498 global locally interpolated estimation of alkalinity, ph, and nitrate, *Limnology and Oceanography: Methods*, 16(2),
1499 119–131, <https://doi.org/10.1002/lom3.10232>, 2017.

1500 [Carter, B. R., Feely, R. A., Lauvset, S. K., Olsen, A., DeVries, T., and Sonnerup, R.: Preformed properties for](#)
1501 [marine organic matter and carbonate mineral cycling quantification. *Global Biogeochemical Cycles*, 35\(1\).](#)
1502 <https://doi.org/10.1029/2020gb006623>, 2020.

1503 Carter, B. R., Bittig, H. C., Fassbender, A. J., Sharp, J. D., Takeshita, Y., Xu, Y.-Y., et al.: New and updated global
1504 empirical seawater property estimation routines, *Limnol. and Oceanogr.: Methods*, 19(12), 785–809,
1505 <https://doi.org/10.1002/lom3.10461>, 2021.

1506 [Carter, B. R., Schwinger, J., Sonnerup, R., Fassbender, A. J., Sharp, J. D., Dias, L. M., and Sandborn, D. E.: Tracer-](#)
1507 [based Rapid Anthropogenic Carbon Estimation \(TRACE\), *Earth Syst. Sci. Data*, 17, 3073–3088,](#)
1508 <https://doi.org/10.5194/essd-17-3073-2025>, 2025.

1509 [Carter, B.: Anthropogenic carbon distributions from preindustrial to 2500 c.e. estimated using Tracer-based Rapid](#)
1510 [Anthropogenic Carbon Estimation \(version 1\) \[Data set\]. Zenodo. <https://doi.org/10.5281/zenodo.15003059>, 2025.](#)

1511 Chakraborty, K., Joshi, A. P., Ghoshal, P. K., Baduru, B., Valsala, V., Sarma, V. V. S. S., Metzl, N., Gehlen, M.,
1512 Chevallier, F., and Lo Monaco, C.: Indian Ocean acidification and its driving mechanisms over the last four decades
1513 (1980–2019), *Global Biogeochemical Cycles*, 38(9), <https://doi.org/10.1029/2024gb008139>, 2024.

1514 Chakraborty, K.; Joshi, A. P.; Ghoshal, P. K.; Baduru, B.; Valsala, V.; Sarma, V. V. S. S.; Metzl, N.; Gehlen, M.;
1515 Chevallier, F.; Lo Monaco, C.: Indian ocean acidification and its driving mechanisms over the last four decades
1516 from 1980-01-01 to 2019-12-31 (NCEI Accession 0307663). NOAA National Centers for Environmental
1517 Information. Dataset. <https://doi.org/10.25921/z2x4-vt48>, 2025.

1518 Chau, T.-T.-T., Gehlen, M., and Chevallier, F.: A seamless ensemble-based reconstruction of surface ocean $p\text{CO}_2$
1519 and air–sea CO_2 fluxes over the global coastal and open oceans. *Biogeosciences*, 19(4), 1087–1109,
1520 <https://doi.org/10.5194/bg-19-1087-2022>, 2022.

1521 Chau, T.-T.-T., Gehlen, M., Metzl, N., and Chevallier, F.: CMEMS-LSCCE: a global, 0.25°, monthly reconstruction
1522 of the surface ocean carbonate system, *Earth Syst. Sci. Data*, 16, 121–160, [https://doi.org/10.5194/essd-16-121-](https://doi.org/10.5194/essd-16-121-2024)
1523 [2024](https://doi.org/10.5194/essd-16-121-2024), 2024a.

1524 Chau, T.-T.-T., Chevallier, F. and Gehlen, M.: Global analysis of surface ocean CO_2 fugacity and air-sea fluxes with
1525 low latency, *Geophys. Res. Lett.*, <https://doi.org/10.1029/2023GL106670>, 2024b.

1526 Chen, C.-T. A., Lui, H.-K., Hsieh, C.-H., Yanagi, T., Kosugi, N., Ishii, M., and Gong, G.-C.: Deep oceans may
1527 acidify faster than anticipated due to global warming, *Nat. Clim. Change.*, 7(12), 890–894,
1528 <https://doi.org/10.1038/s41558-017-0003-y>, 2017.

1529 Clement, D., and Gruber, N.: The EMLR(C*) method to determine decadal changes in the global ocean storage of
1530 Anthropogenic CO_2 . *Global Biogeochemical Cycles*, 32(4), 654–679, <https://doi.org/10.1002/2017gb005819>, 2018.

1531 Cooley, S. R., and Doney, S. C.: Anticipating ocean acidification’s economic consequences for commercial
1532 fisheries. *Environmental Research Letters*, 4(2), 024007, <https://doi.org/10.1088/1748-9326/4/2/024007>, 2009.

1533 Crisp, D., Dolman, H., Tanhua, T., McKinley, G. A., Hauck, J., Bastos, A., Sitch, S., Eggleston, S., and Aich, V.:
1534 How well do we understand the land-ocean-atmosphere carbon cycle? *Reviews of Geophysics*, 60(2),
1535 <https://doi.org/10.1029/2021RG000736>, 2022.

1536 Cyr, F., Gibb, O., Azetsu-Scott, K., Chassé, J., Galbraith, P., Maillet, G., Pepin, P., Punshon, S., and Starr, M.:
1537 Ocean carbonate parameters on the Canadian Atlantic Continental Shelf, Federated Research Data Repository,
1538 <https://doi.org/10.20383/102.0673>, 2022.

1539 Delaigue, L., Sulpis, O., Reichart, G. -J., and Humphreys, M. P.: The changing biological carbon pump of the South
1540 Atlantic Ocean. *Global Biogeochemical Cycles*, 38(9), <https://doi.org/10.1029/2024gb008202>, 2024.

1541 DeVries, T., Holzer, M. and Primeau, F.: Recent increase in oceanic carbon uptake driven by weaker upper-ocean
1542 overturning, *Nature*, 542, 215–218, <https://doi.org/10.1038/nature21068>, 2017.

1543 DeVries, T., Le Quéré, C., Andrews, O., Berthet, S., Hauck, J., Ilyina, T., Landschützer, P., Lenton, A., Lima, I. D.,
1544 Nowicki, M., Schwinger, J., and Séférian, R.: Decadal trends in the ocean carbon sink, *Proceedings of the National
1545 Academy of Sciences*, 116(24), 11646–11651, <https://doi.org/10.1073/pnas.1900371116>, 2019.

1546 DeVries, T.: The Ocean Carbon Cycle, *Annual Review of Environment and Resources*, 47(1), 317–341,
1547 <https://doi.org/10.1146/annurev-environ-120920-111307>, 2022a.

1548 DeVries, T.: Atmospheric CO₂ and sea surface temperature variability cannot explain recent decadal variability of
1549 the Ocean CO₂ Sink. *Geophysical Research Letters*, 49(7), <https://doi.org/10.1029/2021gl096018>, 2022b.

1550 DeVries, T., Yamamoto, K., Wanninkhof, R., Gruber, N., Hauck, J., Müller, J. D., Bopp, L., Carroll, D., Carter, B.,
1551 Chau, T., Doney, S. C., Gehlen, M., Gloege, L., Gregor, L., Henson, S., Kim, J. H., Iida, Y., Ilyina, T.,
1552 Landschützer, P., Le Quéré, C., Munro, D., Nissen, C., Patara, L., Pérez, F. F., Resplandy, L., Rodgers, K. B.,
1553 Schwinger, J., Séférian, R., Sicardi, V., Terhaar, J., Triñanes, J., Tsujino, H., Watson, A., Yasunaka, S., Zeng, J.
1554 (2023). Magnitude, trends, and variability of the Global Ocean Carbon Sink from 1985 to 2018. *Global
1555 Biogeochemical Cycles*, 37(10), <https://doi.org/10.1029/2023gb007780>, 2023.

1556 Dickson, A. G.: Standard potential of the reaction: $\text{AgCl}(s) + 1/2 \text{H}_2(g) = \text{Ag}(s) + \text{HCl}(aq)$, and the standard acidity
1557 constant of the ion HSO_4^- in synthetic seawater from 273.15 to 318.15K, *Journal of Chemical Thermodynamics*,
1558 22(2), 113–127, [https://doi.org/10.1016/0021-9614\(90\)90074-Z](https://doi.org/10.1016/0021-9614(90)90074-Z), 1990.

1559 Doney, S. C., Busch, D. S., Cooley, S. R., and Kroeker, K. J.: The impacts of ocean acidification on marine
1560 ecosystems and reliant human communities, *Annual Review of Environment and Resources*, 45(1), 83–112,
1561 <https://doi.org/10.1146/annurev-environ-012320-083019>, 2020.

1562 Dore, J. E., Lukas, R., Sadler, D. W., and Karl, D. M.: Climate-driven changes to the atmospheric CO₂ sink in the
1563 subtropical North Pacific Ocean, *Nature*, 424, 754–757, <https://doi.org/10.1038/nature01885>, 2003.

1564 Dore, J. E., Lukas, R., Sadler, D. W., Church, M. J., and Karl, D. M.: Physical and biogeochemical modulation of
1565 ocean acidification in the central North Pacific, *Proc. Natl. Acad. Sci.*, 106, 12235-12240,
1566 <https://doi.org/10.1073/pnas.0906044106>, 2009.

1567 Dore, J. E., Church, M. J., Karl, D. M., Sadler, D. W., and Letelier, R. M.: Paired windward and leeward
1568 biogeochemical time series reveal consistent surface ocean CO₂ trends across the Hawaiian Ridge, *Geophys. Res.*
1569 *Lett.*, 41, 6459-6467, <https://doi.org/10.1002/2014GL060725>, 2014.

1570 Dore, J.E., White, A.E., and Karl, D.M.: Hawaii Ocean Time-series (HOT) Carbon Dioxide (Version 1) [Data set].
1571 Zenodo. <https://doi.org/10.5281/zenodo.15060931>, 2025.

1572 Dunne, John P., John, J. G., Shevliakova, E., Stouffer, R. J., Krasting, J. P., Malyshev, S. L., Milly, P. C., Sentman,
1573 L. T., Adcroft, A. J., Cooke, W., Dunne, K. A., Griffies, S. M., Hallberg, R. W., Harrison, M. J., Levy, H.,
1574 Wittenberg, A. T., Phillips, P. J., and Zadeh, N.: GFDL's ESM2 global coupled climate-carbon earth system
1575 models. part II: Carbon system formulation and baseline simulation characteristics, *Journal of Climate*, 26(7), 2247–
1576 2267, <https://doi.org/10.1175/jcli-d-12-00150.1>, 2013.

1577 Dunne, J. P., Hewitt, H. T., Arblaster, J., Bonou, F., Boucher, O., Cavazos, T., Durack, P. J., Hassler, B., Juckes, M.,
1578 Miyakawa, T., Mizielinski, M., Naik, V., Nicholls, Z., O'Rourke, E., Pincus, R., Sanderson, B. M., Simpson, I. R.,
1579 and Taylor, K. E.: An Evolving Coupled Model Intercomparison Project Phase 7 (CMIP7) and Fast Track in
1580 Support of Future Climate Assessment, <https://doi.org/10.5194/egusphere-2024-3874>, 2024.

1581 Durack, P. J., Taylor, K. E., Gleckler, P. J., Meehl, G. A., Lawrence, B. N., Covey, C., Stouffer, R. J., Levvasseur,
1582 G., Ben-Nasser, A., Denvil, S., Stockhause, M., Gregory, J. M., Juckes, M., Ames, S. K., Antonio, F., Bader, D. C.,
1583 Dunne, J. P., Ellis, D., Eyring, V., Fiore, S. L., Joussaume, S., Kershaw, P., Lamarque, J.-F., Lautenschlager, M.,
1584 Lee, J., Mauzey, C. F., Mizielinski, M., Nassisi, P., Nuzzo, A., O'Rourke, E., Painter, J., Potter, G. L., Rodriguez,
1585 S., Williams, D. N.: The Coupled Model Intercomparison Project (CMIP): Reviewing Project History, Evolution,
1586 Infrastructure and Implementation, <https://doi.org/10.5194/egusphere-2024-3729>, 2025.

1587 Edmond, J. M.: High precision determination of titration alkalinity and total carbon dioxide content of sea water by
1588 potentiometric titration, *Deep Sea Research and Oceanographic Abstracts*, 17(4), 737–750,
1589 [https://doi.org/10.1016/0011-7471\(70\)90038-0](https://doi.org/10.1016/0011-7471(70)90038-0), 1970.

1590 Fassbender, A. J., Carter, B. R., Sharp, J. D., Huang, Y., Arroyo, M. C., and Frenzel, H.: Amplified subsurface
1591 signals of ocean acidification, *Global Biogeochemical Cycles*, 37, e2023GB007843,
1592 <https://doi.org/10.1029/2023GB007843>, 2023.

1593 Fassbender, A. J.: Near-global, upper 2000 m estimates of preindustrial and year 2002 ocean pH, aragonite
1594 saturation state, carbon dioxide partial pressure, hydrogen ion concentration, and Revelle factor values, and their
1595 total changes caused by anthropogenic carbon accumulation in addition to the component of the changes induced by

1596 carbonate system nonlinearities (NCEI Accession 0290073). NOAA National Centers for Environmental
1597 Information. Dataset. <https://doi.org/10.25921/rdr-9t74>, 2024.

1598 Fay, A. R., Gregor, L., Landschützer, P., McKinley, G. A., Gruber, N., Gehlen, M., Iida, Y., Laruelle, G. G.,
1599 Rödenbeck, C., Roobaert, A., and Zeng, J.: SeaFlux: harmonization of air–sea CO₂ fluxes from surface pCO₂ data
1600 products using a standardized approach, *Earth Sys. Sci. Data*, 13(10), 4693–4710, [https://doi.org/10.5194/essd-13-](https://doi.org/10.5194/essd-13-4693-2021)
1601 4693-2021, 2021.

1602 Fay, A. R., and McKinley, G. A.: Observed regional fluxes to constrain modelled estimates of the Ocean Carbon
1603 Sink, *Geophysical Res. Lett.*, 48(20), <https://doi.org/10.1029/2021gl095325>, 2021.

1604 Fay, A. R., Munro, D. R., McKinley, G. A., Pierrot, D., Sutherland, S. C., Sweeney, C., and Wanninkhof, R.:
1605 Updated climatological mean Δ /CO₂ and net sea–air CO₂ flux over the global open ocean regions, *Earth Syst. Sci.*
1606 *Data*, 16, 2123–2139, <https://doi.org/10.5194/essd-16-2123-2024>, 2024.

1607 Feely, R. A., Jiang, L.-Q., Wanninkhof, R., Carter, B. R., Alin, S. A., Bednaršek, N., and Cosca, C. E.: Acidification
1608 of the global surface ocean: What we have learned from observations, *Oceanography*, 36, 120-129,
1609 <https://doi.org/10.5670/oceanog.2023.222>, 2023.

1610 Fennel, K., Mattern, J. P., Doney, S. C., Bopp, L., Moore, A. M., Wang, B., and Yu, L.: Ocean biogeochemical
1611 modelling, *Nat. Rev. Methods Primers*, 2, 76, <https://doi.org/10.1038/s43586-022-00154-2>, 2022.

1612 Franco, A. C., Ianson, D., Ross, T., Hamme, R. C., Monahan, A. H., Christian, J. R., Davelaar, M., Johnson, W. K.,
1613 Miller, L. A., Robert, M., and Tortell, P. D.: Anthropogenic and climatic contributions to observed carbon system
1614 trends in the northeast Pacific. *Global Biogeochemical Cycles*, 35(7). <https://doi.org/10.1029/2020GB006829>,
1615 2021a.

1616 Franco, A. C., Ianson, D., Ross, T., Hamme, R. C., Monahan, A. H., Christian, J. R., Davelaar, M., Johnson, W. K.,
1617 Miller, L. A., Robert, M., and Tortell, P. D.: A compilation of inorganic carbon system and other hydrographic and
1618 chemical discrete profile measurements obtained during the fifty five Line P cruises in the Northeast Pacific Ocean
1619 over the period from 1990 to 2019 (NCEI Accession 0234342). NOAA National Centers for Environmental
1620 Information. Dataset. <https://doi.org/10.25921/zrw8-kn24>, 2021b.

1621 Freeland, H.: A short history of Ocean Station Papa and Line P. *Progress in Oceanography*, 75(2), 120–125,
1622 <https://doi.org/10.1016/j.pocean.2007.08.005>, 2007.

1623 Friedlingstein, P., O'Sullivan, M., Jones, M. W., Andrew, R. M., Hauck, J., Landschützer, P., Le Quéré, C., Li, H.,
1624 Lujikx, I. T., Olsen, A., Peters, G. P., Peters, W., Pongratz, J., Schwingshackl, C., Sitch, S., Canadell, J. G., Ciais,
1625 P., Jackson, R. B., Alin, S. R., Armeth, A., Arora, V., Bates, N. R., Becker, M., Bellouin, N., Berghoff, C. F., Bittig,
1626 H. C., Bopp, L., Cadule, P., Campbell, K., Chamberlain, M. A., Chandra, N., Chevallier, F., Chini, L. P., Colligan,

1627 T., Decayeux, J., Djeutchouang, L. M., Dou, X., Duran Rojas, C., Enyo, K., Evans, W., Fay, A. R., Feely, R. A.,
1628 Ford, D. J., Foster, A., Gasser, T., Gehlen, M., Gkritzalis, T., Grassi, G., Gregor, L., Gruber, N., Gürses, Ö., Harris,
1629 I., Hefner, M., Heinke, J., Hurtt, G. C., Iida, Y., Ilyina, T., Jacobson, A. R., Jain, A. K., Jarníková, T., Jersild, A.,
1630 Jiang, F., Jin, Z., Kato, E., Keeling, R. F., Klein Goldewijk, K., Knauer, J., Korsbakken, J. I., Lan, X., Lauvset, S.
1631 K., Lefèvre, N., Liu, Z., Liu, J., Ma, L., Maksyutov, S., Marland, G., Mayot, N., McGuire, P. C., Metzl, N.,
1632 Monacci, N. M., Morgan, E. J., Nakaoka, S.-I., Neill, C., Niwa, Y., Nützel, T., Olivier, L., Ono, T., Palmer, P. I.,
1633 Pierrot, D., Qin, Z., Resplandy, L., Roobaert, A., Rosan, T. M., Rödenbeck, C., Schwinger, J., Smallman, T. L.,
1634 Smith, S. M., Sospedra-Alfonso, R., Steinhoff, T., Sun, Q., Sutton, A. J., Séférian, R., Takao, S., Tatebe, H., Tian,
1635 H., Tilbrook, B., Torres, O., Tourigny, E., Tsujino, H., Tubiello, F., van der Werf, G., Wanninkhof, R., Wang, X.,
1636 Yang, D., Yang, X., Yu, Z., Yuan, W., Yue, X., Zaehle, S., Zeng, N., and Zeng, J.: Global Carbon Budget 2024,
1637 Earth Syst. Sci. Data, 17, 965–1039, <https://doi.org/10.5194/essd-17-965-2025>, 2025.

1638 Garcia, H. E., Locarnini, R. A., Boyer, T. P., Antonov, J. I., Baranova, O. K., Zweng, M. M., Reagan, J. R., and
1639 Johnson, D. R.: World Ocean Atlas 2013, Volume 3: Dissolved Oxygen, Apparent Oxygen Utilization, and Oxygen
1640 Saturation, edited by: Levitus, S. and Mishonov, A., Technical Ed., NOAA Atlas NES- DIS 75, 27 pp., 2014.

1641 Garcia, H. E., Weathers, K., Paver, C. R., Smolyar, I., Boyer, T. P., Locarnini, R. A., Zweng, M. M., Mishonov, A.
1642 V., Baranova, O. K., Seidov, D., and Reagan, J. R.: World Ocean Atlas 2018, Volume 4: Dissolved Inorganic
1643 Nutrients (phosphate, nitrate and nitrate+nitrite, silicate), A. Mishonov Technical Ed., NOAA Atlas NESDIS 84,
1644 35pp, 2018a.

1645 Garcia H. E., Weathers, K. W., Paver, C. R., Smolyar, I. V., Boyer, T. P., Locarnini, R. A., Zweng, M. M.,
1646 Mishonov, A. V., Baranova, O. K., and Reagan, J. R.: World Ocean Atlas 2018, Volume 3: Dissolved Oxygen,
1647 Apparent Oxygen Utilization, and Oxygen Saturation, Mishonov, A., Technical Editor, NOAA Atlas NESDIS 83,
1648 2018b.

1649 Garcia H. E., Boyer, T. P., Locarnini, R. A., Reagan, J. R., Mishonov, A. V., Baranova, O. K., Paver, C. R., Wang,
1650 Z., Bouchard, C. N., Cross, S. L., Seidov, D., and Dukhovskoy, D.: World Ocean Database 2023: User's Manual.
1651 A.V. Mishonov, Technical Ed., NOAA Atlas NESDIS 98, pp 129. <https://doi.org/10.25923/j8gq-eee82>, 2024.

1652 Gattuso, J.-P., and Hansson, L.: Ocean acidification, Oxford University Press, pp. 326, 2011.

1653 Gattuso, J.-P., Epitalon, J.-M., Lavigne, H., and Orr, J.: seacarb: Seawater Carbonate Chemistry, R Package
1654 (Version 3.2.16), <https://CRAN.R-project.org/package=seacarb>, 2021a.

1655 Gattuso, J.-P., Alliouane, S., Mousseau, L.: Seawater carbonate chemistry in the Bay of Villefranche, Point B
1656 (France), January 2007 - June 2023 [dataset], PANGAEA, <https://doi.org/10.1594/PANGAEA.727120>, 2021b.

1657 Gattuso, J.-P., Alliouane, S., and Fischer, P.: High-frequency, year-round time series of the carbonate chemistry in a
1658 high-Arctic fjord (Svalbard), Earth Syst. Sci. Data, 15, 2809–2825, <https://doi.org/10.5194/essd-15-2809-2023>,

1659 2023a.

1660 Gattuso, J.-P., Alliouane, S., and Fischer, P.: High-frequency, year-round time series of the carbonate chemistry in a
1661 high-Arctic fjord (Svalbard) [dataset], PANGAEA, <https://doi.org/10.1594/PANGAEA.957028>, 2023b.

1662 Ghoshal, P. K., Joshi, A. P., and Chakraborty, K.: An improved long-term high-resolution surface $p\text{CO}_2$ data
1663 product for the Indian Ocean using machine learning, *Scientific Data*, 12(1), [https://doi.org/10.1038/s41597-025-](https://doi.org/10.1038/s41597-025-04914-z)
1664 [04914-z](https://doi.org/10.1038/s41597-025-04914-z), 2025a.

1665 Ghoshal, P. K.; Joshi, A. P.; Chakraborty, K.: An improved long-term high-resolution surface $p\text{CO}_2$ data product for
1666 the Indian Ocean using machine learning from 1980-01-01 to 2020-12-31 (NCEI Accession 0307788). NOAA
1667 National Centers for Environmental Information. Dataset. <https://doi.org/10.25921/r2q9-d197>, 2025b.

1668 Gibb, O., Cyr, F., Azetsu-Scott, K., Chassé, J., Childs, D., Gabriel, C.-E., Galbraith, P. S., Maillet, G., Pepin, P.,
1669 Punshon, S., and Starr, M.: Spatiotemporal variability in pH and carbonate parameters on the Canadian Atlantic
1670 continental shelf between 2014 and 2022, *Earth Syst. Sci. Data*, 15, 4127–4162, [https://doi.org/10.5194/essd-15-](https://doi.org/10.5194/essd-15-4127-2023)
1671 [4127-2023](https://doi.org/10.5194/essd-15-4127-2023), 2023.

1672 Gloege, L., Yan, M., Zheng, T., and McKinley, G. A.: Improved quantification of ocean carbon uptake by using
1673 machine learning to merge global models and $p\text{CO}_2$ data, *Journal of Advances in Modeling Earth Systems*, 14(2),
1674 <https://doi.org/10.1029/2021ms002620>, 2022.

1675 González-Dávila, M. and Santana-Casiano J. M.: Long-term trends of pH and inorganic carbon in the Eastern North
1676 Atlantic: the ESTOC site, *Front. Mar. Sci.*, 10, 1236214, <https://doi.org/10.3389/fmars.2023.1236214>, 2023.

1677 Gregor, L.: luke-gregor/OceanSODA-ETHZ: code, Zenodo, <https://doi.org/10.5281/zenodo.4455354>, 2021.

1678 Gregor, L. and Fay, A.: SeaFlux: harmonised sea-air CO_2 fluxes from surface $p\text{CO}_2$ data products using a
1679 standardised approach [Data set], Zenodo, <https://doi.org/10.5281/zenodo.5482547>, 2021.

1680 Gregor, L., Lebehot, A. D., Kok, S., and Monteiro, P. M. S.: A comparative assessment of the uncertainties of
1681 Global Surface Ocean CO_2 Estimates using a machine-learning ensemble (CSIR-ML6 version 2019a) – have we hit
1682 the wall? *Geoscientific Model Development*, 12(12), 5113–5136, <https://doi.org/10.5194/gmd-12-5113-2019>, 2019a.

1683 Gregor, L., Lebehot, A. D., Kok, S., Monteiro, P. M. S.: Global surface-ocean partial pressure of carbon dioxide
1684 ($p\text{CO}_2$) estimates from a machine learning ensemble: CSIR-ML6 v2019a (NCEI Accession 0206205), NOAA
1685 National Centers for Environmental Information, Dataset, <https://doi.org/10.25921/z682-mn47>, 2019b.

1686 Gregor, L., and Gruber, N.: OceanSODA-ETHZ: A global gridded dataset of the surface ocean carbonate system for
1687 seasonal to decadal studies of ocean acidification (v2023) (NCEI Accession 0220059), NOAA National Centers for
1688 Environmental Information, Dataset, <https://doi.org/10.25921/m5wx-ja34>, 2020.

1689 Gregor, L., and Gruber, N.: Oceansoda-ETHZ: A global gridded data set of the surface ocean carbonate system for
1690 seasonal to decadal studies of ocean acidification, *Earth System Science Data*, 13(2), 777–808,
1691 <https://doi.org/10.5194/essd-13-777-2021>, 2021.

1692 Gregor, L., and Gruber, N.: OceanSODA-ETHZ: A global gridded dataset of the surface ocean carbonate system for
1693 seasonal to decadal studies of ocean acidification (v2023) (NCEI accession 0220059) [Dataset], NOAA National
1694 Centers for Environmental Information, <https://doi.org/10.25921/m5wx-ja34>, 2023.

1695 Gregor, L., Shutler, J., and Gruber, N.: High-resolution variability of the Ocean Carbon Sink, *Global*
1696 *Biogeochemical Cycles*, 38(8), <https://doi.org/10.1029/2024gb008127>, 2024a.

1697 Gregor, L., Shutler, J., and Gruber, N.: OceanSODA-ETHZ-v2: Surface ocean sea-air CO₂ fluxes from 1982 to 2022
1698 (8-day by 0.25° x 0.25°) (v2.2024r01), [Data set], Zenodo, <https://zenodo.org/records/11206366>, 2024b.

1699 Gruber, N., Clement, D., Carter, B. R., Feely, R. A., van Heuven, S., Hoppema, M., Ishii, M., Key, R. M., Kozyr,
1700 A., Lauvset, S. K., Lo Monaco, C., Mathis, J. T., Murata, A., Olsen, A., Perez, F. F., Sabine, C. L., Tanhua, T., and
1701 Wanninkhof, R.: The oceanic sink for anthropogenic CO₂ from 1994 to 2007, *Science*, 363(6432), 1193–1199,
1702 <https://doi.org/10.1126/science.aau5153>, 2019a.

1703 Gruber, N., Clement, D., Carter, B. R., Feely, R. A., van Heuven, S., Hoppema, M., Ishii, M., Key, R. M., Kozyr,
1704 A., Lauvset, S. K., Lo Monaco, C., Mathis, J. T., Murata, A., Olsen, A., Perez, F. F., Sabine, C. L., Tanhua, T., and
1705 Wanninkhof, R.: The oceanic sink for anthropogenic CO₂ from 1994 to 2007 - the data (NCEI Accession 0186034),
1706 NOAA National Centers for Environmental Information, Dataset, <https://doi.org/10.25921/wdn2-pt10>, 2019b.

1707 Gruber, N., Bakker, D. C. E., DeVries, T., Gregor, L., Hauck, J., Landschützer, P., McKinley, G. A., and Müller, J.
1708 D.: Trends and variability in the ocean carbon sink, *Nature Reviews Earth and Environment*, 4(2), 119–134,
1709 <https://doi.org/10.1038/s43017-022-00381-x>, 2023.

1710 Hauck, J., Mayot, N., Landschützer, P., and Jersild, A.: Global Carbon Budget 2024, surface ocean fugacity of CO₂
1711 (*f*CO₂) and air-sea CO₂ flux of individual global ocean biogeochemical models and surface ocean *f*CO₂-based data-
1712 products, Zenodo, <https://doi.org/10.5281/zenodo.14639761>, 2025.

1713 [Hollitzer, H. A. L., Patara, L., Terhaar, J., and Oeschler, A.: Competing effects of wind and buoyancy forcing on](https://doi.org/10.1038/s41467-024-53557-y)
1714 [ocean oxygen trends in recent decades. *Nat Commun* 15, 9264. <https://doi.org/10.1038/s41467-024-53557-y>, 2024.](https://doi.org/10.1038/s41467-024-53557-y)

1715 [Huguenin, M. F., Holmes, R. M., and England, M. H.: Drivers and distribution of global ocean heat uptake over the](https://doi.org/10.1038/s41467-022-32540-5)
1716 [last half century. *Nat Commun* 13, 4921. <https://doi.org/10.1038/s41467-022-32540-5>, 2022.](https://doi.org/10.1038/s41467-022-32540-5)

1717 Humphreys, M. P., Lewis, E. R., Sharp, J. D., and Pierrot, D.: PyCO2SYS v1.8: Marine carbonate system
1718 calculations in Python, *Geoscientific Model Development*, 15(1), 15–43, <https://doi.org/10.5194/gmd-15-15-2022>,
1719 2022.

1720 Iida, Y., Takatani, Y., Kojima, A., and Ishii, M.: Global trends of ocean CO₂ sink and ocean acidification: An
1721 observation-based reconstruction of surface ocean inorganic carbon variables, *Journal of Oceanography*, 77(2), 323–
1722 358, <https://doi.org/10.1007/s10872-020-00571-5>, 2021.

1723 IPCC: Climate Change 2023: Synthesis Report, Contribution of Working Groups I, II and III to the Sixth
1724 Assessment Report of the Intergovernmental Panel on Climate Change [Core Writing Team, H. Lee and J. Romero
1725 (eds.)], IPCC, Geneva, Switzerland, pp. 35-115, <https://doi.org/10.59327/IPCC/AR6-9789291691647>, 2023.

1726 Ishii, M., Kosugi, N., Sasano, D., Saito, S., Midorikawa, T., & Inoue, H. Y.: Ocean acidification off the south coast
1727 of Japan: A result from time series observations of CO₂ Parameters from 1994 to 2008. *Journal of Geophysical*
1728 *Research*, 116(C6), <https://doi.org/10.1029/2010jc006831>, 2011a.

1729 Ishii, M., Suzuki, T., and Key, R.: Pacific Ocean Interior Carbon Data Synthesis, PACIFICA, in Progress, PICES
1730 Press, 19(1), 20-23, https://www.pices.int/publications/pices_press/volume19/v19_n1/pp_20-23_PACIFICA_f.pdf,
1731 2011b.

1732 Jersild, A., Landschützer, P., Gruber, N., Bakker, D. C. E.: An observation-based global monthly gridded sea surface
1733 pCO₂ and air-sea CO₂ flux product from 1982 onward and its monthly climatology (NCEI Accession 0160558),
1734 NOAA National Centers for Environmental Information, Dataset, <https://doi.org/10.7289/v5z899n6>, 2017.

1735 Jiang, L.-Q., Feely, R. A., Carter, B. R., Greeley, D. J., Gledhill, D. K., and Arzayus, K. M.: Climatological
1736 distribution of aragonite saturation state in the global oceans, *Global Biogeochemical Cycles*, 29(10), 1656–1673,
1737 <https://doi.org/10.1002/2015GB005198>, 2015a.

1738 Jiang, L.-Q., Feely, R. A.: Aragonite saturation state gridded to 1x1 degree latitude and longitude at depth levels of 0,
1739 50, 100, 200, 500, 1000, 2000, 3000, and 4000 meters in the global oceans (NCEI Accession 0139360), NOAA
1740 National Centers for Environmental Information, Dataset, <https://doi.org/10.7289/v5q81b4p>, 2015b.

1741 Jiang, L.-Q., Carter, B. R., Feely, R. A., Lauvset, S., and Olsen, A.: Surface ocean pH and buffer capacity: Past,
1742 present and future, *Scientific Reports*, 9(1), 18624, <https://doi.org/10.1038/s41598-019-55039-4>, 2019a.

1743 Jiang, L.-Q., Carter, B. R., Feely, R. A., Lauvset, S., and Olsen, A.: Global surface ocean pH, acidity, and Revelle
1744 Factor on a 1x1 degree global grid from 1770 to 2100 (NCEI Accession 0206289), NOAA National Centers for
1745 Environmental Information, Dataset, <https://doi.org/10.25921/kgqr-9h49>, 2019b.

1746 Jiang, L.-Q., Feely, R. A., Wanninkhof, R., Greeley, D., Barbero, L., Alin, S., Carter, B. R., Pierrot, D.,
1747 Featherstone, C., Hooper, J., Melrose, C., Monacci, N., Sharp, J. D., Shellito, S., Xu, Y.-Y., Kozyr, A., Byrne, R. H.,
1748 Cai, W.-J., Cross, J., Johnson, G. C., Hales, B., Langdon, C., Mathis, J., Salisbury, J., and Townsend, D. W.: Coastal
1749 Ocean Data Analysis Product in North America (CODAP-NA, Version 2021) (NCEI Accession 0219960), NOAA
1750 National Centers for Environmental Information, Dataset, <https://doi.org/10.25921/531n-c230>, 2020.

1751 Jiang, L.-Q., Feely, R. A., Wanninkhof, R., Greeley, D., Barbero, L., Alin, S., Carter, B. R., Pierrot, D.,
1752 Featherstone, C., Hooper, J., Melrose, C., Monacci, N., Sharp, J. D., Shellito, S., Xu, Y.-Y., Kozyr, A., Byrne, R. H.,
1753 Cai, W.-J., Cross, J., Johnson, G. C., Hales, B., Langdon, C., Mathis, J., Salisbury, J., and Townsend, D. W.: Coastal
1754 Ocean Data Analysis Product in North America (CODAP-NA) – an internally consistent data product for discrete
1755 inorganic carbon, oxygen, and nutrients on the North American ocean margins, *Earth Syst. Sci. Data*, 13, 2777–
1756 2799, <https://doi.org/10.5194/essd-13-2777-2021>, 2021.

1757 Jiang, L.-Q., Pierrot, D., Wanninkhof, R., Feely, R. A., Tilbrook, B., Alin, S., Barbero, L., Byrne, R. H., Carter, B.
1758 R., Dickson, A. G., Gattuso, J.-P., Greeley, D., Hoppema, M., Humphreys, M. P., Karstensen, J., Lange, N.,
1759 Lauvset, S. K., Lewis, E. R., Olsen, A., Perez, F. F., Sabine, C., Sharp, J. D., Tanhua, T., Trull, T. W., Velo, A.,
1760 Allegra, A. J., Barker, P., Burger, E., Cai, W.-J., Chen, C.-T. A., Cross, J., Garcia, H., Hernandez-Ayon, J. M., Hu,
1761 X., Kozyr, A., Langdon, C., Lee, K., Salisbury, J., Wang, Z. A., and Xue, L.: Best practice data standards for
1762 discrete chemical oceanographic observations. *Frontiers in Marine Science*, 8,
1763 <https://doi.org/10.3389/fmars.2021.705638>, 2022a.

1764 Jiang, L.-Q., Boyer, T. P., Paver, C. R., Yoo, H., Reagan, J. R., Alin, S. R., Barbero, L., Carter, B. R., Feely, R. A.,
1765 and Wanninkhof, R.: Climatological distribution of ocean acidification indicators from surface to 500 meters water
1766 depth on the North American ocean margins from 2003-12-06 to 2018-11-22 (NCEI Accession 0270962), NOAA
1767 National Centers for Environmental Information, Dataset, <https://doi.org/10.25921/g8pb-zy76>, 2022b.

1768 Jiang, L., Dunne, J., Carter, B. R., Tjiputra, J. F., Terhaar, J., Sharp, J. D., Olsen, A., Alin, S., Bakker, D. C., Feely,
1769 R. A., Gattuso, J., Hogan, P., Ilyina, T., Lange, N., Lauvset, S. K., Lewis, E. R., Lovato, T., Palmieri, J., Santana-
1770 Falcón, Y., Schwinger, J., Séférian, R., Strand, G., Swart, N., Tanhua, T., Tsujino, H., Wanninkhof, R., Watanabe,
1771 M., Yamamoto, A., and Ziehn, T.: Global surface ocean acidification indicators from 1750 to 2100 (NCEI
1772 Accession 0259391), NOAA National Centers for Environmental Information, Dataset,
1773 <https://doi.org/10.25921/9ker-bc48>, 2022c.

1774 Jiang, L., Dunne, J., Carter, B. R., Tjiputra, J. F., Terhaar, J., Sharp, J. D., Olsen, A., Alin, S., Bakker, D. C., Feely,
1775 R. A., Gattuso, J., Hogan, P., Ilyina, T., Lange, N., Lauvset, S. K., Lewis, E. R., Lovato, T., Palmieri, J., Santana-
1776 Falcón, Y., Schwinger, J., Séférian, R., Strand, G., Swart, N., Tanhua, T., Tsujino, H., Wanninkhof, R., Watanabe,
1777 M., Yamamoto, A., and Ziehn, T.: Global surface ocean acidification indicators from 1750 to 2100, *Journal of*
1778 *Advances in Modeling Earth Systems*, 15(3), <https://doi.org/10.1029/2022ms003563>, 2023.

1779 Jiang, L.-Q., Boyer, T. P., Paver, C. R., Yoo, H., Reagan, J. R., Alin, S. R., Barbero, L., Carter, B. R., Feely, R. A.,
1780 and Wanninkhof, R.: Climatological distribution of ocean acidification variables along the North American ocean
1781 margins, *Earth System Science Data*, 16(7), 3383–3390, <https://doi.org/10.5194/essd-16-3383-2024>, 2024.

1782 [John, S. G., Liang, H., Weber, T., DeVries, T., Primeau, F., Moore, K., Holzer, M., Mahowald, N., Gardner, W.,](#)
1783 [Mishonov, A., Richardson, M. J., Faugere, Y., & Taburet, G.: Awesome OCIM: A simple, flexible, and powerful](#)

1784 [tool for modeling elemental cycling in the oceans. *Chemical Geology*, 533, 119403.](#)
1785 <https://doi.org/10.1016/j.chemgeo.2019.119403>, 2020.

1786 Johnson, G. C., Robbins, P. E., and Hufford, G. E. (2001). Systematic adjustments of hydrographic sections for
1787 internal consistency. *Journal of Atmospheric and Oceanic Technology*, 18(7), 1234–1244, 2001.

1788 Joshi, A. P., Ghoshal, P. K., Chakraborty, K., and Sarma, V. V. S. S.: Sea-surface $p\text{CO}_2$ maps for the Bay of Bengal
1789 based on Advanced Machine Learning Algorithms, *Scientific Data*, 11(1), [https://doi.org/10.1038/s41597-024-](https://doi.org/10.1038/s41597-024-03236-w)
1790 03236-w, 2024.

1791 Joshi, A. P.; Ghoshal, P. K.; Chakraborty, K.; Sarma, V. V. S. S.: Sea-surface $p\text{CO}_2$ maps for the Bay of
1792 Bengal based on advanced machine learning algorithms from 2015-01-01 to 2015-12-31 (NCEI Accession
1793 0307627). NOAA National Centers for Environmental Information. Dataset. <https://doi.org/10.25921/2sjr-pg16>,
1794 2025a.

1795 Joshi, A. P., Ghoshal, P. K., Chakraborty, K., Roy, R., Jayaram, C., Sridevi, B., and Sarma, V. V. S. S.: Long-term
1796 changes of surface total alkalinity and its driving mechanisms in the north Indian Ocean. *Global Biogeochemical*
1797 *Cycles*, 39, e2024GB008344, <https://doi.org/10.1029/2024GB008344>, 2025b.

1798 Joshi, A. P.; Ghoshal, P. K.; Chakraborty, K.; Roy, R.; Jayaram, C.; Sridevi, B.; Sarma, V. V. S. S.: Long-term
1799 changes of surface total alkalinity and its driving mechanisms in the Northern Indian Ocean from 1993-01-01 to
1800 2020-12-31 (NCEI Accession 0307789). NOAA National Centers for Environmental Information. Dataset.
1801 <https://doi.org/10.25921/7as7-et15>, 2025c.

1802 Kapsenberg, L., Alliouane, S., Gazeau, F., Mousseau, L., and Gattuso, J.-P.: Coastal ocean acidification and
1803 increasing total alkalinity in the northwestern Mediterranean Sea, *Ocean Sci.*, 13, 411–426,
1804 <https://doi.org/10.5194/os-13-411-2017>, 2017.

1805 Karl, D. M., and Lukas, R.: The Hawaii Ocean Time-series (HOT) program: Background, rationale and field
1806 implementation, *Deep Sea Research Part II*, 43(2–3), 129–156, [https://doi.org/10.1016/0967-0645\(96\)00005-7](https://doi.org/10.1016/0967-0645(96)00005-7),
1807 1996.

1808 Karl, D., Dore, J., Lukas, R., Michaels, A., Bates, N., and Knap, A.: Building the long-term picture: The U.S.
1809 JGOFS Time-series programs. *Oceanography*, 14(4), 6–17, <https://doi.org/10.5670/oceanog.2001.02>, 2001.

1810 Kennedy, E. G., Zulian, M., Hamilton, S. L., Hill, T. M., Delgado, M., Fish, C. R., Gaylord, B., Kroeker, K. J.,
1811 Palmer, H. M., Ricart, A. M., Sanford, E., Spalding, A. K., Ward, M., Carrasco, G., Elliott, M., Grisby, G. V.,
1812 Harris, E., Jahncke, J., Rocheleau, C. N., Westerink, S., and Wilmot, M. I.: Multistressor Observations of Coastal
1813 Hypoxia and Acidification (MOCHA) Synthesis (NCEI Accession 0277984), NOAA National Centers for
1814 Environmental Information, Dataset, <https://doi.org/10.25921/2vve-fh39>, 2023.

1815 Kennedy, E. G., Zilian, M., Hamilton, S. L., Hill, T. M., Delgado, M., Fish, C. R., Gaylord, B., Kroeker, K. J.,
1816 Palmer, H. M., Ricart, A. M., Sanford, E., Spalding, A. K., Ward, M., Carrasco, G., Elliott, M., Grisby, G. V.,
1817 Harris, E., Jahncke, J., Rocheleau, C. N., Westerink, S., and Wilmot, M. I.: A high-resolution synthesis dataset for
1818 multistressor analyses along the US West Coast, *Earth Syst. Sci. Data*, 16, 219–243, [https://doi.org/10.5194/essd-](https://doi.org/10.5194/essd-16-219-2024)
1819 16-219-2024, 2024.

1820 Keppler, L., Landschützer, P., Gruber, N., Lauvset, S. K., and Stemmler, I.: Seasonal carbon dynamics in the near-
1821 global ocean, *Global Biogeochemical Cycles*, 34(12), e2020GB006571, <https://doi.org/10.1029/2020GB006571>,
1822 2020.

1823 Keppler, L., Landschützer, P., Lauvset, S. K., and Gruber, N.: Recent trends and variability in the oceanic storage of
1824 dissolved inorganic carbon, *Global Biogeochemical Cycles*, 37(5), <https://doi.org/10.1029/2022gb007677>, 2023a.

1825 Keppler, L.; Landschützer, P.; Lauvset, S. K.; and Gruber, N.: Mapped Observation-Based Oceanic Dissolved
1826 Inorganic Carbon Monthly fields from 2004 through 2019 (MOBO-DIC2004-2019) (NCEI Accession 0277099).
1827 NOAA National Centers for Environmental Information. Dataset. <https://doi.org/10.25921/z31n-3m26>, 2023b.

1828 Key, R. M., Kozyr, A., Sabine, C. L., Lee, K., Wanninkhof, R., Bullister, J. L., Feely, R. A., Millero, F. J., Mordy,
1829 C., and Peng, T. -H.: A global ocean carbon climatology: Results from Global Data Analysis Project (GLODAP),
1830 *Global Biogeochemical Cycles*, 18(4), <https://doi.org/10.1029/2004gb002247>, 2004.

1831 Key, R. M., Tanhua, T., Olsen, A., Hoppema, M., Jutterström, S., Schirnack, C., van Heuven, S., Kozyr, A., Lin, X.,
1832 Velo, A., Wallace, D. W. R., and Mintrop, L.: The CARINA data synthesis project: introduction and overview,
1833 *Earth Syst. Sci. Data*, 2, 105–121, <https://doi.org/10.5194/essd-2-105-2010>, 2010.

1834 Key, R. M., Olsen, A., van Heuven, S., Lauvset, S. K., Velo, A., Lin, X., Schirnack, C., Kozyr, A., Tanhua, T.,
1835 Hoppema, M., Jutterström, S., Steinfeldt, R., Jeansson, E., Ishi, M., Perez, F. F., and Suzuki, T.: Global Ocean Data
1836 Analysis Project, Version 2 (GLODAPv2), ORNL/CDIAC-162, ND-P093, Ocean Carbon and Acidification Data
1837 System, National Centers for Environmental Information, Silver Spring, Maryland,
1838 https://www.ncei.noaa.gov/access/ocean-carbon-acidification-data-system/oceans/GLODAPv2/NDP_093.pdf, 2015.

1839 Khesghi, H. S.: Sequestering atmospheric carbon dioxide by increasing ocean alkalinity, *Energy*, 20(9), 915–922,
1840 [https://doi.org/10.1016/0360-5442\(95\)00035-f](https://doi.org/10.1016/0360-5442(95)00035-f), 1995.

1841 Knor, L. A. C. M., Sabine, C. L., Sutton, A. J., White, A. E., Potemra, J., and Weller, R. A.: Quantifying net
1842 community production and calcification at Station ALOHA near Hawai‘i: Insights and limitations from a dual tracer
1843 carbon budget approach, *Global Biogeochemical Cycles*, 37, e2022GB007672,
1844 <https://doi.org/10.1029/2022GB007672>, 2023.

1845 Knor, L. A. C. M., Sabine, C. L., Dore, J. E., White, A. E., and Potemra, J.: Drivers and variability of intensified

1846 subsurface ocean acidification trends at Station ALOHA, *Journal of Geophysical Research: Oceans*, 130,
1847 e2024JC022251, <https://doi.org/10.1029/2024JC022251>, 2025.

1848 Kwiatkowski, L., Torres, O., Bopp, L., Aumont, O., Chamberlain, M., Christian, J. R., Dunne, J. P., Gehlen, M.,
1849 Ilyina, T., John, J. G., Lenton, A., Li, H., Lovenduski, N. S., Orr, J. C., Palmieri, J., Santana-Falcón, Y., Schwinger,
1850 J., Séférian, R., Stock, C. A., Tagliabue, A., Takano, Y., Tjiputra, J., Toyama, K., Tsujino, H., Watanabe, M.,
1851 Yamamoto, A., Yool, A., and Ziehn, T.: Twenty-first century ocean warming, acidification, deoxygenation, and
1852 upper-ocean nutrient and primary production decline from CMIP6 model projections, *Biogeosciences*, 17, 3439–
1853 3470, <https://doi.org/10.5194/bg-17-3439-2020>, 2020.

1854 Landschützer, P., Gruber, N., Bakker, D. C. E., Schuster, U., Nakaoka, S., Payne, M. R., Sasse, T., and Zeng, J.: A
1855 neural network-based estimate of the seasonal to inter-annual variability of the Atlantic Ocean carbon sink,
1856 *Biogeosciences*, 10, 7793–7815, <https://doi.org/10.5194/bg-10-7793-2013>, 2013.

1857 Landschützer, P., Gruber, N., Bakker, D. C. E., and Schuster, U.: Recent variability of the Global Ocean Carbon
1858 Sink, *Global Biogeochemical Cycles*, 28(9), 927–949, <https://doi.org/10.1002/2014gb004853>, 2014.

1859 Landschützer, P., Gruber, N., and Bakker, D. C. E.: Decadal variations and trends of the Global Ocean Carbon Sink,
1860 *Global Biogeochemical Cycles*, 30(10), 1396–1417. <https://doi.org/10.1002/2015gb005359>, 2016.

1861 Landschützer, P., Laruelle, G. G., Roobaert, A., and Regnier, P.: A uniform $p\text{CO}_2$ climatology combining open and
1862 coastal oceans, *Earth Syst. Sci. Data*, 12, 2537–2553, <https://doi.org/10.5194/essd-12-2537-2020>, 2020a.

1863 Landschützer, P., Laruelle, G. G., Roobaert, A., and Regnier, P.: A combined global ocean $p\text{CO}_2$ climatology
1864 combining open ocean and coastal areas (NCEI Accession 0209633), NOAA National Centers for Environmental
1865 Information, Dataset, <https://doi.org/10.25921/qb25-f418>, 2020b.

1866 Lange, N., Tanhua, T., Pfeil, B., Bange, H. W., Lauvset, S. K., Grégoire, M., Bakker, D. C., Jones, S. D., Fiedler, B.,
1867 O'Brien, K. M., and Körtzinger, A.: A status assessment of selected data synthesis products for ocean
1868 biogeochemistry, *Frontiers in Marine Science*, 10, <https://doi.org/10.3389/fmars.2023.1078908>, 2023.

1869 Lange, N., Fiedler, B., Álvarez, M., Benoit-Cattin, A., Benway, H., Buttigieg, P. L., Coppola, L., Currie, K., Flecha,
1870 S., Gerlach, D. S., Honda, M., Huertas, I. E., Lauvset, S. K., Muller-Karger, F., Körtzinger, A., O'Brien, K. M.,
1871 Ólafsdóttir, S. R., Pacheco, F. C., Rueda-Roa, D., Skjelvan, I., Wakita, M., White, A., and Tanhua, T.: Synthesis
1872 product for ocean time series (spots) – a ship-based biogeochemical pilot, *Earth System Science Data*, 16(4), 1901–
1873 1931, <https://doi.org/10.5194/essd-16-1901-2024>, 2024a.

1874 Lange, N., Fiedler, B., Álvarez, M., Benoit-Cattin, A., Benway, H., Buttigieg, P. L., Coppola, L., Currie, K. I.,
1875 Flecha, S., Gerlach, D. S., Honda, M. C., Huertas, E. I., Kinkade, D., Muller-Karger, F., Lauvset, S. K., Körtzinger,
1876 A., O'Brien, K. M., Ólafsdóttir, S., Pacheco, F. C., Rueda-Roa, D., Skjelvan, I., Wakita, M., White, A. E., Tanhua,

1877 T.: Synthesis Product for Ocean Time Series (SPOTS), Biological and Chemical Oceanography Data Management
1878 Office (BCO-DMO), (Version 2) Version Date 2024-02-22, <https://doi.org/10.26008/1912/bco-dmo.896862.2>,
1879 2024b.

1880 Laruelle, G. G., Landschützer, P., Gruber, N., Tison, J.-L., Delille, B., and Regnier, P.: Global high-resolution
1881 monthly $p\text{CO}_2$ climatology for the coastal ocean derived from neural network interpolation, *Biogeosciences*, 14,
1882 4545–4561, <https://doi.org/10.5194/bg-14-4545-2017>, 2017.

1883 Lauvset, S. K., and Tanhua, T.: A toolbox for secondary quality control on ocean chemistry and Hydrographic Data,
1884 *Limnology and Oceanography: Methods*, 13(11), 601–608, <https://doi.org/10.1002/lom3.10050>, 2015.

1885 Lauvset, S. K., Key, R. M., Olsen, A., van Heuven, S., Velo, A., Lin, X., Schirnack, C., Kozyr, A., Tanhua, T.,
1886 Hoppema, M., Jutterström, S., Steinfeldt, R., Jeansson, E., Ishii, M., Perez, F. F., Suzuki, T., and Watelet, S.: A new
1887 global interior ocean mapped climatology: The $1^\circ \times 1^\circ$ GLODAP version 2, *Earth System Science Data*, 8(2), 325–
1888 340, <https://doi.org/10.5194/essd-8-325-2016>, 2016.

1889 Lauvset, S. K., Lange, N., Tanhua, T., Bittig, H. C., Olsen, A., Kozyr, A., Álvarez, M., Becker, S., Brown, P. J.,
1890 Carter, B. R., Cotrim da Cunha, L., Feely, R. A., van Heuven, S., Hoppema, M., Ishii, M., Jeansson, E., Jutterström,
1891 S., Jones, S. D., Karlsen, M. K., Lo Monaco, C., Michaelis, P., Murata, A., Pérez, F. F., Pfeil, B., Schirnack, C.,
1892 Steinfeldt, R., Suzuki, T., Tilbrook, B., Velo, A., Wanninkhof, R., Woosley, R. J., and Key, R. M.: An updated
1893 version of the global interior ocean biogeochemical data product, GLODAPv2.2021, *Earth Syst. Sci. Data*, 13,
1894 5565–5589, <https://doi.org/10.5194/essd-13-5565-2021>, 2021.

1895 Lauvset, S. K., Lange, N., Tanhua, T., Bittig, H. C., Olsen, A., Kozyr, A., Alin, S., Álvarez, M., Azetsu-Scott, K.,
1896 Barbero, L., Becker, S., Brown, P. J., Carter, B. R., da Cunha, L. C., Feely, R. A., Hoppema, M., Humphreys, M. P.,
1897 Ishii, M., Jeansson, E., Jiang, L.-Q., Jones, S. D., Lo Monaco, C., Murata, A., Müller, J. D., Pérez, F. F., Pfeil, B.,
1898 Schirnack, C., Steinfeldt, R., Suzuki, T., Tilbrook, B., Ulfsbo, A., Velo, A., Woosley, R. J., and Key, R. M.:
1899 GLODAPv2.2022: the latest version of the global interior ocean biogeochemical data product, *Earth Syst. Sci. Data*,
1900 14, 5543–5572, <https://doi.org/10.5194/essd-14-5543-2022>, 2022.

1901 Lauvset, S. K., Key, R. M., Olsen, A., van Heuven, S. M. A. C., Velo, A., Lin, X., Schirnack, C., Kozyr, A., Tanhua,
1902 T., Hoppema, M., Jutterström, S., Steinfeldt, R., Jeansson, E., Ishii, M., Pérez, F. F., Suzuki, T., Watelet, S.: A new
1903 global interior ocean mapped climatology: the $1^\circ \times 1^\circ$ GLODAP version 2 from 1972-01-01 to 2013-12-31 (NCEI
1904 Accession 0286118), NOAA National Centers for Environmental Information, Dataset,
1905 https://doi.org/10.3334/cdiac/otg.ndp093_glodapv2, 2023a.

1906 Lauvset, S. K., Lange, N., Tanhua, T., Bittig, H. C., Olsen, A., Kozyr, A., Álvarez, M., Azetsu-Scott, K., Becker, S.,
1907 Brown, P. J., Carter, B. R., Cotrim da Cunha, L., Feely, R. A., Hoppema, M., Humphreys, M. P., Ishii, M., Jeansson,
1908 E., Jones, S. D., Lo Monaco, C., Murata, A., Müller, J. D., Pérez, F. F., Schirnack, C., Steinfeldt, R., Suzuki, T.,
1909 Tilbrook, B., Ulfsbo, A., Velo, A., Woosley, R. J., Key, R. M.: Global Ocean Data Analysis Project version 2.2023

1910 (GLODAPv2.2023) (NCEI Accession 0283442), NOAA National Centers for Environmental Information, Dataset,
1911 <https://doi.org/10.25921/zyrq-ht66>, 2023b.

1912 Lauvset, S. K., Lange, N., Tanhua, T., Bittig, H. C., Olsen, A., Kozyr, A., Álvarez, M., Azetsu-Scott, K., Brown, P.
1913 J., Carter, B. R., Cotrim da Cunha, L., Hoppema, M., Humphreys, M. P., Ishii, M., Jeansson, E., Murata, A., Müller,
1914 J. D., Pérez, F. F., Schirnack, C., Steinfeldt, R., Suzuki, T., Ulfso, A., Velo, A., Woosley, R. J., and Key, R. M.:
1915 The annual update GLODAPv2.2023: the global interior ocean biogeochemical data product, *Earth Syst. Sci. Data*,
1916 16, 2047–2072, <https://doi.org/10.5194/essd-16-2047-2024>, 2024.

1917 Lee, K., Tong, L. T., Millero, F. J., Sabine, C. L., Dickson, A. G., Goyet, C., Park, G., Wanninkhof, R., Feely, R. A.,
1918 and Key, R. M.: Global relationships of total alkalinity with salinity and temperature in surface waters of the world's
1919 oceans, *Geophysical Research Letters*, 33(19), <https://doi.org/10.1029/2006gl027207>, 2006.

1920 Lee, K., Kim, T.-W., Byrne, R. H., Millero, F. J., Feely, R. A., and Liu, Y.-M.: The universal ratio of boron to
1921 chlorinity for the North Pacific and North Atlantic oceans, *Geochimica et Cosmochimica Acta*, 74(6), 1801–1811,
1922 <https://doi.org/10.1016/j.gca.2009.12.027>, 2010.

1923 Lewis, E., and Wallace, D. W. R.: Program Developed for CO₂ System Calculations, ORNL/CDIAC-105, Carbon
1924 Dioxide Information Analysis Center, Oak Ridge National Laboratory, Oak Ridge, TN, 1998.

1925 Locarnini, R. A., Mishonov, A. V., Antonov, J. I., Boyer, T. P., Garcia, H. E., Baranova, O. K., Zweng, M. M.,
1926 Paver, C. R., Reagan, J. R., Johnson, D. R., Hamilton, M., and Seidov, D.: World Ocean Atlas 2013, Volume 1:
1927 Temperature, edited by: Levitus, S. and Mishonov, A., NOAA Atlas NESDIS 73, 40 pp., 2013.

1928 Locarnini, R. A., Mishonov, A. V., Baranova, O. K., Boyer, T., P., Zweng, M. M., Garcia, H. E., Reagan, J. R.,
1929 Seidov, D., Weathers, K. W., Paver, C. R., Smolyar, I. V.: World Ocean Atlas 2018, Volume 1: Temperature,
1930 Mishonov, A. [Technical Editor], NOAA Atlas NESDIS 81, 2019.

1931 Lueker, T. J., Dickson, A. G., and Keeling, C. D.: Ocean *p*CO₂ calculated from dissolved inorganic carbon,
1932 alkalinity, and equations for K₁ and K₂: Validation based on laboratory measurements of CO₂ in gas and seawater at
1933 equilibrium, *Marine Chemistry*, 70(1–3), 105–119, [https://doi.org/10.1016/s0304-4203\(00\)00022-0](https://doi.org/10.1016/s0304-4203(00)00022-0), 2000.

1934 Ma, D., Gregor, L., and Gruber, N. (2023). Four decades of trends and drivers of global surface ocean acidification,
1935 *Global Biogeochemical Cycles*, 37(7), <https://doi.org/10.1029/2023gb007765>, 2023.

1936 Manzello, D. P., Enochs, I. C., Hendee, J. C.: National Coral Reef Monitoring Program: Carbonate chemistry data
1937 collected in the Atlantic Ocean, NOAA National Centers for Environmental Information, Dataset,
1938 <https://doi.org/10.25921/vfz0-dg77>, 2018.

1939 Mercier, H., Desbruyères, D., Lherminier, P., Velo, A., Carracedo, L., Fontela, M., & Pérez, F. F.: New insights into
1940 the eastern subpolar North Atlantic Meridional overturning circulation from OVIDE. *Ocean Science*, 20(3), 779–

1941 797, <https://doi.org/10.5194/os-20-779-2024>, 2024.

1942 MetzI, N., Tilbrook, B., Bakker, D., le Quéré, C., Doney, S., Feely, R., Hood, M., and Dargaville, R.: Surface Ocean
1943 CO₂ variability and Vulnerability Workshop, Paris, France, 11–14 April 2007. *Eos, Transactions American*
1944 *Geophysical Union*, 88(28), 287–287, <https://doi.org/10.1029/2007eo280005>, 2007.

1945 MetzI, Nicolas; Fin, Jonathan; Lo Monaco, Claire; Mignon, Claude; Alliouane, Samir; Antoine, David; Bourdin,
1946 Guillaume; Boutin, Jacqueline; Bozec, Yann; Conan, Pascal; Coppola, Laurent; Diaz, Frédéric; Douville, Eric;
1947 Durrieu de Madron, Xavier; Gattuso, Jean-Pierre; Gazeau, Frédéric; Golbol, Melek; Lansard, Bruno; Lefèvre,
1948 Dominique; Lefèvre, Nathalie; Lombard, Fabien; Louanchi, Ferial; Merlivat, Liliane; Olivier, Léa; Petrenko, Anne;
1949 Petton, Sébastien; Pujo-Pay, Mireille; Rabouille, Christophe; Reverdin, Gilles; Ridame, Céline; Tribollet, Aline;
1950 Vellucci, Vincenzo; Wagener, Thibaut; Wimart-Rousseau, Cathy (2023). A synthesis of ocean total alkalinity and
1951 dissolved inorganic carbon measurements in the Global Ocean and Mediterranean Sea from 1993 to 2022: the
1952 SNAPO-CO₂-v1 dataset (NCEI Accession 0285681). NOAA National Centers for Environmental Information.
1953 Unpublished Dataset. <https://www.ncei.noaa.gov/archive/accession/0285681>, 2023.

1954 MetzI, N., Fin, J., Lo Monaco, C., Mignon, C., Alliouane, S., Antoine, D., Bourdin, G., Boutin, J., Bozec, Y.,
1955 Conan, P., Coppola, L., Diaz, F., Douville, E., Durrieu de Madron, X., Gattuso, J.-P., Gazeau, F., Golbol, M.,
1956 Lansard, B., Lefèvre, D., Lefèvre, N., Lombard, F., Louanchi, F., Merlivat, L., Olivier, L., Petrenko, A., Petton, S.,
1957 Pujo-Pay, M., Rabouille, C., Reverdin, G., Ridame, C., Tribollet, A., Vellucci, V., Wagener, T., and Wimart-
1958 Rousseau, C.: A synthesis of ocean total alkalinity and dissolved inorganic carbon measurements from 1993 to
1959 2022: the SNAPO-CO₂-v1 dataset, *Earth Syst. Sci. Data*, 16, 89–120, <https://doi.org/10.5194/essd-16-89-2024>,
1960 2024.

1961 Mishonov, A. V., Boyer, T. P., Baranova, O. K., Bouchard, C. N., Cross, S. L., Garcia H. E., Locarnini, R. A., Paver,
1962 C. R., Wang, Z., Seidov, D., Grodsky, A. I., Beauchamp, J. G.: World Ocean Database 2023, C. Bouchard, Technical
1963 Ed., NOAA Atlas NESDIS 97, 206 pp., <https://doi.org/10.25923/z885-h264>, 2024.

1964 Monacci, N. M., Cross, J. N., Danielson, S. L., Evans, W., Hopcroft, R. R., Mathis, J. T., Mordy, C. W., Naber, D.
1965 D., Shake, K. L., Trahanovsky, K., Wang, H., Weingartner, T. J., Whittedge, T. E.: Marine carbonate system
1966 discrete profile data from the Gulf of Alaska (GAK) Seward Line cruises between 2008 and 2017 (NCEI Accession
1967 0277034). NOAA National Centers for Environmental Information. Dataset. <https://doi.org/10.25921/x9sg-9b08>,
1968 2023.

1969 Monacci, N. M., Cross, J. N., Evans, W., Mathis, J. T., and Wang, H.: A decade of marine inorganic carbon
1970 chemistry observations in the northern Gulf of Alaska – insights into an environment in transition, *Earth Syst. Sci.*
1971 *Data*, 16, 647–665, <https://doi.org/10.5194/essd-16-647-2024>, 2024.

1972 Müller, J. D.: RECCAP2-ocean data collection, <https://doi.org/10.5281/zenodo.7990823>, 2023.

1973 Müller, J. D., Gruber, N., Carter, B., Feely, R., Ishii, M., Lange, N., Lauvset, S. K., Murata, A., Olsen, A., Pérez, F.
1974 F., Sabine, C., Tanhua, T., Wanninkhof, R., and Zhu, D.: Decadal trends in the oceanic storage of anthropogenic
1975 carbon from 1994 to 2014, *AGU Advances*, 4(4), <https://doi.org/10.1029/2023av000875>, 2023a.

1976 Müller, J. D.; Gruber, N.; Carter, B. R.; Feely, R. A.; Ishii, M.; Lange, N.; Lauvset, S. K.; Murata, A.; Olsen, A.;
1977 Pérez, F. F.; Sabine, C. L.; Tanhua, T.; Wanninkhof, R.; Zhu, D.: Decadal Trends in the Oceanic Storage of
1978 Anthropogenic Carbon from 1994 to 2014 (NCEI Accession 0279447). NOAA National Centers for Environmental
1979 Information. Dataset. <https://doi.org/10.25921/ppcf-w020>, 2023b.

1980 Müller, J. D., and Gruber, N.: Progression of ocean interior acidification over the industrial era, *Science Advances*,
1981 10(48), <https://doi.org/10.1126/sciadv.ado3103>, 2024a.

1982 Müller, J. D.; and Gruber, N.: Progression of Ocean Interior Acidification over the Industrial Era from 1800-07-01
1983 to 2014-06-30 (NCEI Accession 0298993). NOAA National Centers for Environmental Information. Dataset.
1984 <https://doi.org/10.25921/tefm-x802>, 2024b.

1985 Olsen, A., Key, R. M., van Heuven, S., Lauvset, S. K., Velo, A., Lin, X., Schirmick, C., Kozyr, A., Tanhua, T.,
1986 Hoppema, M., Jutterström, S., Steinfeldt, R., Jeansson, E., Ishii, M., Pérez, F. F., and Suzuki, T.: The Global Ocean
1987 Data Analysis Project version 2 (GLODAPv2) – an internally consistent data product for the world ocean, *Earth
1988 Syst. Sci. Data*, 8, 297–323, <https://doi.org/10.5194/essd-8-297-2016>, 2016.

1989 Olsen, A., Lange, N., Key, R. M., Tanhua, T., Álvarez, M., Becker, S., Bittig, H. C., Carter, B. R., Cotrim da Cunha,
1990 L., Feely, R. A., van Heuven, S., Hoppema, M., Ishii, M., Jeansson, E., Jones, S. D., Jutterström, S., Karlsen, M. K.,
1991 Kozyr, A., Lauvset, S. K., Lo Monaco, C., Murata, A., Pérez, F. F., Pfeil, B., Schirmick, C., Steinfeldt, R., Suzuki,
1992 T., Telszewski, M., Tilbrook, B., Velo, A., and Wanninkhof, R.: GLODAPv2.2019 – an update of GLODAPv2,
1993 *Earth Syst. Sci. Data*, 11, 1437–1461, <https://doi.org/10.5194/essd-11-1437-2019>, 2019.

1994 Olsen, A., Lange, N., Key, R. M., Tanhua, T., Bittig, H. C., Kozyr, A., Álvarez, M., Azetsu-Scott, K., Becker, S.,
1995 Brown, P. J., Carter, B. R., Cotrim da Cunha, L., Feely, R. A., van Heuven, S., Hoppema, M., Ishii, M., Jeansson,
1996 E., Jutterström, S., Landa, C. S., Lauvset, S. K., Michaelis, P., Murata, A., Pérez, F. F., Pfeil, B., Schirmick, C.,
1997 Steinfeldt, R., Suzuki, T., Tilbrook, B., Velo, A., Wanninkhof, R., and Woosley, R. J.: An updated version of the
1998 global interior ocean biogeochemical data product, GLODAPv2.2020, *Earth Syst. Sci. Data*, 12, 3653–3678,
1999 <https://doi.org/10.5194/essd-12-3653-2020>, 2020.

2000 Orr, J. C., Fabry, V. J., Aumont, O., Bopp, L., Doney, S. C., Feely, R. A., Gnanadesikan, A., Gruber, N., Ishida, A.,
2001 Joos, F., Key, R. M., Lindsay, K., Maier-Reimer, E., Matear, R., Monfray, P., Mouchet, A., Najjar, R. G., Plattner,
2002 G.-K., Rodgers, K. B., Sabine, C. L., Sarmiento, J. L., Schlitzer, R., Slater, R. D., Totterdell, I. J., Weirig, M.-F.,
2003 Yamanaka, Y., and Yool, A.: Anthropogenic ocean acidification over the twenty-first century and its impact on
2004 calcifying organisms, *Nature*, 437(7059), 681–686, <https://doi.org/10.1038/nature04095>, 2005.

- 2005 Orr, J. C., Epitalon, J.-M., and Gattuso, J.-P.: Comparison of ten packages that compute ocean carbonate chemistry,
2006 Biogeosciences, 12, 1483–1510, <https://doi.org/10.5194/bg-12-1483-2015>, 2015.
- 2007 Orr, J. C., Epitalon, J.-M., Dickson, A. G., and Gattuso, J.-P.: Routine uncertainty propagation for the Marine
2008 Carbon Dioxide System, *Marine Chemistry*, 207, 84–107. <https://doi.org/10.1016/j.marchem.2018.10.006>, 2018.
- 2009 Oschlies, A., Bach, L. T., Fennel, K., Gattuso, J.-P., and Mengis, N.: Perspectives and challenges of marine carbon
2010 dioxide removal, *Frontiers in Climate*, 6, <https://doi.org/10.3389/fclim.2024.1506181>, 2025.
- 2011 Padin, X. A., Velo, A., & Pérez, F. F.: Arios: A database for ocean acidification assessment in the Iberian Upwelling
2012 System (1976–2018), *Earth System Science Data*, 12(4), 2647–2663, <https://doi.org/10.5194/essd-12-2647-2020>,
2013 2020.
- 2014 Palacio-Castro, A. M., Enochs, I. C., Besemer, N., Boyd, A., Jankulak, M., Kolodziej, G., Hirsh, H. K., Webb, A. E.,
2015 Towle, E. K., Kelble, C., Smith, I., and Manzello, D. P.: Coral Reef carbonate chemistry reveals interannual,
2016 seasonal, and spatial impacts on ocean acidification off Florida, *Global Biogeochemical Cycles*, 37(12),
2017 <https://doi.org/10.1029/2023gb007789>, 2023.
- 2018 Perez, F. F., and Fraga, F.: Association constant of fluoride and hydrogen ions in seawater. *Marine Chemistry*,
2019 21(2), 161–168, [https://doi.org/10.1016/0304-4203\(87\)90036-3](https://doi.org/10.1016/0304-4203(87)90036-3), 1987.
- 2020 Perez, F. F., Fontela, M., García-Ibáñez, M. I., Mercier, H., Velo, A., Lherminier, P., Zunino, P., de la Paz, M.,
2021 Alonso-Pérez, F., Gualart, E. F., & Padin, X. A.: Meridional overturning circulation conveys fast acidification to
2022 the deep Atlantic Ocean. *Nature*, 554(7693), 515–518. <https://doi.org/10.1038/nature25493>, 2018.
- 2023 Pérez, F. F., Velo, A., Padin, X. A., Doval, M. D., and Prego, R.: ARIOS Database: An Acidification Ocean
2024 Database for the Galician Upwelling Ecosystem, Instituto de Investigaciones Marinas, Consejo Superior de
2025 Investigaciones Científicas (CSIC), <https://doi.org/10.20350/digitalCSIC/12498>, 2020.
- 2026 Pérez, F. F., Olafsson, J., Ólafsdóttir, S. R., Fontela, M., & Takahashi, T.: Contrasting drivers and trends of ocean
2027 acidification in the Subarctic Atlantic. *Scientific Reports*, 11(1). <https://doi.org/10.1038/s41598-021-93324-3>, 2021.
- 2028 Pfeil, B., Olsen, A., Bakker, D. C. E., Hankin, S., Koyuk, H., Kozyr, A., Malczyk, J., Manke, A., Metzl, N., Sabine,
2029 C. L., Akl, J., Alin, S. R., Bates, N., Bellerby, R. G. J., Borges, A., Boutin, J., Brown, P. J., Cai, W.-J., Chavez, F.
2030 P., Chen, A., Cosca, C., Fassbender, A. J., Feely, R. A., González-Dávila, M., Goyet, C., Hales, B., Hardman-
2031 Mountford, N., Heinze, C., Hood, M., Hoppema, M., Hunt, C. W., Hydes, D., Ishii, M., Johannessen, T., Jones, S.
2032 D., Key, R. M., Körtzinger, A., Landschützer, P., Lauvset, S. K., Lefèvre, N., Lenton, A., Lourantou, A., Merlivat,
2033 L., Midorikawa, T., Mintrop, L., Miyazaki, C., Murata, A., Nakadate, A., Nakano, Y., Nakaoka, S., Nojiri, Y.,
2034 Omar, A. M., Padin, X. A., Park, G.-H., Paterson, K., Perez, F. F., Pierrot, D., Poisson, A., Ríos, A. F., Santana-
2035 Casiano, J. M., Salisbury, J., Sarma, V. V. S. S., Schlitzer, R., Schneider, B., Schuster, U., Sieger, R., Skjelvan, I.,

2036 Steinhoff, T., Suzuki, T., Takahashi, T., Tedesco, K., Telszewski, M., Thomas, H., Tilbrook, B., Tjiputra, J.,
2037 Vandemark, D., Veness, T., Wanninkhof, R., Watson, A. J., Weiss, R., Wong, C. S., and Yoshikawa-Inoue, H.: A
2038 uniform, quality controlled Surface Ocean CO₂ Atlas (SOCAT), *Earth Syst. Sci. Data*, 5, 125–143,
2039 <https://doi.org/10.5194/essd-5-125-2013>, 2013.

2040 Qi, D., Chen, L., Chen, B., Gao, Z., Zhong, W., Feely, R. A., Anderson, L. G., Sun, H., Chen, J., Chen, M., Zhan,
2041 L., Zhang, Y., & Cai, W.-J.: Increase in acidifying water in the Western Arctic ocean. *Nature Climate Change*, 7(3),
2042 195–199. <https://doi.org/10.1038/nclimate3228>, 2017.

2043 Qi, D., Ouyang, Z., Chen, L., Wu, Y., Lei, R., Chen, B., Feely, R. A., Anderson, L. G., Zhong, W., Lin, H.,
2044 Polukhin, A., Zhang, Y., Zhang, Y., Bi, H., Lin, X., Luo, Y., Zhuang, Y., He, J., Chen, J. and Cai, W.-J.: Climate
2045 change drives rapid decadal acidification in the Arctic Ocean from 1994 to 2020, *Science*, 377, 1544–1550,
2046 doi:10.1126/science.abo0383, 2022.

2047 Resplandy, L., Hogikyan, A., Müller, J. D., Najjar, R. G., Bange, H. W., Bianchi, D., Weber, T., Cai, W. -J., Doney,
2048 S. C., Fennel, K., Gehlen, M., Hauck, J., Lacroix, F., Landschützer, P., Le Quéré, C., Roobaert, A., Schwinger, J.,
2049 Berthet, S., Bopp, L., Chau, T. T. T., Dai, M., Gruber, N., Ilyina, T., Kock, A., Manizza, M., Lachkar, Z., Laruelle,
2050 G. G., Liao, E., Lima, I. D., Nissen, C., Rödenbeck, C., Séférian, R., Toyama, K., Tsujino, H., and Regnier, P.: A
2051 synthesis of global coastal Ocean Greenhouse Gas Fluxes, *Global Biogeochemical Cycles*, 38(1),
2052 <https://doi.org/10.1029/2023gb007803>, 2024.

2053 Revelle, R., and Suess, H. E.: Carbon dioxide exchange between atmosphere and ocean and the question of an
2054 increase of atmospheric CO₂ during the past decades. *Tellus*, 9(1), 18–27, [https://doi.org/10.1111/j.2153-](https://doi.org/10.1111/j.2153-3490.1957.tb01849.x)
2055 [3490.1957.tb01849.x](https://doi.org/10.1111/j.2153-3490.1957.tb01849.x), 1957.

2056 Rödenbeck, C., Keeling, R. F., Bakker, D. C., Metzl, N., Olsen, A., Sabine, C., and Heimann, M.: Global surface-
2057 ocean *p*CO₂ and sea-air CO₂ flux variability from an observation-driven ocean mixed-layer scheme, *Ocean Science*,
2058 9(2), 193–216, <https://doi.org/10.5194/os-9-193-2013>, 2013.

2059 Rödenbeck, Christian, DeVries, T., Hauck, J., Le Quéré, C., & Keeling, R. F.: Data-based estimates of interannual
2060 sea-air CO₂ flux variations 1957-2020 and their relation to environmental drivers, *Biogeosciences*, 19(10), 2627–
2061 2652, <https://doi.org/10.5194/bg-19-2627-2022>, 2022.

2062 Roobaert, A.: Regnier, P., Landschützer, P., Laruelle, G. G.: A novel sea surface partial pressure of carbon dioxide
2063 (*p*CO₂) data product for the global coastal ocean resolving trends over the 1982-2020 period (NCEI Accession
2064 0279118), NOAA National Centers for Environmental Information, Dataset, <https://doi.org/10.25921/4sde-p068>,
2065 2023.

2066 Roobaert, A., Regnier, P., Landschützer, P., and Laruelle, G. G.: A novel sea surface *p*CO₂-product for the global
2067 coastal ocean resolving trends over 1982–2020, *Earth System Science Data*, 16(1), 421–441,

2068 <https://doi.org/10.5194/essd-16-421-2024>, 2024.

2069 Sabine, C. L., Feely, R. A., Gruber, N., Key, R. M., Lee, K., Bullister, J. L., Wanninkhof, R., Wong, C. S., Wallace,
2070 D. W., Tilbrook, B., Millero, F. J., Peng, T.-H., Kozyr, A., Ono, T., and Rios, A. F.: The oceanic sink for
2071 anthropogenic CO₂, *Science*, 305(5682), 367–371, <https://doi.org/10.1126/science.1097403>, 2004a.

2072 [Sabine, C. L., Feely, R. A., Key, R. M., Wanninkhof, R., Millero, F. J., Kozyr, A.: GLObal Ocean Data Analysis](#)
2073 [Project \(GLODAP\) version 1.1 \(NCEI Accession 0001644\). NOAA National Centers for Environmental](#)
2074 [Information. Dataset. <https://doi.org/10.25921/pkjs-5w29>, 2004b.](#)

2075 Sabine, C. L., Key, R. M., Kozyr, A., Feely, R. A., Wanninkhof, R., Millero, F. J., Peng, T.-H., Bullister, J. L., and
2076 Lee, K.: Global Ocean Data Analysis Project (GLODAP): Results and data. ORNL/CDIAC-145, NDP-083, Carbon
2077 Dioxide Information Analysis Center, Oak Ridge National Laboratory, U.S. Department of Energy, Oak Ridge, TN,
2078 110 pp. plus 6 Appendices, 2005.

2079 Sabine, C. L., Feely, R. A., Millero, F. J., Dickson, A. G., Langdon, C., Mecking, S., and Greeley, D.: Decadal
2080 changes in Pacific Carbon, *Journal of Geophysical Research: Oceans*, 113(C7),
2081 <https://doi.org/10.1029/2007jc004577>, 2008.

2082 Sabine, C. L., Hankin, S., Koyuk, H., Bakker, D. C. E., Pfeil, B., Olsen, A., Metzl, N., Kozyr, A., Fassbender, A.,
2083 Manke, A., Malczyk, J., Akl, J., Alin, S. R., Bellerby, R. G. J., Borges, A., Boutin, J., Brown, P. J., Cai, W.-J.,
2084 Chavez, F. P., Chen, A., Cosca, C., Feely, R. A., González-Dávila, M., Goyet, C., Hardman-Mountford, N., Heinze,
2085 C., Hoppema, M., Hunt, C. W., Hydes, D., Ishii, M., Johannessen, T., Key, R. M., Körtzinger, A., Landschützer, P.,
2086 Lauvset, S. K., Lefèvre, N., Lenton, A., Lourantou, A., Merlivat, L., Midorikawa, T., Mintrop, L., Miyazaki, C.,
2087 Murata, A., Nakadate, A., Nakano, Y., Nakaoka, S., Nojiri, Y., Omar, A. M., Padin, X. A., Park, G.-H., Paterson, K.,
2088 Perez, F. F., Pierrot, D., Poisson, A., Ríos, A. F., Salisbury, J., Santana-Casiano, J. M., Sarma, V. V. S. S., Schlitzer,
2089 R., Schneider, B., Schuster, U., Sieger, R., Skjelvan, I., Steinhoff, T., Suzuki, T., Takahashi, T., Tedesco, K.,
2090 Telszewski, M., Thomas, H., Tilbrook, B., Vandemark, D., Veness, T., Watson, A. J., Weiss, R., Wong, C. S., and
2091 Yoshikawa-Inoue, H.: Surface Ocean CO₂ Atlas (SOCAT) gridded data products, *Earth Syst. Sci. Data*, 5, 145–153,
2092 <https://doi.org/10.5194/essd-5-145-2013>, 2013.

2093 Sarma, V. V. S. S., Krishna, M. S., Paul, Y. S., and Murty, V. S. N.: Observed changes in ocean acidity and carbon
2094 dioxide exchange in the coastal bay of Bengal—A link to air pollution, *Tellus B: Chemical and Physical*
2095 *Meteorology*, 67(1), 24638, <https://doi.org/10.3402/tellusb.v67.24638>, 2015.

2096 Schimel, D. S., and Carroll, D.: Carbon cycle–climate feedbacks in the post-paris world, *Annual Review of Earth*
2097 *and Planetary Sciences*, 52(1), <https://doi.org/10.1146/annurev-earth-031621-081700>, 2024.

2098 Schoderer, M., Bittig, H., Klein, B., Hägele, R., Steinhoff, T., Castro-Morales, K., Cotrim da Cunha, L., Hornidge,
2099 A., and Körtzinger, A.: From individual observations to global assessments: Tracing the Marine Carbon Knowledge

2100 Value Chain, Ocean and Society, 2, <https://doi.org/10.17645/oas.8891>, 2024.

2101 Sharp, J. D., Pierrot, D., Humphreys, M. P., Epitalon, J.-M., Orr, J. C., Lewis, E. R., Wallace, D. W. R.: CO2SYSv3
2102 for MATLAB (Version v3.2.1), Zenodo, <http://doi.org/10.5281/zenodo.3950562>, 2023.

2103 Sharp, J. D., Jiang, L.-Q., Carter, B. R., Lavin, P. D., Yoo, H., and Cross, S. L.: A mapped dataset of surface ocean
2104 acidification indicators in large marine ecosystems of the United States, *Sci. Data*, 11, 715,
2105 <https://doi.org/10.1038/s41597-024-03530-7>, 2024a.

2106 Sharp, J. D., Jiang, L.-Q., Carter, B. R., Lavin, P. D., Yoo, H., Cross, S. L. RFR-LME Ocean Acidification Indicators
2107 from 1998 to 2023 (NCEI Accession 0287551). NOAA National Centers for Environmental Information. Dataset.
2108 <https://doi.org/10.25921/h8vw-e872>, 2024b.

2109 Sridevi, B., and Sarma, V. V. S. S.: Role of river discharge and warming on ocean acidification and pco2 levels in
2110 the Bay of Bengal, *Tellus B: Chemical and Physical Meteorology*, 73 (1), 1–20,
2111 <https://doi.org/10.1080/16000889.2021.1971924>, 2021.

2112 Sutton, A. J., Feely, R. A., Maenner-Jones, S., Musielwicz, S., Osborne, J., Dietrich, C., Monacci, N., Cross, J.,
2113 Bott, R., Kozyr, A.: Autonomous seawater partial pressure of carbon dioxide (pCO₂) and pH time series from 40
2114 surface buoys between 2004 and 2017 (NCEI Accession 0173932), NOAA National Centers for Environmental
2115 Information, Dataset, <https://doi.org/10.7289/v5db8043>, 2018.

2116 Sutton, A. J., Feely, R. A., Maenner-Jones, S., Musielwicz, S., Osborne, J., Dietrich, C., Monacci, N., Cross, J.,
2117 Bott, R., Kozyr, A., Andersson, A. J., Bates, N. R., Cai, W.-J., Cronin, M. F., De Carlo, E. H., Hales, B., Howden, S.
2118 D., Lee, C. M., Manzello, D. P., McPhaden, M. J., Meléndez, M., Mickett, J. B., Newton, J. A., Noakes, S. E., Noh,
2119 J. H., Olafsdottir, S. R., Salisbury, J. E., Send, U., Trull, T. W., Vandemark, D. C., and Weller, R. A.: Autonomous
2120 seawater pCO₂ and pH time series from 40 surface buoys and the emergence of anthropogenic trends, *Earth Syst.*
2121 *Sci. Data*, 11, 421–439, <https://doi.org/10.5194/essd-11-421-2019>, 2019.

2122 Suzuki, T., Ishii, M., Aoyama, M., Christian, J. R., Enyo, K., Kawano, T., Key, R. M., Kosugi, N., Kozyr, A.,
2123 Miller, L. A., Murata, A., Nakano, T., Ono, T., Saino, T., Sasaki, K., Sasano, D., Takatani, Y., Wakita, M., Sabine,
2124 C. L. The Pacific Ocean Interior Carbon (PACIFICA) Database (NCEI Accession 0110865). NOAA National
2125 Centers for Environmental Information. Dataset. <https://doi.org/10.25921/n9nn-8324>, 2013.

2126 Swift, J. (2022), [Quality Edited Hydrographic Data](https://joa.ucsd.edu/Data_homepage), https://joa.ucsd.edu/Data_homepage (Last
2127 accessed: 2025-02-08).

2128 Takahashi, T., Feely, R. A., Weiss, R. F., Wanninkhof, R. H., Chipman, D. W., Sutherland, S. C., and Takahashi, T.
2129 T.: Global Air-Sea Flux of CO₂: An estimate based on measurements of sea–air pCO₂ difference, *Proceedings of the*
2130 *National Academy of Sciences*, 94(16), 8292–8299, <https://doi.org/10.1073/pnas.94.16.8292>, 1997.

2131 Takahashi, T., Sutherland, S. C., Sweeney, C., Poisson, A., Metz, N., Tilbrook, B., Bates, N., Wanninkhof, R.,
2132 Feely, R. A., Sabine, C., Olafsson, J., and Nojiri, Y.: Global sea–air CO₂ flux based on climatological surface ocean
2133 pCO₂, and seasonal biological and temperature effects, Deep Sea Research Part II: Topical Studies in
2134 Oceanography, 49(9–10), 1601–1622, [https://doi.org/10.1016/s0967-0645\(02\)00003-6](https://doi.org/10.1016/s0967-0645(02)00003-6), 2002.

2135 Takahashi, T., Sutherland, S. C., Wanninkhof, R., Sweeney, C., Feely, R. A., Chipman, D. W., Hales, B., Friederich,
2136 G., Chavez, F., Sabine, C., Watson, A., Bakker, D. C. E., Schuster, U., Metz, N., Yoshikawa-Inoue, H., Ishii, M.,
2137 Midorikawa, T., Nojiri, Y., Körtzinger, A., Steinhoff, T., and de Baar, H. J. W.: Climatological mean and decadal
2138 change in Surface Ocean pCO₂, and net sea–air CO₂ flux over the Global Oceans, Deep Sea Research Part II:
2139 Topical Studies in Oceanography, 56(8–10), 554–577, <https://doi.org/10.1016/j.dsr2.2008.12.009>, 2009.

2140 Takahashi, T., Sutherland, S. C., Kozyr, A.: LDEO Database (Version 2019): Global Ocean Surface Water Partial
2141 Pressure of CO₂ Database: Measurements Performed During 1957-2019 (NCEI Accession 0160492), NOAA
2142 National Centers for Environmental Information, Dataset, [https://doi.org/10.3334/cdiac/otg.ndp088\(v2015\)](https://doi.org/10.3334/cdiac/otg.ndp088(v2015)), 2017.

2143 [Takano, Y., Ilyina, T., Tjiputra, J., Eddebban, Y. A., Berthet, S., Bopp, L., Buitenhuis, E., Butenschön, M., Christian,](#)
2144 [J. R., Dunne, J. P., Gröger, M., Hayashida, H., Hieronymus, J., Koenigk, T., Krasting, J. P., Long, M. C., Lovato, T.,](#)
2145 [Nakano, H., Palmieri, J., Schwinger, J., Séférian, R., Suntharalingam, P., Tatebe, H., Tsujino, H., Urakawa, S.,](#)
2146 [Watanabe, M., and Yool, A.: Simulations of ocean deoxygenation in the historical era: insights from forced and](#)
2147 [coupled models. Front. Mar. Sci. 10:1139917. doi: 10.3389/fmars.2023.1139917, 2023.](#)

2148 Tanhua, T., Jones, E. P., Jeansson, E., Jutterström, S., Smethie, W. M., Wallace, D. W., and Anderson, L. G.:
2149 Ventilation of the Arctic Ocean: Mean ages and inventories of Anthropogenic CO₂ and CFC-11, Journal of
2150 Geophysical Research: Oceans, 114(C1), <https://doi.org/10.1029/2008jc004868>, 2009.

2151 Tanhua, T., van Heuven, S., Key, R. M., Velo, A., Olsen, A., and Schirnack, C.: Quality control procedures and
2152 methods of the CARINA database, Earth Syst. Sci. Data, 2, 35-49, <https://doi.org/10.5194/essd-2-35-2010>, 2010.

2153 Tanhua, T., Olsen, A., Hoppema, M., Jutterström, S., Schirnack, C., van Heuven, S. M. A. C., Velo, A., Lin, X.,
2154 Kozyr, A., Álvarez, M., Bakker, D. C. E., Brown, P. J., Falck, E., Jeansson, E., Lo Monaco, C., Ólafsson, J., Pérez,
2155 F. F., Pierrot, D., Ríos, A. F., Sabine, C. L., Schuster, U., Steinfeldt, R., Stendardo, I., Anderson, L. G., Bates, N.,
2156 Bellerby, R. G. J., Blindheim, J., Bullister, J. L., Gruber, N., Ishii, M., Johannessen, T., Jones, E. P., Köhler, J.,
2157 Körtzinger, A., Metz, N., Murata, A., Musielewicz, S., Omar, A. M., Olsson, K. A., de la Paz, M., Pfeil, B., Rey, F.,
2158 Rhein, M., Skjelvan, I., Tilbrook, B., Wanninkhof, R., Mintrop, L. J., Wallace, D. W. R., Key, R. M.: The CARBON
2159 dioxide IN the Atlantic Ocean (CARINA) Database V1.1 2010 (NCEI Accession 0113899). NOAA National
2160 Centers for Environmental Information. Dataset. <https://doi.org/10.3334/cdiac/otg.ndp091>, 2013.

2161 Tans, P., and Keeling, R.: Trends in atmospheric carbon dioxide, NOAA Global Monitoring Laboratory (Boulder,
2162 Colorado, USA) and Scripps Institution of Oceanography (LaJolla, California, USA),
2163 <https://gml.noaa.gov/ccgg/trends/> and <https://scrippsco2.ucsd.edu/>, 2025.

2164 [Terhaar, J.: Composite model-based estimate of the ocean carbon sink from 1959 to 2022, *Biogeosciences*, 22,](#)
2165 [1631–1649, <https://doi.org/10.5194/bg-22-1631-2025>, 2025.](#)

2166 Terhaar, J., Orr, J. C., Ethé, C., Regnier, P., and Bopp, L.: Simulated Arctic Ocean response to doubling of riverine
2167 carbon and nutrient delivery, *Global Biogeochemical Cycles*, 33, 1048–1070,
2168 <https://doi.org/10.1029/2019GB006200>, 2019.

2169 Terhaar, J., Tanhua, T., Stöven, T., Orr, J. C., and Bopp, L.: Evaluation of data-based estimates of anthropogenic
2170 carbon in the Arctic Ocean, *Journal of Geophysical Research: Oceans*, 125(6),
2171 <https://doi.org/10.1029/2020jc016124>, 2020.

2172 Terhaar, J., Torres, O., Bourgeois, T., and Kwiatkowski, L.: Arctic Ocean acidification over the 21st century co-
2173 driven by anthropogenic carbon increases and freshening in the CMIP6 model ensemble, *Biogeosciences*, 18, 2221–
2174 2240, <https://doi.org/10.5194/bg-18-2221-2021>, 2021a.

2175 Terhaar, Jens, Frölicher, T. L., & Joos, F.: Southern Ocean anthropogenic carbon sink constrained by sea surface
2176 salinity, *Science Advances*, 7(18), <https://doi.org/10.1126/sciadv.abd5964>, 2021b.

2177 Terhaar, J., Frölicher, T. L., Joos, F.: Simulated and constrained Southern Ocean carbon sink from 1850 to 2100
2178 based on CMIP5 and CMIP6 models. SEANOE. <https://doi.org/10.17882/103938>, 2021c.

2179 Terhaar, J., Frölicher, T. L., and Joos, F.: Observation-constrained estimates of the Global Ocean Carbon Sink from
2180 earth system models, *Biogeosciences*, 19(18), 4431–4457, <https://doi.org/10.5194/bg-19-4431-2022>, 2022a.

2181 Terhaar, J., Frölicher, T. L., and Joos, F.: Simulated and constrained ocean carbon sink from 1850 to 2100 based on
2182 CMIP6 models. SEANOE. <https://doi.org/10.17882/103934>, 2022b.

2183 Terhaar, J., Frölicher, T. L., and Joos, F.: Ocean acidification in emission-driven temperature stabilization scenarios:
2184 The role of TCRE and non-CO₂ greenhouse gases, *Environmental Research Letters*, 18(2), 02403,
2185 <https://doi.org/10.1088/1748-9326/acaf91>, 2023.

2186 Terhaar, J., Tanhua, T., Stöven, T., Orr, J. C., Bopp, L.: Observation-based anthropogenic carbon estimates in the
2187 Arctic Ocean. SEANOE. <https://doi.org/10.17882/103920>, 2024.

2188 van Heuven, S., Pierrot, D., Rae, J. W. B., Lewis, E., Wallace, D. W. R.: MATLAB Program Developed for CO₂
2189 System Calculations, ORNL/CDIAC-105b, Carbon Dioxide Information Analysis Center, Oak Ridge National
2190 Laboratory, Oak Ridge, TN, USA, 2011.

2191 van Hooijdonk, R.: Modeled ocean acidification data in the Gulf of Mexico and wider Caribbean using satellites and
2192 climate model data for the Ocean Acidification Products for the Gulf of Mexico and East Coast project from 2014-
2193 01-01 to 2020-12-31 (NCEI Accession 0245950), NOAA National Centers for Environmental Information, Dataset,

2194 <https://doi.org/10.25921/tt1c-dx53>, 2022.

2195 Velo, A., Pérez, F. F., Tanhua, T., Gilcoto, M., Ríos, A. F., and Key, R. M.: Total alkalinity estimation using MLR
2196 and neural network techniques, *J. Mar. Syst.*, 111–112, 11–18, <https://doi.org/10.1016/j.jmarsys.2012.09.002>, 2013.

2197 Wanninkhof, R., Pierrot, D., Sullivan, K., Barbero, L., and Triñanes, J.: Gridded surface water fugacity of CO₂
2198 observations, and calculated pH, aragonite saturation state and air–sea CO₂ fluxes in the northern Caribbean Sea
2199 from 2002 through 2019 (NCEI Accession 0207749), NOAA National Centers for Environmental Information,
2200 Dataset, <https://doi.org/10.25921/2swk-9w56>, 2019.

2201 Wanninkhof, R., Pierrot, D., Sullivan, K., Barbero, L., and Triñanes, J.: A 17-year dataset of surface water fugacity
2202 of CO₂ along with calculated pH, aragonite saturation state and air–sea CO₂ fluxes in the northern Caribbean Sea,
2203 *Earth Syst. Sci. Data*, 12, 1489–1509, <https://doi.org/10.5194/essd-12-1489-2020>, 2020.

2204 Wanninkhof, R., Triñanes, J., Pierrot, D., Munro, D. R., Sweeney, C., and Fay, A. R.: AOML_ET: Partial pressure
2205 of CO₂ (*p*CO₂) and sea-air CO₂ fluxes for the global ocean, along with the predictor variables from 1998-01-01 to
2206 2023-12-30, using an Extra Trees (extremely randomized trees) machine learning (NCEI Accession 0298989),
2207 NOAA National Centers for Environmental Information, Dataset, <https://doi.org/10.25921/0s8y-q287>, 2024.

2208 Wanninkhof, R., Triñanes, J., Pierrot, D., Munro, D. R., Sweeney, C., and Fay, A. R.: Trends in sea-air CO₂ fluxes
2209 and sensitivities to atmospheric forcing using an extremely randomized trees machine learning approach, *Global
2210 Biogeochemical Cycles*, 39, <https://doi.org/10.1029/2024GB008315>, 2025.

2211 Watson, A. J., Schuster, U., Shutler, J. D., Holding, T., Ashton, I. G., Landschützer, P., Woolf, D., and Goddijn-
2212 Murphy, L.: Revised estimates of ocean-atmosphere CO₂ flux are consistent with ocean carbon inventory, *Nature
2213 Communications*, 11(1), 1–6, <https://doi.org/10.1038/s41467-020-18203-3>, 2020.

2214 Watson, A. J., Schuster, U., Shutler, J. D., Holding, T., Ashton, I. G., Landschützer, P., Woolf, D., and Goddijn-
2215 Murphy, L.: Revised estimates of ocean-atmosphere CO₂ flux accounting for near-surface temperature and salinity
2216 deviations from 1985-01-01 to 2019-12-31 (NCEI Accession 0301544), NOAA National Centers for Environmental
2217 Information, Dataset, <https://doi.org/10.25921/2dp5-xm29>, 2025.

2218 Wilkinson, M. D., Dumontier, M., Aalbersberg, I. J., Appleton, G., Axton, M., Baak, A., Blomberg, N., Boiten, J.-
2219 W., da Silva Santos, L. B., Bourne, P. E., Bouwman, J., Brookes, A. J., Clark, T., Crosas, M., Dillo, I., Dumon, O.,
2220 Edmunds, S., Evelo, C. T., Finkers, R., Gonzalez-Beltran, A., Gray, A. J. G., Groth, P., Goble, C., Grethe, J. S.,
2221 Heringa, J., Hoen, P., Hooft, R., Kuhn, T., Kok, R., Kok, J., Scott J. Lusher, S. J., Martone, M. E., Mons, A., Packer,
2222 A. L., Persson, B., Rocca-Serra, P., Roos, M., van Schaik, R., Sansone, S.-A., Schultes, E., Sengstag, T., Slater, T.,
2223 Strawn, G., Swertz, M. A., Thompson, M., van der Lei, J., van Mulligen, E., Velterop, J., Waagmeester, A.,
2224 Wittenburg, P., Wolstencroft, K., Zhao, J., Mons, B.: The Fair Guiding Principles for Scientific Data Management
2225 and Stewardship, *Scientific Data*, 3(1), <https://doi.org/10.1038/sdata.2016.18>, 2016.

2226 Winn, C. D., MacKenzie, F. T., Carrillo, C. J., Sabine, C. L., and Karl, D. M.: Air-sea carbon dioxide exchange in
2227 the North Pacific Subtropical Gyre: Implications for the global carbon budget, *Global Biogeochem Cycles*, 8, 157-
2228 163, <https://doi.org/10.1029/94GB00387>, 1994.

2229 Winn, C. D., Li, Y.-H., Mackenzie, F. T., and Karl, D. M.: Rising surface ocean dissolved inorganic carbon at the
2230 Hawaii Ocean Time-series site, *Mar. Chem.*, 60, 33-47, [https://doi.org/10.1016/S0304-4203\(97\)00085-6](https://doi.org/10.1016/S0304-4203(97)00085-6), 1998.

2231 Wu, Z., Lu, W., Roobaert, A., Song, L., Yan, X.-H., and Cai, W.-J.: A machine-learning reconstruction of sea
2232 surface $p\text{CO}_2$ in the North American Atlantic Coastal Ocean Margin from 1993 to 2021, *Earth Syst. Sci. Data*.
2233 <https://doi.org/10.5194/essd-17-43-2025>, 2025.

2234 Zeng, J., Iida, Y., Matsunaga, T., Shirai, T.: Surface ocean CO_2 concentration and air-sea flux estimate by machine
2235 learning with modelled variable trends, *Front. Mar. Sci.*, 9, 989233, <https://doi.org/10.3389/fmars.2022.989233>,
2236 2022.

2237 Zeng, J.: NIES-ML3 ensemble product of surface ocean CO_2 concentrations and air-sea CO_2 fluxes reconstructed by
2238 using three machine learning models with new CO_2 trends, National Institute for Environmental Studies (NIES),
2239 Japan, <https://doi.org/10.17595/20220311.001>, 2022.

2240 Zhang, H., Menemenlis, D., and Fenty, I. G.: ECCO LLC270 ocean-ice state estimate (Tech. Rep.), Jet Propulsion
2241 Laboratory, California Institute of Technology, <http://hdl.handle.net/1721.1/119821>, 2018.

2242 Zhong, G., Li, X., Song, J., Qu, B., Wang, F., Wang, Y., ... & Duan, L. Reconstruction of global surface ocean $p\text{CO}_2$
2243 using region-specific predictors based on a stepwise FFNN regression algorithm. *Biogeosciences*, 19, 845-859,
2244 <https://doi.org/10.5194/bg-19-845-2022>, 2022.

2245 Zhong, G., Li, X., Song, J., Qu, B., Wang, F., Wang, Y., Zhang, B., Cheng, L., Ma, J., Yuan, H., Duan, L., Li, N.,
2246 Wang, Q., Xing, J., and Dai, J.: A global monthly 3D field of seawater pH over 3 decades: a machine learning
2247 approach, *Earth Syst. Sci. Data*, 17, 719–740, <https://doi.org/10.5194/essd-17-719-2025>, 2025.

2248 Zweng, M. M., Reagan, J. R., Antonov, J. I., Locarnini, R. A., Mishonov, A. V., Boyer, T. P., Garcia, H. E.,
2249 Baranova, O. K., Johnson, D. R., Seidov, D., and Biddle, M. M.: World Ocean Atlas 2013, Volume 2: Salinity,
2250 edited by: Levitus, S. and Mishonov, A., NOAA Atlas NESDIS 74, 39 pp., 2013.

2251 Zweng, M. M., Reagan, J. R., Seidov, D., Boyer, T. P., Locarnini, R. A., Garcia, H. E., Mishonov, A. V., Baranova,
2252 O. K., Weathers, K. W., Paver, C. R., Smolyar, I. V.: World Ocean Atlas 2018, Volume 2: Salinity, edited by
2253 Mishonov, A., NOAA Atlas NESDIS 82, 2019.